INVESTIGATION OF THE VISCOUS DISSIPATION OF ENERGY IN TURBULENT FLOWS

By

JIMMY ELSTER COX

Bachelor of Science in Mechanical Engineering
Southern Methodist University
1958

Master of Science in Mechanical Engineering
Southern Methodist University
1960

Submitted to the faculty of the Graduate School of
Oklahoma State University
in partial fulfillment of the requirements
for the degree of
DOCTOR OF PHILOSOPHY
August, 1963

INVESTIGATION OF THE VISCOUS DISSIPATION OF

ENERGY IN TURBULENT FLOWS

Thesis Approved:

Gerald W. Parker
Thesis Adviser

O. H. Hamilton

M. K. Jovanovic

J. H. Boggs

Robert MacVicar
Dean of the Graduate School

PREFACE

The author wishes to express his appreciation to all those who have so graciously contributed support by example and encouragement--most of whom shall be nameless here but who are important in the eyes of the author.

The author wishes to thank the committee members, Dr. J. H. Boggs, Dr. O. H. Hamilton, Dr. M. K. Jovanovic, and Dr. J. D. Parker, for their patient direction. Dr. Boggs deserves special recognition for encouraging the author to continue his education and for providing the opportunities to make it possible. The author is grateful to Oklahoma State University and Boeing Airplane Company for financial assistance during this period of study.

A debt of gratitude is due those who have taken time from their busy schedules to serve in a reference capacity for the author.

TABLE OF CONTENTS

TABLE OF CONTENTS (CONT.)

LIST OF TABLES

LIST OF FIGURES

LIST OF FIGURES (CONT.)

LIST OF SYMBOLS

A	Coefficient
a	Dimensionless quantity
a_1	Empirical constant
B	Coefficient
B_1	Coefficient
$\overline{B}$	Coefficient
$\overline{B}_1$	Coefficient
C	Constant
c_v	Specific heat
c^2	Mixing length parameter
e	Specific internal energy
h	Specific enthalpy
K	Mass momentum
k	Thermal conductivity
L	Length
ℓ	Turbulent fluctuation distance
ℓ^2	Mixing length squared
P	Pressure
Q	Heat transfer rate
q_f	Viscous dissipated energy per unit time
$\dot{q}$	Flow rate
R	Radius of container

R_o	Orifice radius
R_x	Boundary of circular jet
r	Radial coordinate
r_o	Boundary of jet in exit regions
r_1	Boundary of core in Exit Region A
t	Time
T	Temperature
$\bar{T}$	Bulk fluid temperature
T'	Turbulent fluctuation temperature
T_s	Temperature of surroundings
u	Velocity in the x direction
$\bar{u}$	Average velocity in the x direction
u'	Turbulent fluctuation velocity in the x direction
u_o	Stream velocity in the x direction
u_x	Center-line velocity in Exit Region B
v	Specific volume
v	Velocity perpendicular to the axis
v'	Turbulent fluctuation velocity in the r direction
Wk	Work rate
x	Axial coordinate
x_o	Axial distance from the source to the orifice plate
x_1	Axial distance from the source to the Fully-Developed Region
x_A	Axial distance from the orifice plate to the interface of Region A-B
y	Coordinate perpendicular to the axial coordinate
Y	Container dimension

Y_x	Boundary of plane jet
z	Elevation above reference plane
β	Viscosity exponent
η	Dimensionless distance
η_o	Dimensionless distance to the edge of the jet
$\mathcal{K}$	Coefficient
μ	Molecular viscosity
μ_J	Joule-Thomson Coefficient
μ_t	Eddy viscosity
υ	Kinematic viscosity
υ_t	Eddy kinematic viscosity
ϕ	Dissipation function
ρ	Density
τ	Shearing stress

CHAPTER I

INTRODUCTION

Viscosity is a physical property of fluids which characterizes the resistance of a fluid to flow. More specifically, it is the transport property expressing the transport of momentum across a velocity gradient. The effects of viscosity are evident in simple flow situations such as forced convection in a pipe and flow over a flat plate; the no-slip requirement at the surface together with the viscosity characteristics of the fluid determine the shape of the velocity gradient. The conversion of mechanical energy into thermal energy by the shearing action is called the viscous dissipation of energy. This is a familiar term in the fields of fluid mechanics and heat transfer and is often thought of as "heat generation." This terminology is poor from two standpoints - first, it seems to indicate a violation of the first law of thermodynamics; and second, it implies the transfer of heat across a boundary.

The relative importance of the viscous dissipation of energy depends upon the fluid medium and the flow patterns. Generally, its quantitative contribution is small. In many cases it is difficult to detect viscous dissipation in the fluid by temperature measurements, but its presence can be established in some cases by determining the decrease in mechanical energy - more commonly called pressure drop.

In the development of the energy equation for the fluid element, the shearing action is found to have two effects on the fluid element.

The viscous forces produce mechanical work, (i.e., compressing or expanding the fluid element) as well as increase internal energy. The general energy equation contains four individual sets of terms representing the energy stored in the element, the energy transferred by convection, the energy transferred by conduction and the viscous dissipation of energy. Since the quantitative contribution of the last set of terms is usually small as compared to the other terms, the viscous dissipation function has received little attention and is usually neglected altogether. Its inclusion in the energy equation complicates the mathematical solution significantly.

According to Lamb(1)[1], the viscous dissipation of energy can be evaluated independently of the energy equation by the relation

$$dq_f = \mu \Phi \, dV \tag{I-1}$$

where Φ is the dissipation function as it appears in the general energy equation. If the viscous dissipation function is to result in a significant quantity relative to the conduction and convection terms, the change in mechanical energy must be substantial. The magnitude of the dissipated energy is a function of the velocity gradients, so that flow situations having as a characteristic large velocity gradients should be investigated.

Two-dimensional flow situations having large changes in mechanical energy are the flow of fluids through restrictions. Using an analytical model, equations are developed to describe the viscous dissipation of energy for the case of free boundary expansions downstream of restrictions. These expressions furnish a means of determining the distributions

[1]Numbers in parentheses indicate references in the Bibliography

of the dissipated energy in both the axial and radial directions. The effects of the various physical situations may be considered by changing the input parameters in the expressions. The results are compared to the values obtained from a thermodynamic system approach.

CHAPTER II

THE THERMODYNAMIC ROLE OF VISCOUS DISSIPATION

In order to illustrate the important role of the viscous dissipation of energy in satisfying the fundamentals of classical thermodynamics, the steady flow of a fluid through a restriction may be considered. The steady-flow energy equation is

$$\dot{g}\rho h_1 + \dot{g}\rho\frac{\bar{u}_1^2}{2} + \dot{g}\rho z_1 + Q = \dot{g}\rho h_2 + \dot{g}\rho\frac{\bar{u}_2^2}{2} + \dot{g}\rho z_2 + Wk. \qquad \text{(II-1)}$$

The necessary conversion factors are not shown in the relations presented. If the thermodynamic system or the control volume is selected as shown in Figure 1 in such a manner that the kinetic and potential energy terms may be neglected, and if there is no work or heat involved, the steady-flow energy equation reduces to

$$h_1 = h_2 .$$

Using the definition of enthalpy and differentiating yields,

$$dh = de + P dv + v dP. \qquad \text{(II-2)}$$

In the event that the working fluid is of an incompressible nature, then the term containing the specific volume variation may be omitted so that the expression simplifies to

$$-de = v dP \qquad \text{(II-3)}$$

when h = constant.

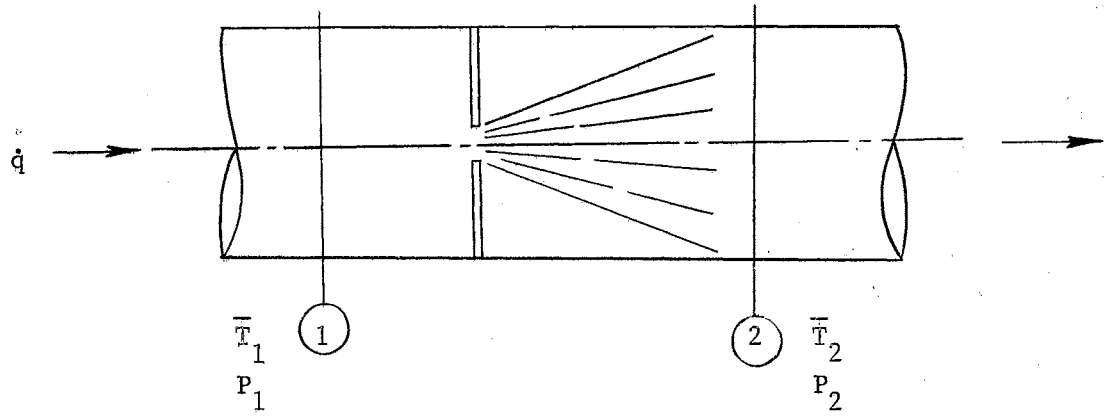

Figure 1. Flow Through a Restriction

By letting

$$de = c_v dT$$

and integrating the above equation assuming c_v = constant or an average specific heat

$$-c_v(\bar{T}_2-\bar{T}_1) = \frac{1}{\rho}(P_2-P_1)$$

$$\bar{T}_2-\bar{T}_1 = \frac{1}{\rho c_v}(P_1-P_2) . \qquad \text{(II-4)}$$

The internal energy of the fluid may be expressed as the function

$$E = f(P,T)$$

but since the dependence on pressure is negligible for the incompressible fluid, the internal energy level of the fluid is proportional to the bulk fluid temperature, which is defined by the relation

$$T = \frac{\iint Tu\,dA}{\iint u\,dA} \qquad \text{(II-5)}$$

where T and u are the local fluid temperature and velocity, respectively.

Therefore, for a case of an incompressible fluid, the bulk fluid temperature increase is directly proportional to the pressure drop. This is presented graphically in Figure 2 for MIL-H-5606A hydraulic fluid.

It is this mechanism for the conversion of energy which is of interest from a fluid mechanics and heat transfer standpoint. Bird, Stewart and Lightfoot (2) call this mechanism the "irreversible degradation" of mechanical energy into thermal energy. The steady-flow energy equation for the non-adiabatic case in the absence of kinetic and potential energy considerations is obtained from the condition:

Decrease in Mechanical Energy = Increase in Thermal Energy + Heat Transferred

$$\dot{g}\rho(P_1-P_2) = \dot{g}\rho(e_1-e_2) + Q \,. \tag{II-6}$$

Bennett and Myers (3) refer to the conversion of flow energy into internal energy and perhaps to heat transfer to the surroundings as "lost work."

For a compressible fluid, the term involving the change in specific volume must be considered. In this case, the relation is

$$-de = Pdv + vdP \,. \tag{II-7}$$

Since both the pressure and the specific volume are variables, it is necessary to establish how one is dependent on the other. In the case of a compressible fluid, the Joule-Thomson coefficient characterizes a throttling process. The Joule-Thomson coefficient is defined as

$$\mu_J = \left(\frac{\partial T}{\partial P}\right)_h \,. \tag{II-8}$$

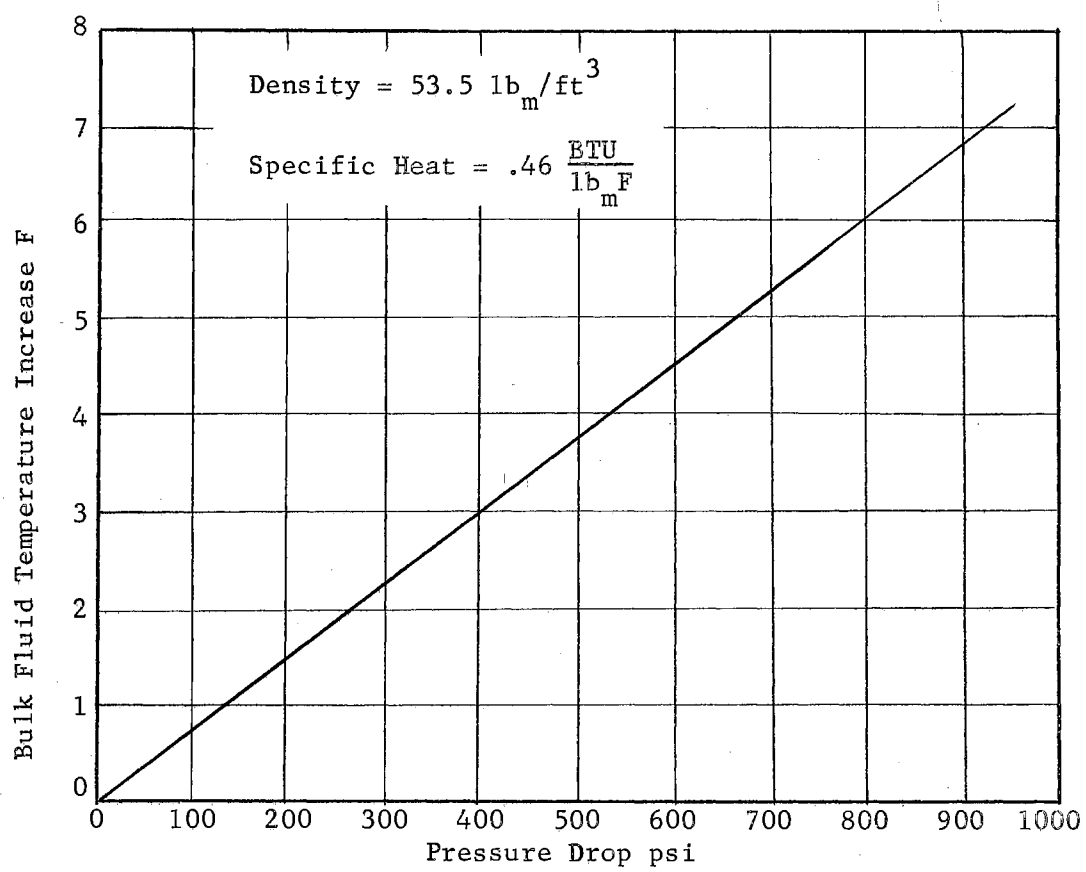

Figure 2. Temperature and Pressure Changes for Adiabatic Flow of Hydraulic Fluid

For a perfect gas, it can easily be shown that μ_J is equal to zero. Jones and Hawkins (4) show the variation in the Joule-Thomson coefficient for air at various pressures and temperatures, as shown in Figure 3. Using the approximation

$$\mu_J \approx \left(\frac{\Delta \bar{T}}{\Delta P}\right)_h , \qquad \text{(II-9)}$$

it can be seen that when μ_J is positive, a decrease in pressure results in a decrease in temperature. This can be explained by the fact that

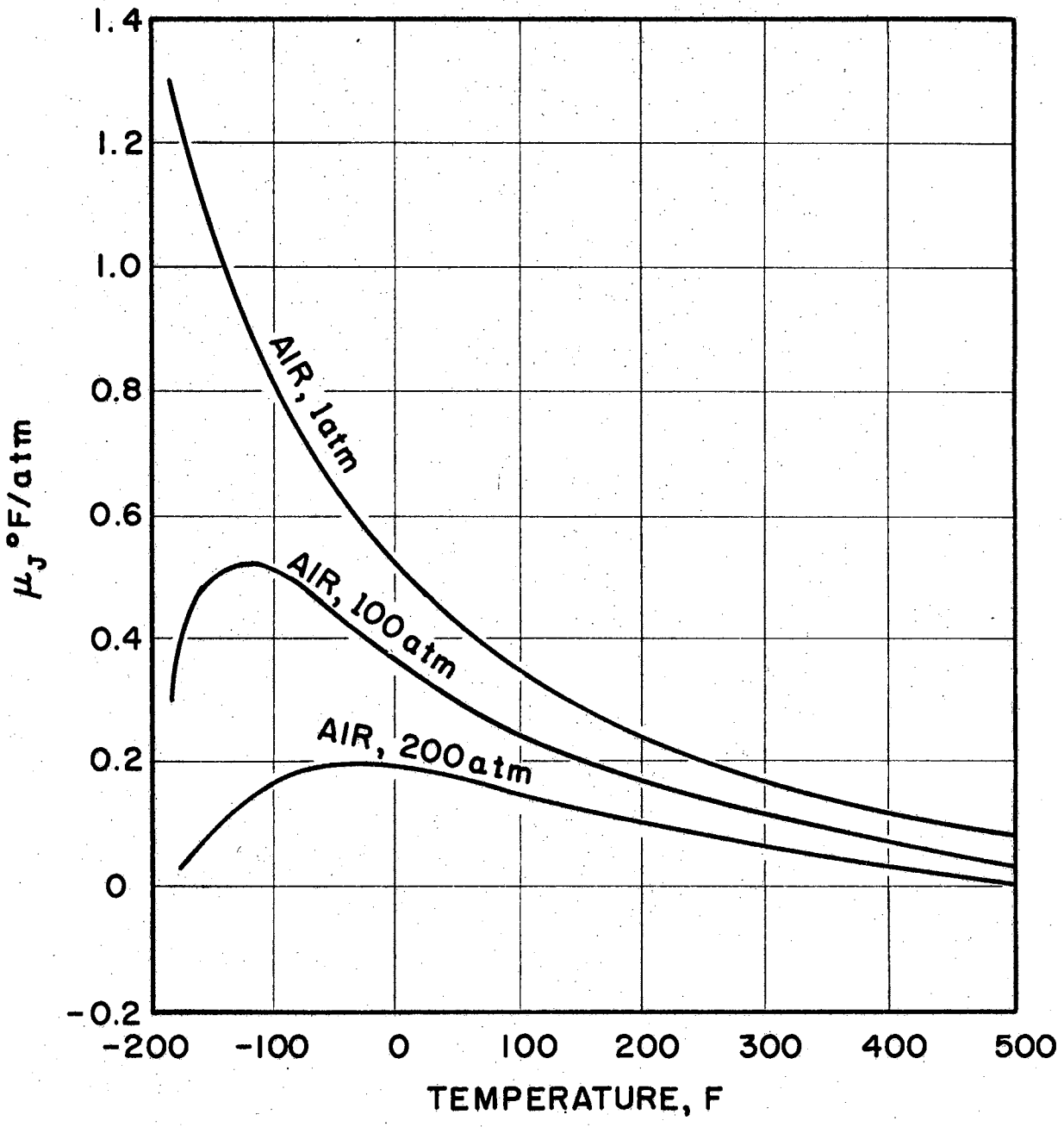

FIGURE 3

JOULE-THOMSON COEFFICIENTS FOR AIR

the viscous dissipation of energy contributes to the increase in the energy level of the fluid; however, the expansion work in the case of a compressible fluid decreases the thermal energy level of the fluid by a greater amount. Thus, the decrease in temperature with a corresponding decrease in pressure for a compressible fluid is the result of an expansion process. The viscous dissipation function does not account for the expansion work in a compressible fluid.

CHAPTER III

ADVANCES IN FREE TURBULENT FLOW ANALYSIS

Since the turn of the century considerable attention has been given to analytical solutions describing the free turbulent flow phenomena. There are three basic types of free turbulent flow situations - the jet boundary, the wake, and the free jet - as illustrated in Figure 4. Solutions of each of these types of flow are similar in nature. Free turbulent flow situations have been described by three basic theories - first, the momentum transfer theory; second, the vorticity theory; and third, the vorticity theory with symmetrical turbulence.

The Momentum Transfer Theory

The momentum transfer theory is based on Prandtl's mixing length theory (6) for the evaluation of the relation

$$\tau = \rho \overline{v'} \qquad \text{(III-1)}$$

The quantity ℓ is a distance term appearing in the analytical model and illustrated in Figure 5. Suppose that a fluid element is located at some arbitrary location $\bar{r}$ from the x axis and that the fluid element has an average velocity $\bar{u}$ in the x direction. If, due to mixing, the element relocates to a new position $\bar{r} \pm \ell$ and at the same time retains the same average velocity, then the average velocity of the fluid in

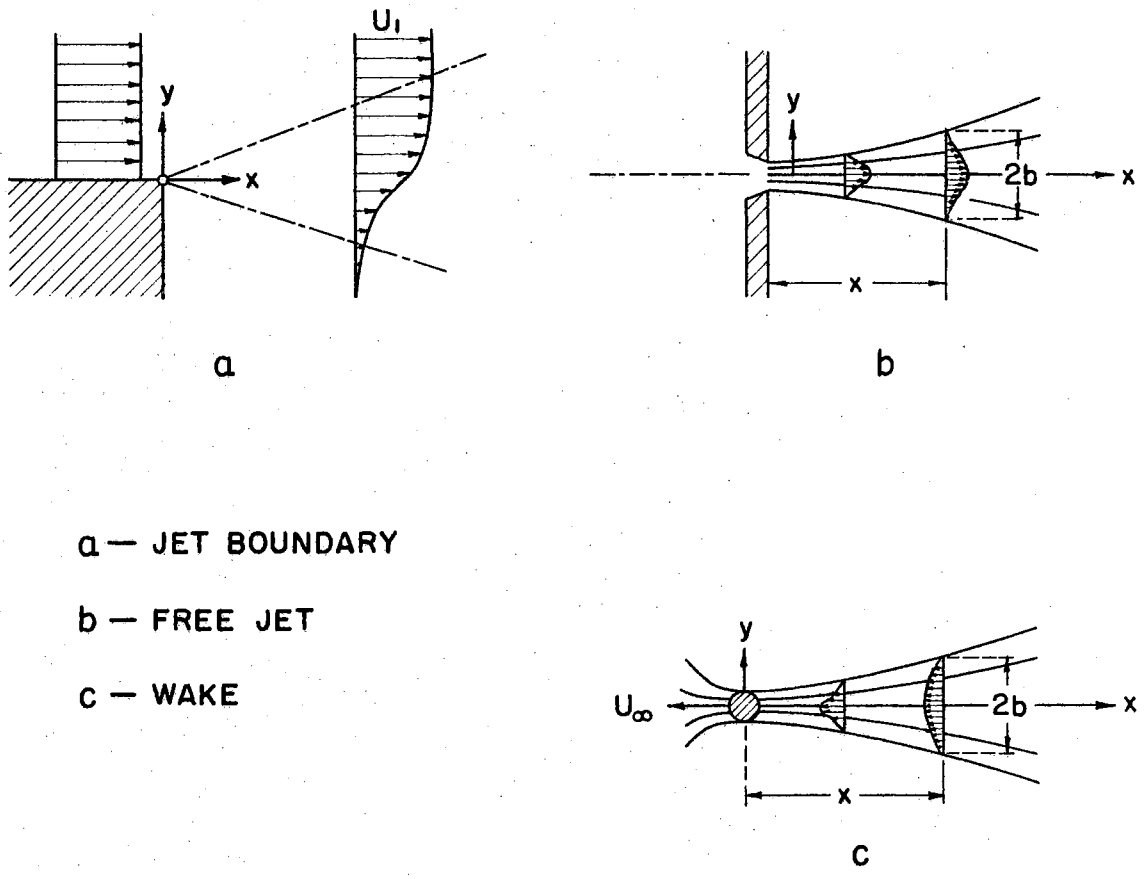

FIGURE 4

FREE TURBULENT FLOWS

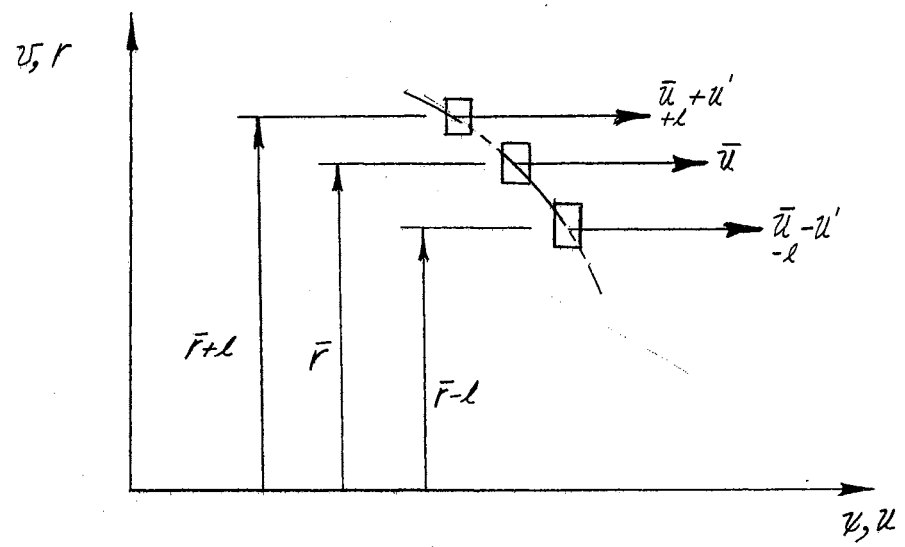

Figure 5. Prandtl's Mixing-Length Model

the new location may be expressed as

$$\bar{u}_{\pm\ell} = \bar{u} \pm \ell \frac{\partial \bar{u}_{\bar{r}}}{\partial r} ,$$

so that the turbulent fluctuation velocity is

$$u' = \ell \left| \frac{\partial u}{\partial r} \right| . \qquad \text{(III-2)}$$

By assuming the turbulent fluctuation velocity in the radial direction is proportional to the turbulent fluctuation velocity in the axial direction, then

$$\kappa = \ell^2 \left| \frac{\partial u}{\partial r} \right| . \qquad \text{(III-3)}$$

Prandtl's technique of analysis is based on the conservation of momentum in the turbulent mixing process. Prandtl stipulates the following restrictions on his mixing length theory;

a. ℓ^2 is proportional to the width of the flow pattern at a sufficient distance downstream

b. ℓ^2 is constant across any section

The Vorticity Theory

The vorticity theory is based on the supposition that the vorticity is independent of position. According to Taylor (6), the effects of the variation of static pressure in the axial direction may have such an effect on the momentum balance technique of Prandtl that the u' will not average to zero. Therefore, Taylor proposes a conservation of vorticity. The fundamental assumption in the vorticity theory is that the vorticity remains constant throughout the mixing process.

Taylor develops the vorticity theory after studying the data of the temperature distribution in the wake of a cylinder. Using the similarity principle between the momentum transfer theory and the temperature profile, the experimental data exhibits a spreading tendency which is not described by the analytical profile. The profiles obtained by Taylor's vorticity theory present a better correlation.

The Vorticity Theory with Symmetrical Turbulence

The vorticity theory with symmetrical turbulence for axially symmetrical flow is proposed by Goldstein (7). The theory is based on symmetrical eddy velocities. In this approach, a more general mixing length is employed which is a function of the radii of the sections and is not assumed to be a constant across any particular section.

Further Developments in Free Flows

Rayleigh (8) discusses the results and reasoning of experimental

work of his contemporaries concerning the flow phenomena of jets issuing from various shaped openings. The effect of head pressure on the jet characteristics is among the results cited. The work represents the state of advancement just after the mid-nineteenth century.

Chaplygin (9) makes an early contribution in the analysis of jets; his analysis considers ideal gas jets and employs the treatment of potential flow theory. The velocity potential and the stream function are presented in the form of series, and the series are investigated for convergence. Chaplygin considers the problem of outflow of a gas from an infinite vessel with plane walls. He describes the phenomena of a gas jet impacting a plate.

Tollmien (10) is among the first to study analytically the jet expansion process employing the momentum transfer theory with Prandtl's mixing length theory as given by

$$\tau_{xr} = \rho l^2 \frac{\partial u}{\partial r} \left| \frac{\partial u}{\partial r} \right| . \qquad \text{(III-4)}$$

Certain limiting assumptions are employed to simplify the equation of motion - namely that the axial velocity is large as compared to the radial velocity and the derivatives with respect to x are small as compared to those with respect to r. The equation of motion reduces to

$$u\left(\frac{\partial u}{\partial x}\right) + v\left(\frac{\partial u}{\partial r}\right) = \frac{1}{\rho} \frac{\partial}{\partial r}\left(\tau_{rx}\right) . \qquad \text{(III-5)}$$

Appendix A presents the general equations of motion. Tollmien presents an analysis for the mixing of an air stream with adjacent still air, a two-dimensional jet expansion, and a rotationally symmetrical jet expansion. The reduction of the partial differential equation to an

ordinary differential equation is accomplished by defining the dimensionless distance η as

$$\eta \propto \frac{r}{x^m}$$

and by using the stream function ψ as

$$\psi \propto x^p F(\eta) .$$

By employing a dimensional analysis technique to the stream function expressions, a simplified equation of motion, and a momentum expression, the partial differential equation is transformed into the ordinary differential equation. For the two-dimensional jet, the equation of motion is reduced to

$$FF' - 2\epsilon^2 (F'')^2 = 0 \qquad \text{(III-6)}$$

where

$$F(\eta) = \int f(\eta)\, d\eta \qquad \text{(III-7)}$$

and for the case of the rotationally symmetrical jet, the equation of motion reduces to

$$FF' - \epsilon^2 \left(F'' - \frac{F'}{\eta}\right)^2 = 0 \qquad \text{(III-8)}$$

where in this case

$$F(\eta) = \int \eta f(\eta)\, d\eta \qquad \text{(III-9)}$$

Förthmann (11) obtains experimental data for an open jet using air as the working fluid; he points out that there are "minor systematic discrepancies" from the velocity distributions predicted by Tollmien.

Kuethe (12) extends the work of Tollmien to include the mixing phenomena of two parallel streams at different velocities. The equation of motion is reduced to an ordinary differential equation similar to

that of Tollmien. Kuethe divides the jet expansion into three separate regions as illustrated in Figure 6. These regions are based on the axial distance from the orifice opening.

Region A is characterized by an annular mixing region surrounding the core of potential flow. In Region B the entire jet is the mixing region. In Region C the center-line velocity is inversely proportional to the distance from some point near the mouth of the orifice and all profiles are similar. Kuethe points out that Tollmien's analysis is valid in Region C for an axial distance of approximately eight orifice diameters downstream of the orifice opening.

Howarth (13) determines the velocity profiles for symmetrical jets using each of the three basic approaches independently. Each approach starts with an equation of motion of

$$u\frac{\partial u}{\partial x}+v\frac{\partial u}{\partial r}=\frac{1}{r}\frac{\partial}{\partial r}\left[\varkappa r\frac{\partial u}{\partial r}\right] \qquad \text{(III-10)}$$

where $\varkappa$ is defined by equation (III-1). The momentum transfer theory uses $\varkappa$ from equation (IV-3), in which case, the equation of motion reduces to the ordinary differential equation,

$$FF'-b\left(F''-\frac{F'}{\eta}\right)^2=0\ , \qquad \text{(III-11)}$$

where

$$F(\eta)=\int \eta f(\eta)\,d\eta\ . \qquad \text{(III-12)}$$

This equation is similar to that of Tollmien (10) for the rotationally symmetrical jet. The vorticity theory modifies the equation by treating $\varkappa$ as a constant; then

$$u\frac{\partial u}{\partial x}+v\frac{\partial u}{\partial r}=\frac{\varkappa}{r}\frac{\partial}{\partial r}\left[r\frac{\partial u}{\partial r}\right] \qquad \text{(III-13)}$$

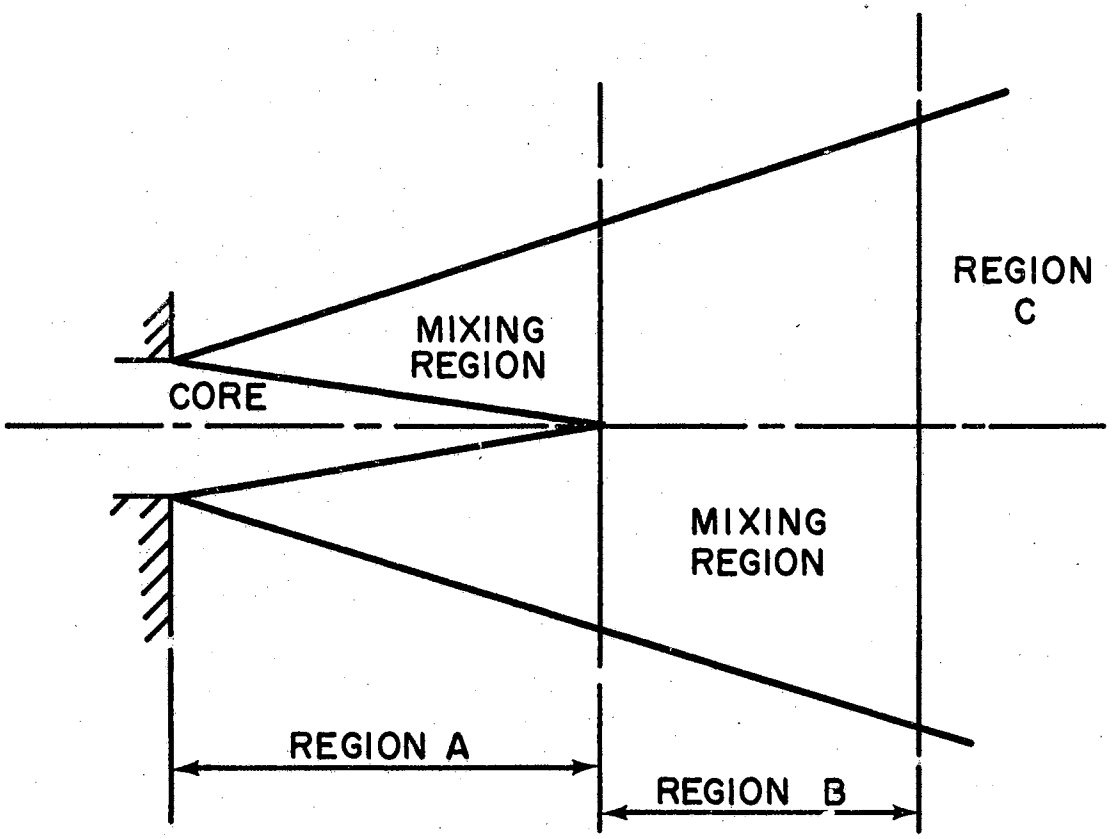

FIGURE 6

KUETHE'S EXIT REGION MODEL

where κ is defined as

$$\kappa = \overline{\ell v'} \quad , \tag{III-14}$$

The modified vorticity theory results in an ordinary differential equation

$$\frac{FF'' + (F')^2}{\eta^2} - \frac{FF'}{\eta^3} = b\left\{\frac{F'''}{\eta} - \frac{F''}{\eta^2} + \frac{F'}{\eta^3}\right\}\left\{\frac{F''}{\eta} - \frac{F'}{\eta^2}\right\} \tag{III-15}$$

where F is the same as defined above. The vorticity theory with symmetrical turbulence reduces the equation of motion to

$$\frac{FF'' + (F')^2}{\eta^2} - \frac{FF'}{\eta^3} = \phi(\eta)\left\{\frac{F'''}{\eta} - \frac{F''}{\eta^2} + \frac{F'}{\eta^3}\right\}\left\{\frac{F''}{\eta} - \frac{F'}{\eta^2}\right\} \tag{III-16}$$

and for this case

$$\ell^2 = \phi(\eta)\kappa^2 = b\eta^p\kappa^2 \quad .$$

The results of these independent analyses are shown in Figures 7 and 8. The temperature profiles are established on a similarity principle between the temperature and velocity distributions. Howarth compares the various analytical solutions to the experimental results of Ruden (14) and finds that the momentum transfer theory provides the best correlation for the velocity distribution and that the vorticity theory provides the best correlation for the temperature distribution. The temperature distributions for the three analyses are shown in Figure 9.

Bickley (15) presents some modifications on an early publication of Schlichting for the case of the plane jet. Bickley performs a direct integration to obtain an exact solution for the equations of Schlichting.

Prandtl (16) - as an introduction to the presentation of Görtler (17) - presents a new formulation for the exchange coefficient for the free

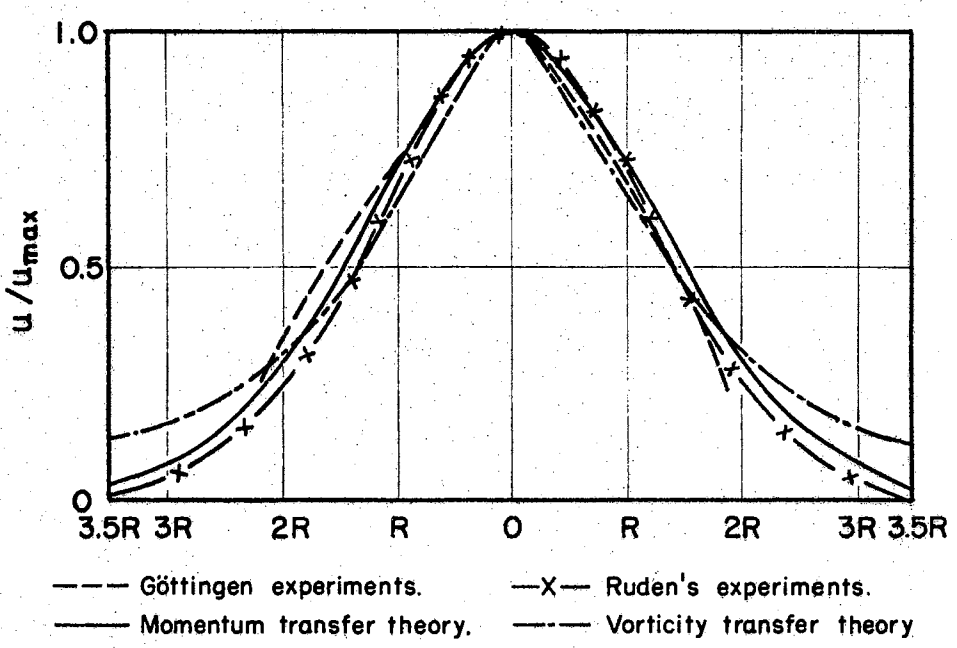

FIGURE 7

VELOCITY DISTRIBUTION IN AN AXIALLY SYMMETRICAL JET. – I (HOWARTH)

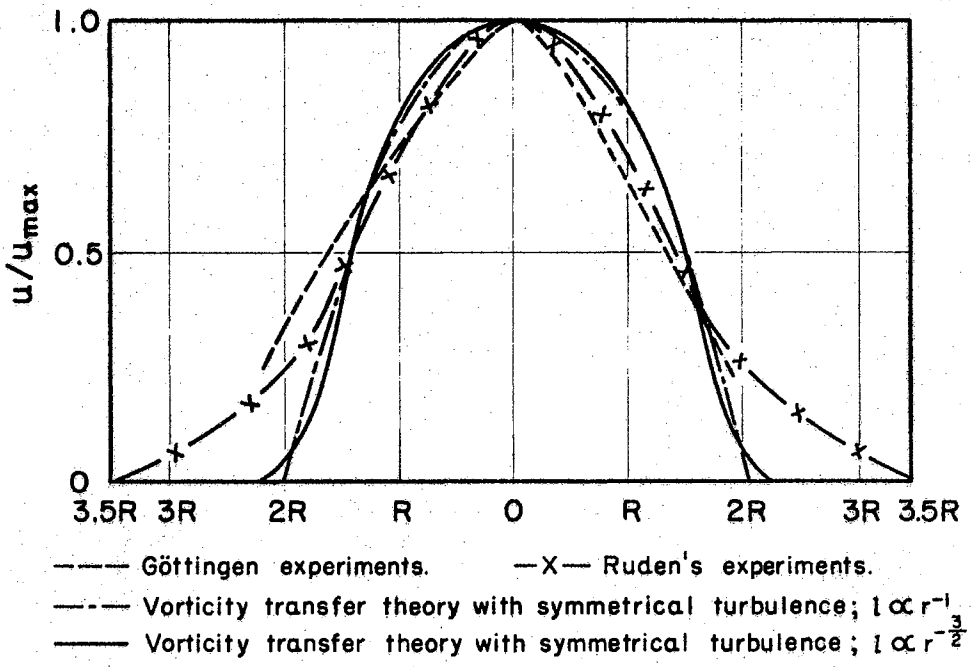

FIGURE 8

VELOCITY DISTRIBUTION IN AN AXIALLY SYMMETRICAL JET.—II (HOWARTH)

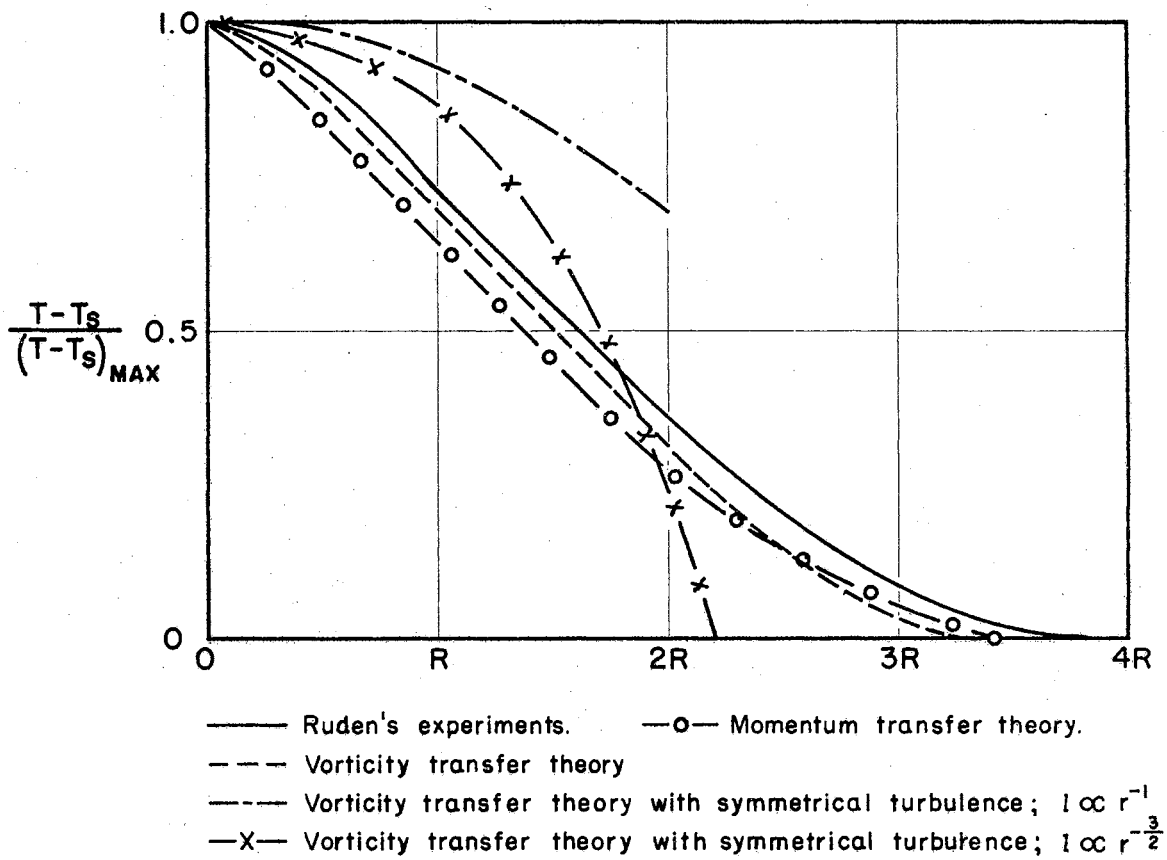

FIGURE 9

TEMPERATURE DISTRIBUTION IN AN AXIALLY SYMMETRICAL JET. (HOWARTH)

turbulence application. In this new formulation, the quantity

$$K = \ell^2 \left| \frac{\partial u}{\partial r} \right| \qquad \text{(III-17)}$$

is replaced by

$$K = C_1 b \left[\bar{u}_{max} - \bar{u}_{min} \right] \qquad \text{(III-18)}$$

where C_1 is a constant, b is the width of the mixing zone at a particular section and $\bar{u}_{max}$ and $\bar{u}_{min}$ are the values of u at the section. Görtler applies the new formulation of Prandtl to several free turbulence problems. He considers the mixing of two parallel streams of different average speeds. Using Prandtl's new evaluation, K is proportional to x. For the plane jet, K is proportional to $\sqrt{x}$ and a more rounded profile near the center of the jet is obtained than that of Tollmien (10).

Squire (18) presents a summary of his results for several types of free turbulent situations including circular and plane jets. The results are qualitative in nature since the constants are not evaluated.

Squire's Plane Jet

$$u\frac{\partial u}{\partial x} + v\frac{\partial u}{\partial y} = -\frac{\partial}{\partial y}\left(\overline{u'v'}\right) \qquad u\frac{\partial T}{\partial x} + v\frac{\partial T}{\partial y} = -\frac{\partial}{\partial y}\left(\overline{v'T'}\right)$$

$$\int u^2 dy = \text{CONSTANT} \qquad \int T u\, dy = \text{CONSTANT}$$

$$u = \frac{A}{\sqrt{x}} f(\eta)\,; \quad \eta = \frac{By}{x} \qquad T = \frac{A_1}{\sqrt{x}} f_1(\eta)$$

$$\overline{u'v'} = -\frac{A^2}{x} g(\eta) \qquad \overline{v'T'} = -\frac{AA_1}{\sqrt{x}} g_1(\eta)$$

$$g(\eta) = \frac{B}{2} f(\eta) \int_0^{\eta} f(\eta)\, d\eta \qquad g_1(\eta) = \frac{B_1}{2} f_1(\eta) \int f_1(\eta)\, d\eta \qquad \text{(III-19)}$$

Squire's Circular Jet

$$
\begin{aligned}
&u\frac{\partial u}{\partial x}+v\frac{\partial u}{\partial r}=-\frac{1}{r}\frac{\partial}{\partial r}\left(r\overline{u'v'}\right) && u\frac{\partial T}{\partial x}+v\frac{\partial T}{\partial r}=-\frac{1}{r}\frac{\partial}{\partial r}\left(r\overline{v'T'}\right)\\
&\int u^2 r\,dr=\text{CONSTANT} && \int uTr\,dr=\text{CONSTANT}\\
&u=\frac{A}{x}f'(\eta) && T=\frac{A_1}{x}f_1(\eta)\\
&\overline{u'v'}=-\frac{A^2}{x^2}g(\eta) && \overline{v'T'}=-\frac{AA_1}{x^2}g_1(\eta)\\
&g(\eta)=\frac{B}{2}f(\eta)\int f(\eta)\,d\eta && g_1(\eta)=\frac{B_1}{2}f_1(\eta)\int f_1(\eta)\,d\eta
\end{aligned}
\qquad \text{(III-20)}
$$

In the above relations, the constant B and B_1 control the spread of the jet. Squire believes that the existing theories of free turbulence are unsatisfactory and the distinction between physical analysis and dimensional analysis is not definite. He points out that heat spreads radially faster than momentum. This fact is first stated by Taylor (6).

Squire and Trouncer (19) extend the work of Kuethe for the axially symmetrical jet; they investigate each of the flow regimes independently and fit the solutions at the interfaces. The authors consider a general case where the jet issues into a parallel stream which has a velocity in the axial direction of u_o. The solutions can be simplified in the case where the jet issues into a fluid at rest. The velocity at the orifice opening is assumed to be constant and equal to $\bar{u}$. The velocity of the fluid in the core remains constant as the core itself diminishes. As the core decreases, the mixing annulus increases in size. When the core has disappeared, the apex of the cone of the core signals the end of Region A. Prandtl's mixing theory is

$$l = \kappa (r_o - r_1) \tag{III-21}$$

for this region where r_o is the edge of the jet and r_1 is the edge of the core. The axial velocity distribution in the mixing annulus is

$$u = u_o + \frac{\bar{u} - u_o}{2}\left[1 - \cos\left(\pi \frac{r_o - r}{r_o - r_1}\right)\right] \tag{III-22}$$

which reduces to

$$u = \frac{\bar{u}}{2}\left[1 - \cos\left(\pi \frac{r_o - r}{r_o - r_1}\right)\right] \tag{III-23}$$

for the case where $u_o = 0$. The jet boundaries are established by use of the momentum relation.

In Region B - where the central core has disappeared - the velocity along the axis begins to decrease. In this region, the velocity distribution is assumed to be of the form

$$u = u_o + \frac{u_x}{2}\left(1 + \cos\frac{\pi r}{r_o}\right) \tag{III-24}$$

and for the case where $u_o = 0$ becomes

$$u = \frac{u_x}{2}\left(1 + \cos\frac{\pi r}{r_o}\right).$$

The mixing length relation for Region B is given by

$$l = \kappa r_o \tag{III-25}$$

which is identical to that for Region A with the core absent. The velocity on the axis in Region B is a function of x. At a point approximately eight diameters downstream of the orifice, the profiles become similar and this signals the entrance to Region C, the fully-developed region.

According to a review by Emmons (20) of a presentation of Lin (21), solutions of laminar and turbulent, two-dimensional and axially symmetrical jets are presented. The method of approach is similar to that of other investigations. It is found that the width of the jet is proportional to x for the laminar case, and for the turbulent case it is proportional to x for the two-dimensional jet; for the axially symmetrical jet, the width is proportional to x for both the laminar and turbulent cases.

Hinze and Van der Hegge Zijnen (22) present the results of some interesting measurements of circular fully-developed jets. The primary fluid is air. The velocity profile is presented in Figure 10. Results indicate that the point source theoretical analysis seems to be valid downstream of the orifice beyond eight diameters. The temperature profile is shown in Figure 11. Measurements of Hinze and Van der Hegge Zijnen for the temperature distribution in the axial direction with $r = 0$ are shown in Figure 12. Temperature measurements are made with a bare chromel-alumel thermocouple.

The significant result of these experiments is that the diffusion process for matter is very similar to the heat transfer process. The diffusion process is investigated by the injection of a foreign gas into the air stream. In the free jet a pressure probe is used to extract gas samples for analysis; as a result of these tests, it seems evident that the heat transport process or temperature profile is closely associated with the diffusion process or concentration profile.

Corrsin and Uberoi (23) perform experiments with turbulent circular jets of air and find that the rate of spread of the jet increases

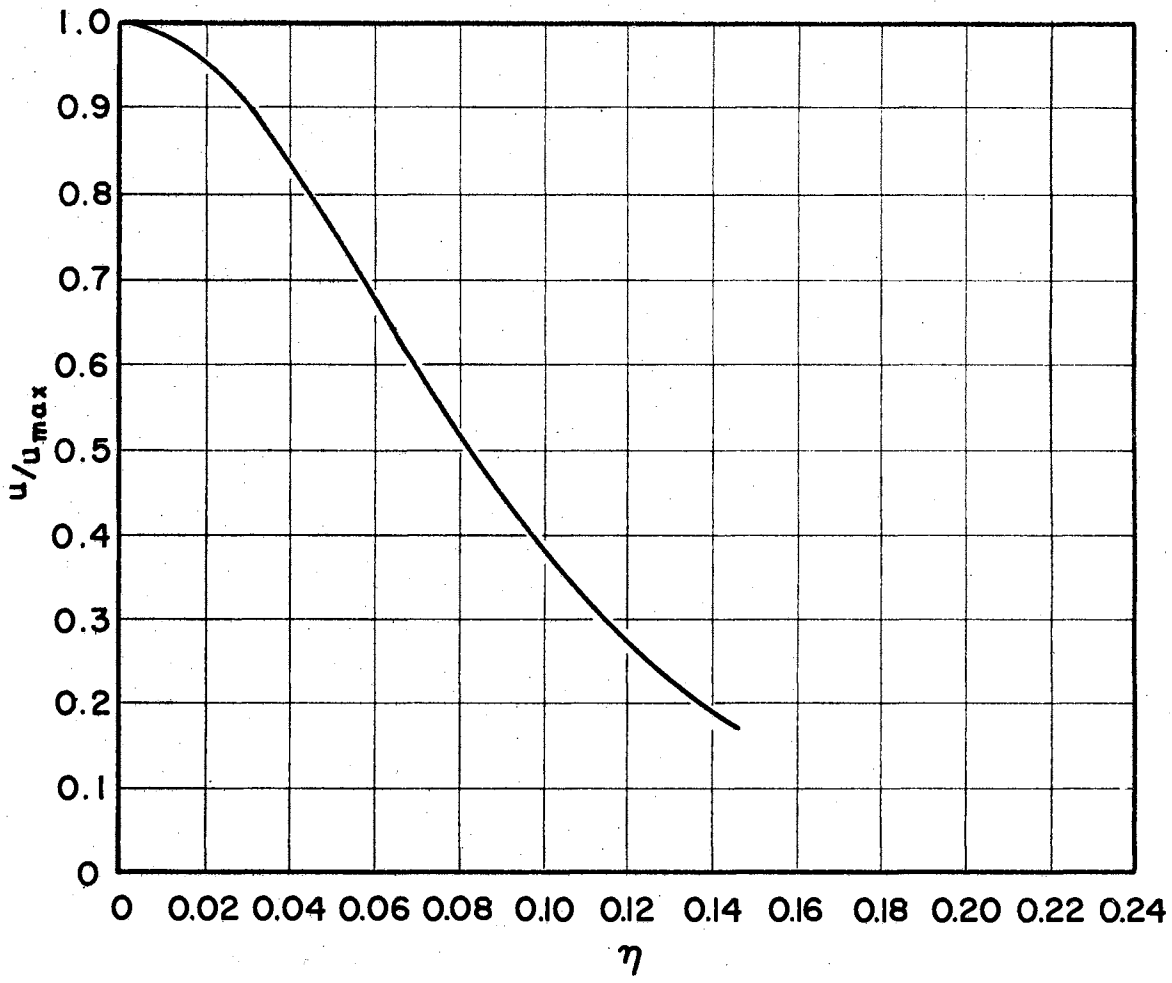

FIGURE 10

VELOCITY-DISTRIBUTION IN AN AXIALLY SYMMETRICAL JET. (HINZE)

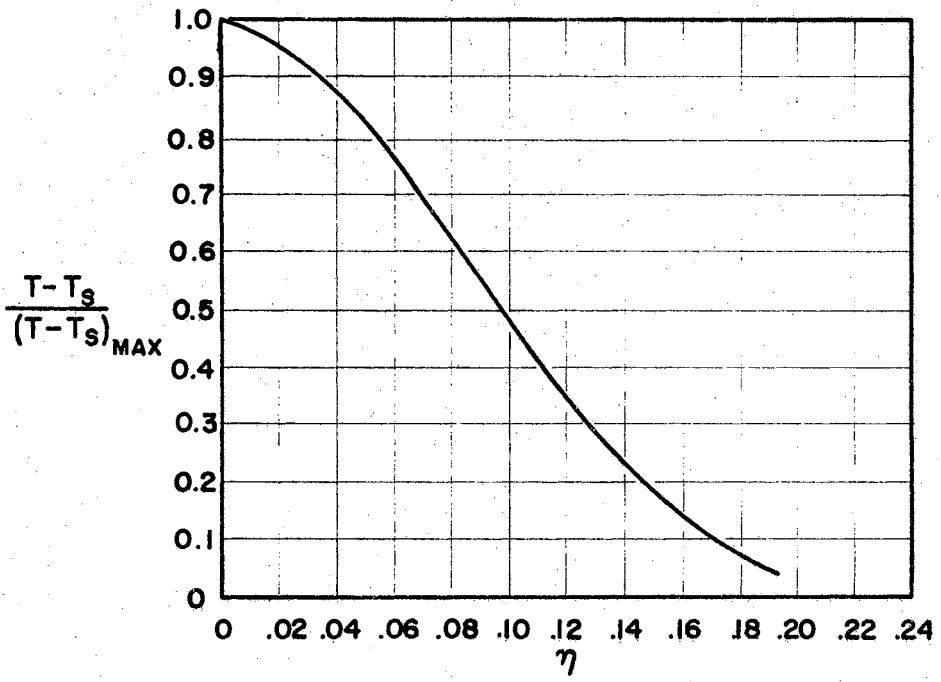

FIGURE 11

TEMPERATURE DISTRIBUTION IN AN AXIALLY SYMMETRICAL JET (HINZE)

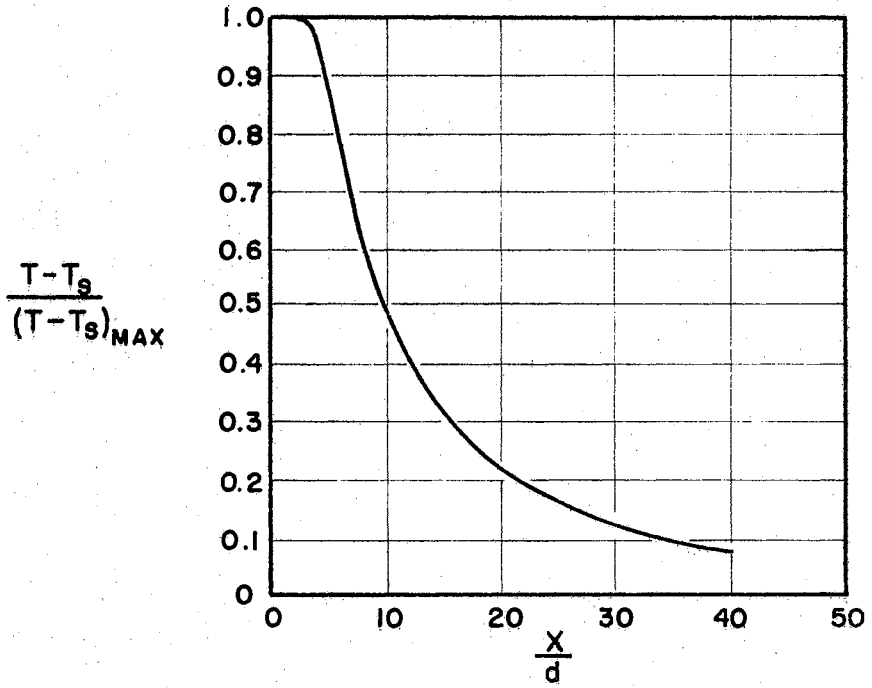

FIGURE 12

TEMPERATURE-DISTRIBUTION ALONG THE AXIS OF THE JET (HINZE)

with a decrease in the density of the jet relative to downstream surroundings. This change in density is obtained by heating the jet gas.

Pai (24) publishes a text dealing with the general subject of the dynamics of jets. Pai compiles information from many different sources many of which are included in this review.

Schlichting (25) presents a comprehensive collection of free turbulence information collected through many years of direct association with the problems. He suggests the following relations for describing the flow for the fully developed plane and circular jets:

Schlichting's Plane Jet

$$u = \frac{B_1}{\sqrt{x}}\left(1-\tanh^2\eta\right) = \sqrt{\frac{3KA_1}{4x}}\left(1-\tanh^2\eta\right)$$

$$v = \frac{B_1}{\sqrt{x}}\left[2\eta\left(1-\tanh^2\eta\right)-\tanh\eta\right] = \sqrt{\frac{3}{16}\frac{K}{A_1 x}}\left[2\eta\left(1-\tanh^2\eta\right)-\tanh\eta\right] \qquad \text{(III-26)}$$

$$\eta = A_1 y/x$$

Schlichting's Circular Jet

$$u = \frac{B}{x}\left(1+\tfrac{1}{4}\eta^2\right)^{-2} = \frac{3K}{8\pi\mu_t x}\left(1+\tfrac{1}{4}\eta^2\right)^{-2}$$

$$v = \frac{B}{x}\frac{\eta-\frac{1}{4}\eta^2}{\left(1+\frac{1}{4}\eta^2\right)^2} = \sqrt{\frac{3}{16}\frac{K}{\pi}}\frac{1}{x}\left[\frac{\eta-\frac{1}{4}\eta^2}{\left(1+\frac{1}{4}\eta^2\right)^2}\right] \qquad \text{(III-27)}$$

$$\eta = \frac{Ar}{x} = \sqrt{\frac{3K}{16\pi}}\frac{1}{\mu_t}\frac{r}{x}$$

The coefficient B may be expressed in terms of the coefficient A as

$$B = \sqrt{\frac{3K}{4\pi}}A \qquad \text{(III-28)}$$

The μ_t is the turbulent viscosity which - according to the presentations of Schlichting - remains constant over the entire jet. The quantity K is the mass momentum as defined by the relation

$$K = 2\pi \int_0^\infty u^2 r\,dr \quad , \tag{III-29}$$

In the development of the equations of motion for free jets, the pressure drop in the axial direction downstream of the orifice is assumed negligible. Therefore, the mass momentum is also assumed to be a constant in this area. Since the velocity distribution in the orifice is assumed constant and equal to $\bar{u}$, it is convenient to evaluate the mass momentum at this point by

$$K = 2\pi \int_0^{R_o} \bar{u}^2 r\,dr = \pi R_o^2 \bar{u}^2 \quad , \tag{III-30}$$

Since the flow rate is given by

$$\dot{q} = \pi R_o^2 \bar{u} \tag{III-31}$$

the mass momentum is expressed as a function of the flow rate by

$$K = \frac{1}{\pi}\left(\frac{\dot{q}^2}{R_o^2}\right) = C_1 \dot{q}^2 \quad . \tag{III-32}$$

The velocity distribution for a circular jet is shown in Figure 13 based on Schlichting's relations. The relations presented by Schlichting for the description of the phenomena downstream of a circular and plane orifice are representative of those in the literature survey. Several authors present identical relations and others present similar relations. The expressions presented above will be chosen as those to be used in determining the viscous dissipation of energy in free turbulent jets for the fully-developed jet.

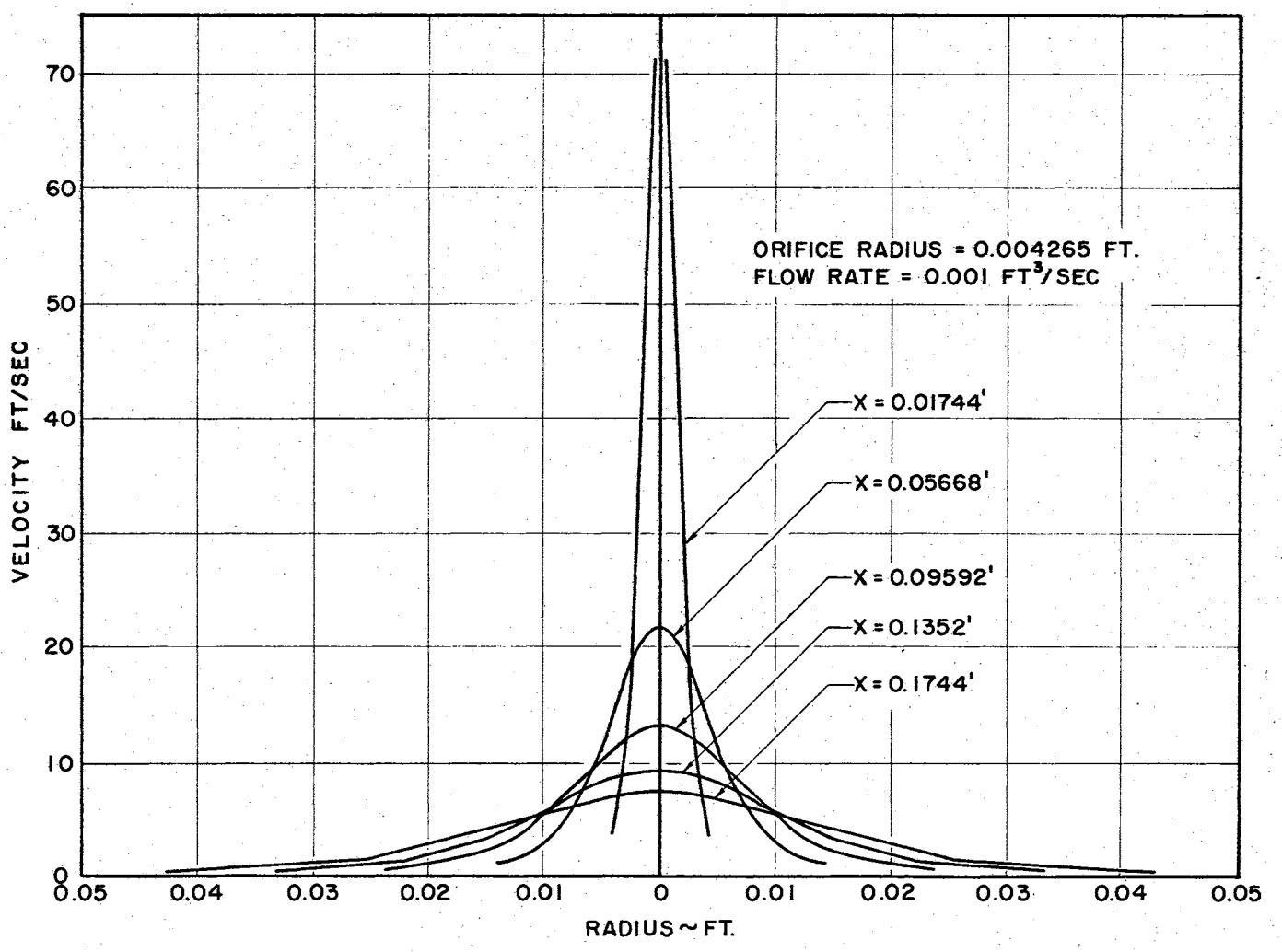

FIGURE 13

SCHLICHTING'S VELOCITY DISTRIBUTION IN AN AXIALLY SYMMETRICAL JET

CHAPTER IV

THE ENERGY EQUATION INCLUDING VISCOUS DISSIPATION

The general energy equation is developed by performing an energy balance on a small element of fluid undergoing change. Appendix B presents a summary of the forms of the general energy equation. Solving the resulting partial differential equation provides information concerning the distribution of energy in the moving fluid.

There are four basic assumptions which predominate in the literature in obtaining solutions of the general energy equation:

1. Simplification of the specific flow situation may be accomplished by reducing the flow pattern to a two-dimensional pattern or even in special cases to a one-dimensional pattern.

2. The similarity principle is assumed valid in establishing a relationship between the temperature and velocity distributions. This technique is valid for a fluid such as air where the Prandtl Number is approximately unity. However, for a fluid which has a Prandtl Number significantly different from unity, the temperature profile is no longer similar to the velocity profile.

3. Relations used in solving the energy equation usually consider all properties of the fluid to be constant and a Newtonian fluid is specified. A Newtonian fluid is one which obeys the relation

$$\tau = -\mu \left(\frac{\partial u}{\partial r} \right) \qquad \text{(IV-1)}$$

Many fluids can be considered to be Newtonian fluids.

There has been some attempt at solving the energy equation for variable viscosity for the simple case of flow in a pipe. For

example, Wilson and Mitchell (26) consider the dependence of viscosity on temperature using the relation

$$\mu = \mu_0 e^{-\beta T} \qquad \text{(IV-2)}$$

Toor (27) presents a solution for both the Newtonian and non-Newtonian fluids obeying the relation

$$\frac{\partial u}{\partial r} = A(\tau)^{N-1} \qquad \text{(IV-3)}$$

where n = 2 for the Newtonian case.

4. Most solutions of the energy equation assume the viscous dissipation of energy to be insignificant. The viscous action may be a significant factor where a highly viscous fluid is involved and where there is capillary flow. Brinkman (28) presents an analysis for capillary flow. An energy balance technique is employed and a term for the viscous dissipation is included. The analysis considers constant fluid properties and a Poiseille velocity distribution.

   Wilson and Mitchell (26) analyze the flows by considering a special fluid element with viscous action at the fluid-wall interface. Several types of laminar flow situations are considered - first, flow between stationary plates; second, flow between one stationary plate and one moving plate; and third, flow in a circular tube.

   Several presentations solve special cases of internal "heat generation" without specifying the type of "heat generation." Sparrow and Seigel (29) present several types of heat sources for laminar flow. A uniform constant heat source, a parabolic radial source, and an arbitrary radial and longitudinal source are developed. Tao (30) develops a highly mathematical approach to laminar flow with internal heat source. However, these references do not discuss how the viscous dissipation of energy can be accurately evaluated and substituted into these solutions.

For the study of the circular free jet, the cylindrical coordinate system applies. For the two-dimensional case, i.e., disregarding all terms involving angular notation, the energy equation is

$$\rho c_v\left[\frac{\partial T}{\partial t}+v\frac{\partial T}{\partial r}+u\frac{\partial T}{\partial x}\right]=k\left[\frac{1}{r}\frac{\partial}{\partial r}\left(r\frac{\partial T}{\partial r}\right)+\frac{\partial^2 T}{\partial x^2}\right]+\mu\phi \qquad \text{(IV-4)}$$

The following assumptions are imposed:

a. ρ, c_v, k, and μ are constant,

b. the fluid is a Newtonian fluid,

c. the two-dimensional case is specified;

and stipulating the further limitations:

d. steady state operation is considered,

e. conduction in the axial direction is small compared with conduction in the radial direction.

The energy equation reduces to

$$v\frac{\partial T}{\partial r}+u\frac{\partial T}{\partial x}=\frac{k}{\rho c_v}\frac{1}{r}\frac{\partial}{\partial r}\left(r\frac{\partial T}{\partial r}\right)+\frac{\mu}{\rho c_v}\phi \qquad \text{(IV-5)}$$

And, in a similar manner, the energy equation reduces to

$$v_1\frac{\partial T_1}{\partial y}+u_1\frac{\partial T_1}{\partial x}=\frac{k}{\rho c_v}\frac{\partial^2 T_1}{\partial y^2}+\frac{\mu}{\rho c_v}\phi_1 \qquad \text{(IV-6)}$$

for the two-dimensional plane jet in the rectangular coordinate system notation. In each of the above equations describing the energy processes, the dependent variables are:

Circular Jet	Plane Jet	
$T = T(r,x)$	$T_1 = T_1(y,x)$	
$u = u(r,x)$	$u_1 = u_1(y,x)$	
$v = v(r,x)$	$v_1 = v_1(y,x)$	(IV-7)
$\phi = \phi(r,x)$	$\phi_1 = \phi_1(y,x)$.	

The equations may be written in the general form as

$$A(x,y)\,u_x + B(x,y)\,u_y = u_{xx} + F(x,y)\,. \qquad \text{(IV-8)}$$

The difficulty in applying the general equation results not from the physical limitations in the derivation of the equation but rather from the limitation of solving the resulting partial differential equation. Since the solution of the partial differential equation is not immediately obvious, a comprehensive literature survey was conducted to ascertain if this type of equation had been solved previously. No solution was found.

The solution for the case of the free jet is complicated by the fact that the boundaries of the flow pattern are functions of the independent variables. Since a solution for the partial differential equation for the free jet with viscous dissipation considerations does not exist, alternate approaches may establish the distribution of energy in the free jet. This additional criterion is established by the evaluation of the viscous dissipation function as suggested by Lamb (1).

CHAPTER V

THE VISCOUS DISSIPATION OF ENERGY IN A FULLY-DEVELOPED TWO-DIMENSIONAL CIRCULAR JET

The flow chamber downstream of a restriction is shown in Figure 14. The jet is assumed to originate from a point source located upstream of the mouth of the orifice. The radius of the orifice is R_o and the radius of the downstream chamber is R. As the jet of fluid expands in a linear manner, the outer boundary of the jet increases according to the expression

$$R_x = R\frac{x}{L} \quad , \tag{V-1}$$

The relations describing the axial velocity in the circular jet as presented by Schlichting (25) are valid in the range where the velocity profiles are similar in nature as bounded by the region

$$x_1 \leq x \leq L \tag{V-2}$$

where x_1 is specified to be

$$x_1 = x_o + 16R_o \quad . \tag{V-3}$$

When the boundaries of the jet approach the wall of the downstream chamber at X = L, the free turbulent flow analysis is no longer valid. The viscous dissipation of energy is neglected downstream of this point. The axial velocity is given as

$$u = \frac{B}{x} f(\eta) = \frac{B}{x}\left(1 + \frac{1}{4}\eta^2\right)^{-2} \tag{V-4}$$

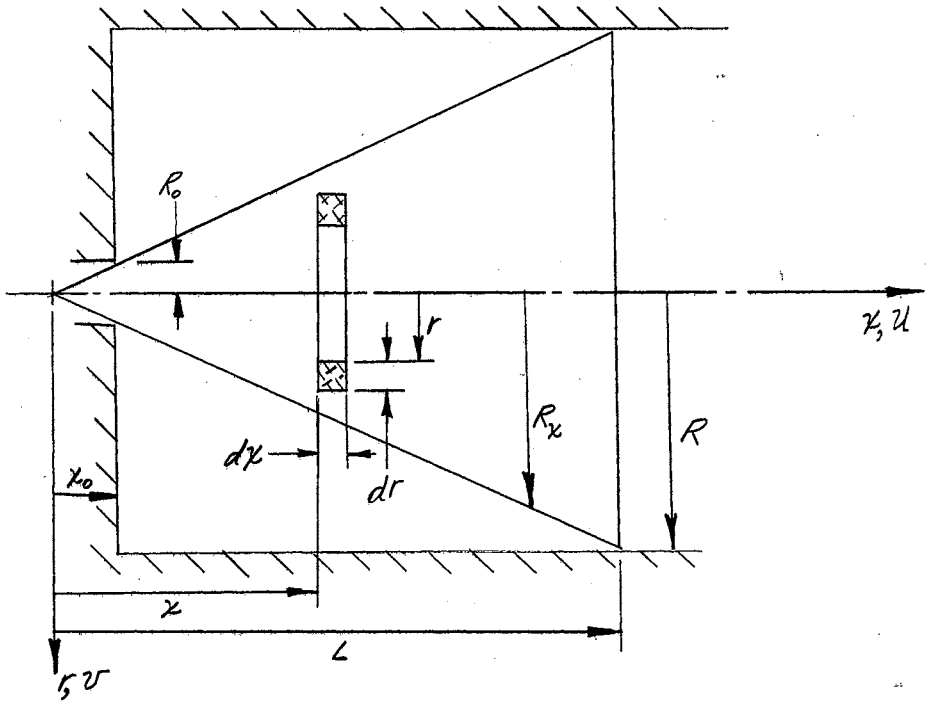

Figure 14. Mathematical Model for Free Jet Analysis

where the dimensionless parameter η is defined by

$$\eta = \frac{Ar}{x} . \tag{V-5}$$

The viscous dissipation of energy can be evaluated from the simplified expression

$$q_f = \mu \iiint_V \left[\left(\frac{\partial u}{\partial r}\right)^2 + 2\left(\frac{\partial u}{\partial x}\right)^2 \right] dV . \tag{V-6}$$

The volume element is of the ring form, and its volume is

$$dV = 2\pi r\, dr\, dx . \tag{V-7}$$

In order to evaluate the integral after substitutions, the variables will be expressed in terms of the two independent variables x and r rather than the dimensionless parameter η. This is necessary since the integrand cannot be expressed entirely in terms of η.

The following quantities will aid in the performing of the differentiating process:

$$\frac{\partial \eta}{\partial x} = -\frac{\eta}{x} \tag{V-8}$$

$$\frac{\partial \eta}{\partial r} = \frac{A}{x} \tag{V-9}$$

Taking derivatives of the axial velocity first with respect to the radial coordinate gives

$$\frac{\partial u}{\partial r} = \frac{AB}{x^2} f'(\eta) \tag{V-10}$$

and then with respect to the axial coordinate gives

$$\frac{\partial u}{\partial x} = -\frac{B}{x^2} f(\eta) - \frac{B}{x^2} \eta f'(\eta) \tag{V-11}$$

Squaring these quantities and substituting into Equation (V-6) yields

$$\mathcal{D}_f = \mu_e \iiint_V \left\{ \frac{2B^2}{x^4} \left[f^2(\eta) + 2\eta f(\eta) f'(\eta) + \eta^2 f'^2(\eta) \right] + \frac{A^2 B^2}{x^4} f'^2(\eta) \right\} dV \tag{V-12}$$

This equation is integrated mathematically in Appendix C. The results of this evaluation show that the increase in the energy of the fluid is proportional to the inverse-square of the axial distance. Upon integration, the numerical value of the viscous dissipation of energy is expressed as

$$\mathcal{D}_f = \mu_e \pi \frac{B^2}{A^2} \left[1.33 + 0.792 A^2 \right] \left(\frac{1}{x_1} - \frac{1}{L} \right) \tag{V-13}$$

$$= C \left(\frac{1}{x_1} - \frac{1}{L} \right) \tag{V-14}$$

Referring to the definitions expressed by Schlichting concerning the velocities in the circular jet, it can be shown that

$$\frac{B^2}{A^2} = \frac{3}{4\pi} K \tag{V-15}$$

where $K = \frac{1}{\pi}(\dot{q}/R_o)^2$ and since $\mu_t = \rho \nu_t$ then the expression becomes

$$q_f = \rho \nu_t (\dot{q}/R_o)^2 (1.0 + 0.593 A^2)\left(\frac{1}{x_1} - \frac{1}{L}\right). \qquad \text{(V-16)}$$

Schlichting states that the velocity expressions are valid for either the laminar or turbulent jet with the proper value for the kinematic viscosity in each case; therefore, the above relation describes each case. Since "A" is defined in Equation (III-27) and K is given in Equation (III-32), then

$$A^2 = \frac{3K}{16\pi} \frac{1}{\nu^2} (\dot{q}/R_o)^2$$

However, in the laminar jet, the kinematic viscosity is a constant so that the viscous dissipation of energy may be written as

$$q_f = \rho \nu (\dot{q}/R_o)^2 \left[1.0 + 0.593 \left(\frac{3}{16\pi}\right)^2 \frac{1}{\nu^2} (\dot{q}/R_o)^2\right]\left(\frac{1}{x_1} - \frac{1}{L}\right) \qquad \text{(V-17)}$$

$$= \left[C_1 \dot{q}^2 + C_2 \dot{q}^4\right]\left(\frac{1}{x_1} - \frac{1}{L}\right) \qquad \text{(V-18)}$$

According to this relation, the viscous dissipation of energy in the laminar free jet is a function of the flow rate raised to the second and fourth powers.

In the turbulent jet, the kinematic viscosity is not a constant. According to Schlichting, the eddy viscosity is a function of the mass momentum as expressed by

$$\frac{\sqrt{K}}{\nu_t} = a_1 = \text{CONSTANT} \qquad \text{(V-19)}$$

Therefore, in the turbulent free jet, the viscous dissipation of energy

is given by

$$g_f = \rho \nu_t \left(\dot{g}/K_o\right)^2 \left(1.00 + 0.593A^2\right)\left(\frac{1}{x_1} - \frac{1}{L}\right) . \qquad \text{(V-20)}$$

Using Equation (V-19) along with the definition of mass momentum, Equation (III-32), Equation (V-20) reduces to

$$g_f = \frac{\rho}{\sqrt{\pi}} \frac{1}{a_1} \left(\dot{g}/K_o\right)^3 \left(1.00 + 0.593A^2\right)\left(\frac{1}{x_1} - \frac{1}{L}\right) \qquad \text{(V-21)}$$

so that in this case the viscous dissipation terms are related to the cube of the flow rate.

The fact that the eddy viscosity in the turbulent range is a variable makes it useful as a method of identifying the type of jet present under various flow conditions. A possible criterion for the distinction may be the point where the eddy viscosity is larger than the kinematic viscosity

$$\nu_t \geq \nu , \qquad \text{(V-22)}$$

so that a relation may be found in terms of the mass momentum

$$\sqrt{K} \geq \text{CONSTANT} \qquad \text{(V-23)}$$

or flow rate and orifice opening according to

$$\frac{\dot{g}}{K_o} \geq \text{CONSTANT} . \qquad \text{(V-24)}$$

An interesting point concerning the transition between the laminar and turbulent jet is that a transition zone is present due to the change in the type of flow. A discontinuity is apparent in the velocity relations as well as in the viscous dissipation relations. For example, for the laminar circular jet, the velocity distribution is expressed as

$$u = \frac{C_1 \dot{q}^2}{x}\left(1 + C_2 \dot{q}^2 \frac{r^2}{x^2}\right)^{-2} \tag{V-25}$$

and the corresponding dissipated energy is

$$q_f = \left(C_3 \dot{q}^2 + C_4 \dot{q}^4\right)\left(\frac{1}{x_1} - \frac{1}{L}\right) .$$

For the turbulent jet where ν_t is a function of flow rate,

$$u = \frac{C_4 \dot{q}}{x}\left(1 + C_5 \frac{r^2}{x^2}\right)^{-2} \tag{V-26}$$

and

$$q_f = C_3 \dot{q}^3 \left(\frac{1}{x_1} - \frac{1}{L}\right) . \tag{V-27}$$

Therefore, since the influence of flow rate on u and q_f undergoes a change in the transition from laminar to turbulent flow regimes, a transition zone must be present.

As a result of performing the analytical evaluation of the viscous dissipation of energy, it was found that the term which contributed to nearly the entire numerical value was the term representing $(\partial u/\partial r)$. From the previous evaluation, the results show the increase in the energy level of the fluid as a function of the axial coordinate, but the results do not describe the behavior of the process as a function of the radial coordinate. Therefore, another expression may be developed to provide this information. In order to maintain simplicity where possible, only those terms representing the $(\partial u/\partial r)$ contribution will be considered. Therefore, the viscous dissipation of energy for an element of fluid from Equation (V-12) is given as

$$\begin{aligned} dq_f &= 2\pi A^2 B^2 \mu_t \frac{r}{x^4}\left(f'(\eta)\right)^2 dr\,dx \\ &= 2\pi A^2 B^2 \mu_t \frac{C^3}{x^6}\left(1 + \frac{A^2 r^2}{4x^2}\right)^{-6} dr\,dx \end{aligned} \tag{V-28}$$

which may be simplified to

$$dq_A = \frac{3\sqrt{3}}{8\pi^2}\rho A^5\left(\frac{\dot{q}}{k_0}\right)^3\frac{r^3}{x^6}\left(1+\frac{A^2r^2}{4x^2}\right)^{-6}dr\,dx \qquad \text{(V-29)}$$

This expression is valid between the limits

$$x_1 = x_0 + 16R_0 = \left(\frac{A}{\eta_0}+16\right)R_0 \leq x \leq L$$

$$0 \leq r \leq \eta_0 x/A$$

The above expression and the corresponding limits or boundaries are used in a computer evaluation technique to determine the distributions of the viscous dissipation of energy. These reults are presented in a later section.

CHAPTER VI

THE VISCOUS DISSIPATION OF ENERGY IN REGIONS A AND B

The expressions describing free turbulent flows are valid for distances greater than eight diameters downstream of the orifice; in the vicinity of the orifice the velocity profiles are not similar in nature but are in the developing stage. The fluid discharges from the face of the orifice with a constant velocity $\bar{u}$ and further downstream enters the fully-developed region with an established profile. In the case of duct flows, this phenomenon is called the "entrance region." A similar nomenclature for the jet expansion process will be designated as the "exit region."

The exit region is important in the study of the viscous dissipation phenomena. This importance may stem from two facts. First the quantitative contribution of the viscous dissipation of energy in the exit region is a significant portion of the total viscous dissipation of energy in the entire expansion process. Second, when the characteristic dimension of the opening is not much smaller than the characteristic dimension of the downstream chamber, the exit region may describe the entire expansion process. Considering these facts, the viscous dissipation function is evaluated in the exit regions.

According to Kuethe (12) the exit region is actually comprised of two separate regions. In the region nearest the orifice, the core of the fluid diminishes to a point as the mixing region enlarges. The

velocity in the core is a constant $\bar{u}$. In the second region, the core of the fluid has disappeared and the entire jet is the mixing region.

Squire and Trouncer (19) present an analysis to describe the velocity distributions in these exit regions for the case of the orifice. The solutions are fitted at the interface through momentum and velocity considerations. In the region nearest the orifice, Region A, the velocity distribution is

$$u = \frac{1}{2}\bar{u}\left[1 - \cos\left(\pi \frac{r_o - r}{r_o - r_1}\right)\right]. \qquad \text{(VI-1)}$$

The quantities r_o and r_1 designate the locations from the axis of the edge of the jet and the edge of the core. In the second region, Region B, the entire jet is the mixing region and the velocity distribution is

$$u = \frac{1}{2}u_x\left(1 + \cos\frac{\pi r}{r_o}\right). \qquad \text{(VI-2)}$$

These velocity distributions are illustrated in Figures 15 and 16. The center-line velocity in Region B is a function of the axial coordinate as shown in Figure 17. The boundaries of the jet and core are also functions of the axial coordinate as shown in Figure 18. Since the velocity distributions are to be employed in the analytical evaluation of the viscous dissipation function, the variations of r_o, r_1, and u_x will be assumed to be linear and given analytically for Region A as

$$r_o = R_o + 33.7\,c^2\chi \qquad \text{(VI-3)}$$

$$r_1 = R_o - 22.4\,c^2\chi \qquad \text{(VI-4)}$$

and for Region B as:

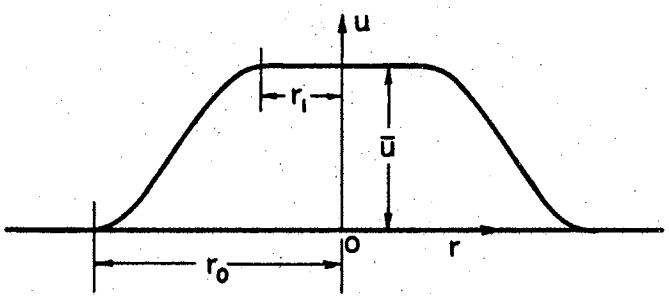

FIGURE 15

VELOCITY DISTRIBUTION FOR EXIT REGION A IN A CIRCULAR JET

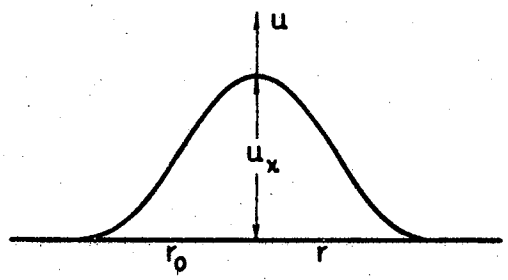

FIGURE 16

VELOCITY DISTRIBUTION FOR EXIT REGION B IN A CIRCULAR JET

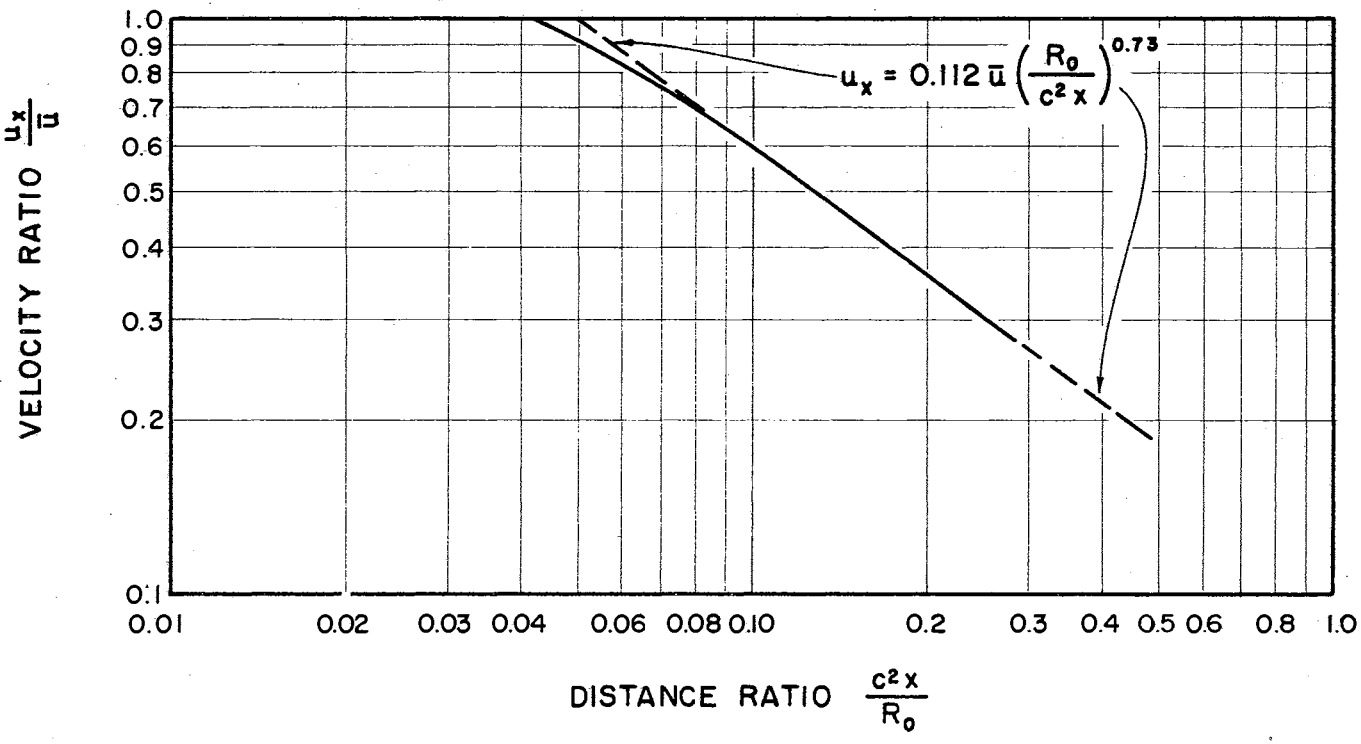

FIGURE 17

CENTER LINE VELOCITY IN EXIT REGION B

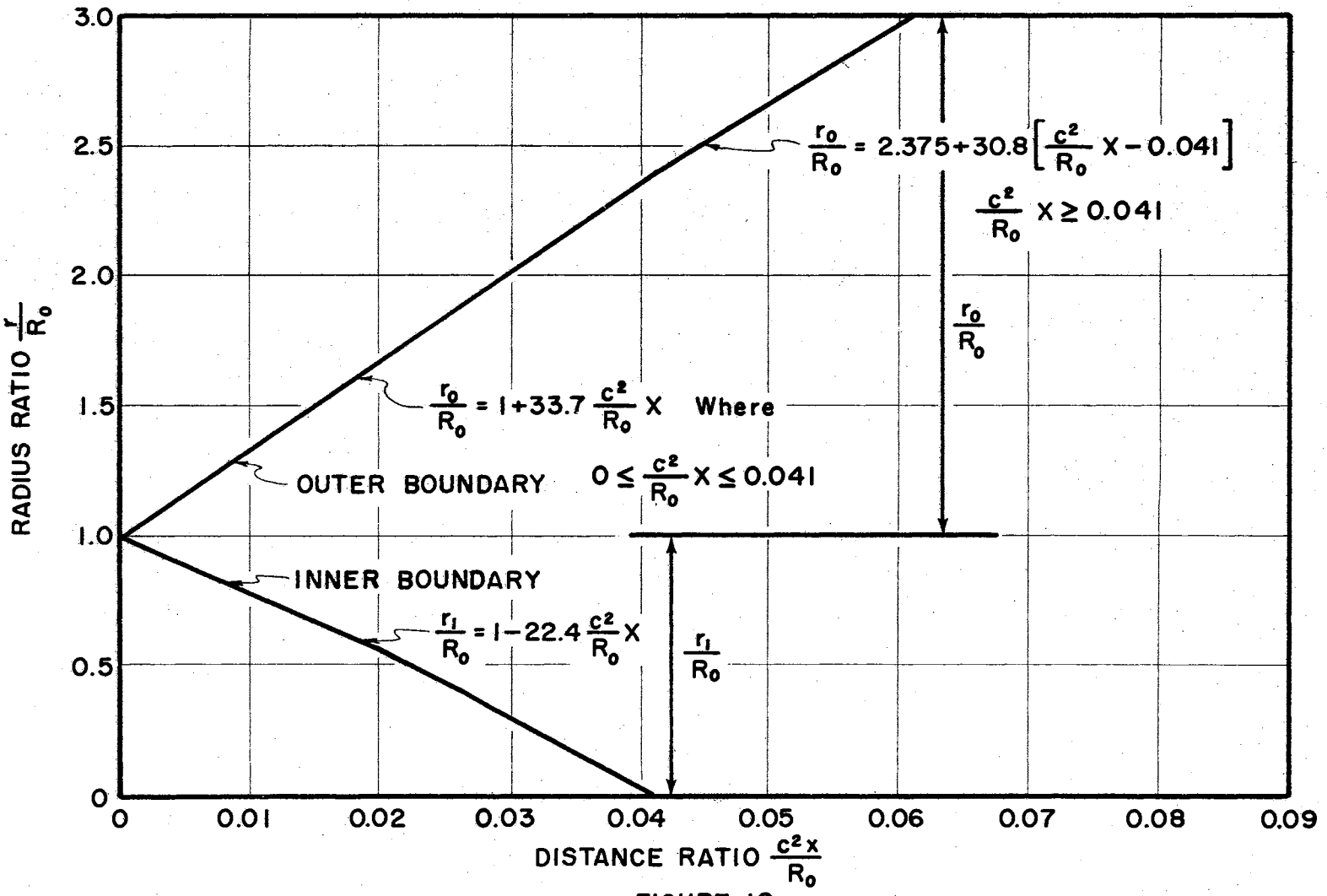

FIGURE 18

BOUNDARIES OF THE FREE JET IN THE EXIT REGIONS

$$r_o = 1.112 R_o + 30.8 c^2 x \qquad \text{(VI-5)}$$

$$r_i = R_o - 22.4 c^2 x \qquad \text{(VI-6)}$$

For both exit regions, the axial coordinate is measured from the face of the orifice. The quantity c^2 is a parameter related to the mixing length ℓ^2 by the expressions:

$$\ell^2 = c^2 (r_o - r_i)^2 \qquad \text{(Region A)} \qquad \text{(VI-7)}$$

$$\ell^2 = c^2 r_o^2 \qquad \text{(Region B)} \qquad \text{(VI-8)}$$

which may be related to the shearing stress by

$$\tau = \ell^2 \left(\frac{\partial u}{\partial r}\right)^2 \qquad \text{(VI-9)}$$

In evaluating the viscous dissipation of energy in these exit regions, it is necessary for the turbulent viscosity μ_t to remain under the integral sign since it is a variable. The general expression of the viscous dissipation of energy for the simplified cases is

$$\phi_f = \iiint_V \mu_t \left[\left(\frac{\partial u}{\partial r}\right)^2 + 2\left(\frac{\partial u}{\partial x}\right)^2\right] dV \qquad \text{(VI-10)}$$

EXIT REGION A

In order to evaluate the viscous dissipation of energy, it is necessary to evaluate the partial derivatives of the velocity distributions for substitution purposes. Using the velocity distributions suggested by Squire and Trouncer (19), the axial velocity in Region A is

$$u = \frac{\bar{u}}{2}\left[1 - \cos\left(\pi \frac{r_o - r}{r_o - r_i}\right)\right] \qquad \text{(VI-11)}$$

Taking the partial derivative with respect to the radial coordinate yields

$$\frac{\partial u}{\partial r} = \frac{\bar{u}}{2} \sin\left(\pi \frac{r_o - r}{r_o - r_i}\right) \frac{\partial}{\partial r}\left(\pi \frac{r_o - r}{r_o - r_i}\right)$$

$$= \frac{\bar{u}}{2} \sin\left(\pi \frac{r_o - r}{r_o - r_i}\right) \frac{\pi}{r_i - r_o}$$

$$= -\frac{\pi}{2} \bar{u} (r_o - r_i)^{-1} \sin\left(\pi \frac{r_o - r}{r_o - r_i}\right) \qquad \text{(VI-12)}$$

Taking the partial derivative with respect to the axial coordinate is

$$\frac{\partial u}{\partial x} = \frac{\bar{u}}{2} \sin\left(\pi \frac{r_o - r}{r_o - r_i}\right) \frac{\partial}{\partial x}\left(\pi \frac{r_o - r}{r_o - r_i}\right) \qquad \text{(VI-13)}$$

It has been previously pointed out that r_o and r_1 are functions of x only; therefore,

$$\frac{\partial}{\partial x}\left(\frac{r_o - r}{r_o - r_i}\right) = \left[(r_o - r_i)\frac{dr_o}{dx} - (r_o - r_i)\frac{d}{dx}(r_o - r)\right](r_o - r_i)^{-2}$$

and upon simplification

$$\frac{\partial}{\partial x}\left(\frac{r_o - r}{r_o - r_i}\right) = \frac{(r - r_i)\frac{dr_o}{dx} + (r_o - r)\frac{dr_i}{dx}}{(r_o - r_i)^2} \qquad \text{(VI-14)}$$

Substitution of this result into the partial derivative gives

$$\frac{\partial u}{\partial x} = \frac{\pi}{2} \bar{u} \sin\left(\pi \frac{r_o - r}{r_o - r_i}\right)\left[(r - r_i)\frac{dr_o}{dx} + (r_o - r)\frac{dr_i}{dx}\right](r_o - r_i)^{-2} \qquad \text{(VI-15)}$$

and squaring produces

$$\left(\frac{\partial u}{\partial x}\right)^2 = \left(\frac{\partial u}{\partial r}\right)^2 (r_o - r_i)^{-2}\left[(r - r_i)\frac{dr_o}{dx} + (r_o - r)\frac{dr_i}{dx}\right] \qquad \text{(VI-16)}$$

which expands to

$$\left(\frac{\partial u}{\partial x}\right)^2 = \left(\frac{\partial u}{\partial r}\right)^2 (r_0 - r_1)^{-2} \left\{ (r^2 - 2rr_1 + r_1^2)\left(\frac{dr_0}{dx}\right)^2 + (2rr_0 - 2r^2 - 2r_1 r_0 + 2r_1 r)\frac{dr_0}{dx}\frac{dr_1}{dx} + (r_0^2 - 2r_0 r + r^2)\left(\frac{dr_1}{dx}\right)^2 \right\} \tag{VI-17}$$

and rearranging terms

$$\left(\frac{\partial u}{\partial x}\right)^2 = \left(\frac{\partial u}{\partial r}\right)^2 (r_0 - r_1)^{-2} \left\{ r^2\left(\frac{dr_0}{dx} - \frac{dr_1}{dx}\right)^2 + 2r\left(\frac{dr_0}{dx} - \frac{dr_1}{dx}\right)\left(r_0\frac{dr_1}{dx} - r_1\frac{dr_0}{dx}\right) + \left(r_1\frac{dr_0}{dx} - r_0\frac{dr_1}{dx}\right)^2 \right\}. \tag{VI-18}$$

In order to simplify the expression, the following substitutions will be made:

$$F(x) = \left(\frac{dr_0}{dx} - \frac{dr_1}{dx}\right)^2 \tag{VI-19}$$

$$F_1(x) = \left(\frac{dr_0}{dx} - \frac{dr_1}{dx}\right)\left(r_0\frac{dr_1}{dx} - r_1\frac{dr_0}{dx}\right) \tag{VI-20}$$

$$F_2(x) = \left(r_1\frac{dr_0}{dx} - r_0\frac{dr_1}{dx}\right) \tag{VI-21}$$

The general expression for the viscous dissipation of energy may now be written as

$$q_f = \iiint_V \mu_t \left\{ \left(\frac{\partial u}{\partial r}\right)^2 + 2\left(\frac{\partial u}{\partial r}\right)^2 (r_0 - r_1)^{-2} \left[r^2 F(x) + 2r F_1(x) + F_2(x) \right] \right\} dV \tag{VI-22}$$

and since the turbulent viscosity is

$$\mu_t = \rho \ell^2 \left(\frac{\partial u}{\partial r}\right) = \rho \kappa^2 (r_0 - r_1)^2 \left(\frac{\partial u}{\partial r}\right) \tag{VI-23}$$

then

$$g_t = \iiint_V \rho c^2 (r_0 - r_1)^2 \left(\frac{\partial u}{\partial r}\right)^3 \left[1 + \frac{2}{(r_0 - r_1)^2}\left\{r^2 F(x) + 2r F_1(x) + F_2(x)\right\}\right] dV$$

$$= \rho c^2 \frac{\pi^3}{8} \bar{u}^3 \iiint_V \frac{1}{(r_0 - r_1)} \sin^3\left(\pi \frac{r_0 - r}{r_0 - r_1}\right)\left[1 + \frac{2r^2 F(x)}{(r_0 - r_1)^2}\right.$$

$$\left. + \frac{4r F_1(x)}{(r_0 - r_1)^2} + \frac{2F_2(x)}{(r_0 - r_1)^2}\right] dV . \qquad \text{(VI-24)}$$

The element of volume is given as a ring expressed by

$$dV = 2\pi r\, dr\, dx \qquad \text{(VI-25)}$$

then

$$g_t = \rho c^2 \frac{\pi^4}{4} \bar{u}^3 \int_{x=0}^{x=x_A} \int_{r=r_1}^{r=r_0} \frac{1}{(r_0 - r_1)} \sin^3\left(\pi \frac{r_0 - r}{r_0 - r_1}\right)\left[1 + \frac{2r^2 F(x)}{(r_0 - r_1)^2}\right.$$

$$\left. + \frac{4r F_1(x)}{(r_0 - r_1)^2} + \frac{2F_2(x)}{(r_0 - r_1)^2}\right] r\, dr\, dx . \qquad \text{(VI-26)}$$

In Region A the boundaries of the jet and of the core are

$$r_0 = a_2 + b_2 x \qquad \text{(VI-27)}$$

$$r_1 = a_1 + b_1 x \qquad \text{(VI-28)}$$

and the derivative of these expressions is:

$$\frac{dr_0}{dx} = b_2 \; ; \; \frac{dr_1}{dx} = b_1 . \qquad \text{(VI-29)}$$

The functions of x defined earlier become for these boundaries:

$$F(x) = (b_2 - b_1)^2 = \text{CONSTANT}$$

$$F_1(x) = (b_2 - b_1)(b_1 a_2 - b_2 a_1) = \text{CONSTANT}$$

$$F_2(x) = 2(b_1 a_2 - b_2 a_1) = \text{CONSTANT}.$$

Using the following values of the constants from Figure 18:

$$a_1 = R_o \qquad a_2 = R_o$$

$$b_1 = 33.1c^2 \qquad b_2 = -22.4c^2$$

and Squire and Trouncer suggest a value of $c^2 = .0067$; the functions of x become:

$$F(x) = 0.1415 \tag{VI-30}$$

$$F_1(x) = -0.1415 R_o \tag{VI-31}$$

$$F_2(x) = 0.1415 R_o^2. \tag{VI-32}$$

Therefore, the expression for the energy is now

$$\mathcal{J}_p = 0.00527 \rho \dot{q}^3 / R_o^6 \int_{x=0}^{x=x_A} \int_{r=r_1}^{r=r_o} \frac{1}{(r_o - r_1)} \sin^3\left(\pi \frac{r_o - r}{r_o - r_1}\right) \Bigg[1 + 0.282 \frac{r^2}{(r_o - r_1)^2} - 0.564 \frac{r R_o}{(r_o - r_1)^2} + 0.282 \frac{R_o^2}{(r_o - r_1)^2} \Bigg] r \, dr \, dx. \tag{VI-33}$$

This equation represents the viscous dissipation of energy in Exit Region A. This relation will be used in determining the distribution of the viscous dissipation of energy across the jet in the first region.

REGION B

For Region B, Squire and Trouncer (19) give the axial velocity as

$$u = \frac{u_x}{2}\left(1 + \cos\frac{\pi r}{r_o}\right) \tag{VI-34}$$

where u_x and r_o are functions of the axial coordinate only. The partial derivatives must also be evaluated for substitution purposes. Taking the partial derivative with respect to the radial coordinate gives

$$\frac{\partial u}{\partial r} = -\frac{u_x}{2}\sin\left(\frac{\pi r}{r_o}\right)\frac{\partial}{\partial r}\left(\pi\frac{r}{r_o}\right) = -\frac{\pi}{2r_o}u_x\sin\left(\frac{\pi r}{r_o}\right) \tag{VI-35}$$

and with respect to the axial coordinate gives

$$\begin{aligned}\frac{\partial u}{\partial x} &= \frac{u_x}{2}\frac{\partial}{\partial x}\left(1+\cos\frac{\pi r}{r_o}\right) + \frac{1}{2}\left(1+\cos\frac{\pi r}{r_o}\right)\frac{du_x}{dx}\\ &= -\frac{u_x}{2}\sin\left(\frac{\pi r}{r_o}\right)\frac{\partial}{\partial x}\left(\pi\frac{r}{r_o}\right) + \frac{1}{2}\left(1+\cos\frac{\pi r}{r_o}\right)\frac{du_x}{dx}\\ &= \frac{u_x}{2}\frac{\pi r}{r_o^2}\sin\left(\frac{\pi r}{r_o}\right)\frac{dr_o}{dx} + \frac{1}{2}\left(1+\cos\frac{\pi r}{r_o}\right)\frac{du_x}{dx}\end{aligned} \tag{VI-36}$$

Squaring this relation produces the expression

$$\begin{aligned}\left(\frac{\partial u}{\partial x}\right)^2 &= \frac{1}{4}\left\{u_x^2\frac{\pi^2 r^2}{r_o^4}\sin^2\left(\frac{\pi r}{r_o}\right) + \frac{2u_x\pi r}{r_o^2}\sin\left(\frac{\pi r}{r_o}\right)\left[1\right.\right.\\ &\quad \left.\left. + \cos\left(\frac{\pi r}{r_o}\right)\right]\frac{dr_o}{dx}\frac{du_x}{dx} + \left[1+2\cos\left(\frac{\pi r}{r_o}\right)+\cos^2\left(\frac{\pi r}{r_o}\right)\right]\left(\frac{du_x}{dx}\right)^2\right\}\\ &= \frac{1}{4}\left\{\left(\frac{\partial u}{\partial r}\right)^2\frac{r^2}{r_o^2}\left(\frac{dr_o}{dx}\right)^2 + \frac{2u_x}{r_o^2}\sin\left(\frac{\pi r}{r_o}\right)\left[1+\cos\left(\frac{\pi r}{r_o}\right)\right]\frac{dr_o}{dx}\frac{du_x}{dx}\right.\\ &\quad \left. + \left[1+2\cos\frac{\pi r}{r_o}+\cos^2\frac{\pi r}{r_o}\right]\left(\frac{du_x}{dx}\right)^2\right\}.\end{aligned} \tag{VI-37}$$

Substituting the turbulent viscosity

$$\mu_t = \rho \ell^2 \left(\frac{\partial u}{\partial r}\right) = \rho c^2 r_o^2 \left(\frac{\partial u}{\partial r}\right) \tag{VI-38}$$

into the general expression for the energy gives

$$q_t = \rho c^2 \iiint_V r_o^2 \left[\left(\frac{\partial u}{\partial r}\right)^3 + 2\left(\frac{\partial u}{\partial r}\right)\left(\frac{\partial u}{\partial x}\right)^2\right] dV \tag{VI-39}$$

$$= \frac{\rho c^2}{8} \iiint_V \left\{ \frac{\pi^3 u_x^3}{r_o} \sin^3 \frac{\pi r}{r_o} + 2 r_o \pi u_x \sin\left(\frac{\pi r}{r_o}\right)\left[\left(\frac{\partial u}{\partial r}\right)^2 \frac{r^2}{r_o^2}\left(\frac{dr_o}{dx}\right)^2 \right.\right.$$

$$+ 2\pi u_x \frac{r}{r_o^2} \sin\left(\pi \frac{r}{r_o}\right)\left(1 + \cos\frac{\pi r}{r_o}\right)\frac{dr_o}{dx}\frac{du_x}{dx} + \left[1 + 2\cos\frac{\pi r}{r_o}\right.$$

$$\left.\left. + \cos^2\frac{\pi r}{r_o}\right]\left(\frac{du_x}{dx}\right)^2\right\} dV , \tag{VI-40}$$

Since r_o and u_x are variables as described by

$$r_o = 1.112 R_o + 30.8 c^2 x \tag{VI-41}$$

$$u_x = 0.112 \bar{u} (R_o/c^2)^{.73} x^{-.73} \tag{VI-42}$$

again $c^2 = .0067$; then, the derivative is simply

$$\frac{dr_o}{dx} = 0.206$$

$$\frac{du_x}{dx} = -1.0 R_o^{-1.27} x^{-1.73} \dot{g} , \tag{VI-43}$$

Performing these substitutions into the energy expression gives

$$q_f = -\frac{\pi C_c^2 \rho}{4} \int_{z=z_4}^{z=z_1} \int_{r=0}^{r=r_0} \left\{ \frac{\pi^2 u_x^3}{r_0} \sin^3\left(\frac{\pi r}{r_0}\right)\left[1 + \frac{2r^2}{r_0^2}(0.206)^2\right] \right.$$

$$+ \frac{4 u_x^2 \pi r}{r_0} \sin^2\left(\frac{\pi r}{r_0}\right)\left[1 + \cos\left(\frac{\pi r}{r_0}\right)\right](0.206)(-1.0) R_0^{-1.27-1.73} z^{\dot{q}}$$

$$+ 2 r_0 u_x \sin\left(\frac{\pi r}{r_0}\right) R_0^{-2.54-3.46} z^{\dot{q}^2}\left[1 + 2\cos\left(\frac{\pi r}{r_0}\right)\right.$$

$$\left. \left. + \cos^2\left(\frac{\pi r}{r_0}\right)\right](1.0)^2 \right\} r\,dr\,dz$$

$$q_f = \frac{0.1328}{8} \rho \int_{z=z_4}^{z=z_1} \int_{r=0}^{r=r_0} \left\{ \frac{\pi^2 u_x^3}{r_0} \sin^3\left(\frac{\pi r}{r_0}\right)\left[1 + 0.0848 \frac{r^2}{r_0^2}\right] \right.$$

$$-0.824 u_x^2 \frac{\pi r}{r_0} \sin^2\left(\frac{\pi r}{r_0}\right) R_0^{-1.27-1.73} z^{\dot{q}}\left(1 + \cos\frac{\pi r}{r_0}\right)$$

$$+ 2 r_0 u_x \sin\left(\frac{\pi r}{r_0}\right) R_0^{-2.54-3.46} z^{\dot{q}^2}\left[1 + 2\cos\frac{\pi r}{r_0}\right.$$

$$\left. \left. + \cos^2\left(\frac{\pi r}{r_0}\right)\right] \right\} r\,dr\,dz \,. \qquad \text{(VI-44)}$$

The above expression represents the viscous dissipation of energy in Exit Region B. By evaluating this relation in the same manner as the relation for Exit Region A, the distribution of the viscous dissipation of energy is established.

CHAPTER VII

THE VISCOUS DISSIPATION OF ENERGY IN THE SIMPLIFIED TWO-DIMENSIONAL PLANE JET

The plane jet is the issuing of a fluid from a slit opening. Since the slit opening is so common an occurrence in practical application to fluid flow situations, it is necessary to establish the similarities between the plane jet and the circular jet with a change in the notation from r to y. The height of the slip opening is Y_o and the height of the chamber is Y. The jet is assumed to expand in a linear manner with the boundary of the jet being described by the relation

$$Y_x = Y\left(\frac{x}{L}\right) \tag{VII-1}$$

The velocity distributions for the plane jet are similar in shape to those of the circular jet except that the analytical relation is expressed in terms of hyperbolic functions. The axial velocity distribution is given as

$$u = \frac{B_1}{\sqrt{x}} f_1'(\eta) = \frac{B_1}{\sqrt{x}} \left(1 - \tanh^2 \eta\right) \tag{VII-2}$$

by Schlichting (25) and Pai (24). The dimensionless parameter η is given as

$$\eta = A_1 \frac{y}{x} \tag{VII-3}$$

The slit opening is assumed to be long and slender so that the problem may be considered two-dimensional in nature thus neglecting all terms in the z notation. The dissipation function is

$$\Phi = 2\left(\frac{\partial u}{\partial x}\right)^2 + \left(\frac{\partial u}{\partial y}\right)^2 \tag{VII-4}$$

for the simplified case ignoring all velocities in the y direction. The element of volume is a rectangular element given simply as

$$dV = dx\,dy\,. \tag{VII-5}$$

The viscous dissipation of energy is given by the relation

$$q_f = \mu_2 \int_{x=y_1}^{x=L} \int_{y=-y_2}^{y=y_2} \left[2\left(\frac{\partial u}{\partial x}\right)^2 + \left(\frac{\partial u}{\partial y}\right)^2\right] dy\,dx\,. \tag{VII-6}$$

In order to aid in the differentiation process, the following quantities will be useful:

$$\frac{\partial \eta}{\partial y} = \frac{A_1}{x} \tag{VII-7}$$

$$\frac{\partial \eta}{\partial x} = -\frac{\eta}{x}\,. \tag{VII-8}$$

Taking derivatives of the axial velocity with respect to the y direction yields

$$\frac{\partial u}{\partial y} = -\frac{2B_1}{\sqrt{x}} \tanh\eta\, \operatorname{sech}^2\eta \frac{\partial \eta}{\partial y} = -\frac{2A_1B_1}{x^{3/2}} \tanh\eta \operatorname{sech}^2\eta \tag{VII-9}$$

and with respect to the x direction gives

$$\frac{\partial u}{\partial x} = -\frac{2B_1}{\sqrt{x}} \tanh\eta \operatorname{sech}^2\eta \frac{\partial \eta}{\partial x} - \frac{B_1}{2}\left(1-\tanh^2\eta\right)x^{-3/2}$$

$$= \frac{2B_1}{x^{3/2}} \operatorname{sech}^2\eta \left(\eta \tanh\eta - \frac{1}{4}\right) \tag{VII-10}$$

Squaring the above relations and substituting into the energy relation produces the equation to be evaluated.

$$\dot{q}_f = \mu_t \int_{x=x_1}^{x=L} \int_{y=-Y_2}^{y=+Y_2} \left\{ \frac{8B_1^2}{x^3} \left[\frac{\eta^2 \sinh^2\eta}{\cosh^6\eta} - \frac{\eta \sinh\eta}{2\cosh^5\eta} + \frac{1}{16\cosh^4\eta} \right] + \frac{4A_1^2 B_1^2}{x^3} \frac{\sinh^2\eta}{\cosh^6\eta} \right\} dy\,dx. \tag{VII-11}$$

This expression is evaluated analytically in Appendix D. The resulting equation is

$$\begin{aligned} \dot{q}_f &= \mu_t \frac{B_1^2}{A_1^2} \left[0.3669 + 1.0712 A_1^2 \right] \left(\frac{1}{x_1} - \frac{1}{L} \right) \\ &= C \left(\frac{1}{x_1} - \frac{1}{L} \right). \end{aligned} \tag{VII-12}$$

From this analysis it is evident that the qualitative description of the plane jet issuing from a slit opening is similar to the description of the circular jet issuing from an orifice. Therefore, the information obtained by studying the circular jet may be applied to the plane jet situation. The orifice is studied in greater detail since there is more information available concerning this type of flow.

CHAPTER VIII

THE DISTRIBUTION OF THE VISCOUS DISSIPATION OF ENERGY IN A FREE CIRCULAR JET

The relations derived for determining the viscous dissipation of energy in the three regions of a circular jet are evaluated by means of computer techniques. The results of these calculations provide radial as well as axial distributions of this energy conversion process. The information is presented in normalized manner. Figures 19, 20, and 21 describe the distribution of the viscous dissipation of energy in Exit Region A, Exit Region B and the Fully-Developed Region, respectively. In each of these regions the radial distribution is shown at different axial locations in each region. The normalization technique presents the local distribution divided by the maximum value for each particular region and the radius in terms of the orifice radius.

These graphical representations are based on previously derived expressions - equations (VI-33), (VI-44) and (V-29). The programs used in the evaluation process on the 1620 Computer are shown in Appendix E.

In Region A as illustrated in Figure 19 the local quantitative value of the viscous dissipation of energy does not vary significantly with the axial distance. As the fluid discharges from the orifice, the energy conversion occurs near the edge of the jet; as the fluid continues down-

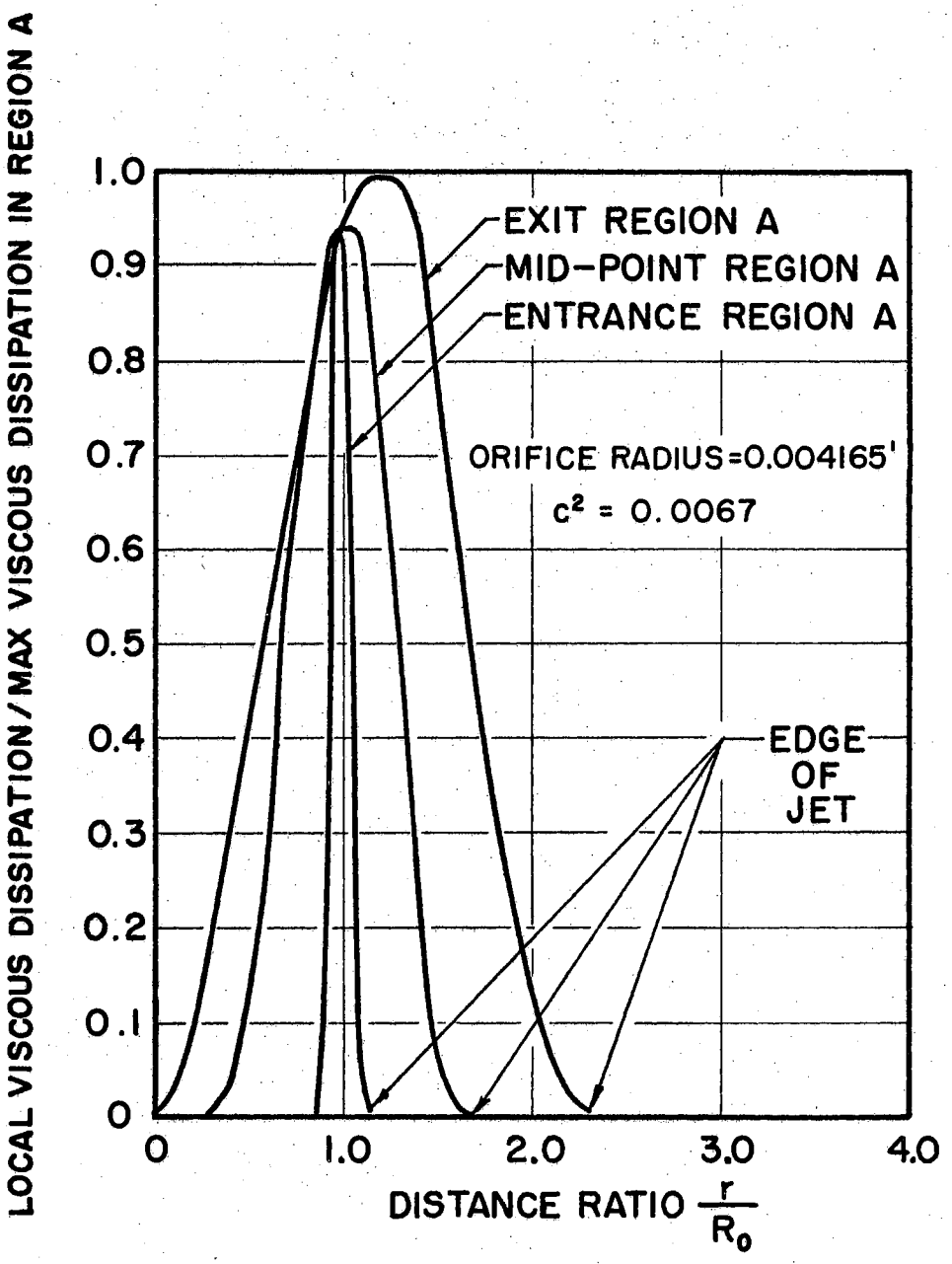

FIGURE 19

DISTRIBUTION OF THE DISSIPATED ENERGY IN EXIT REGION A.

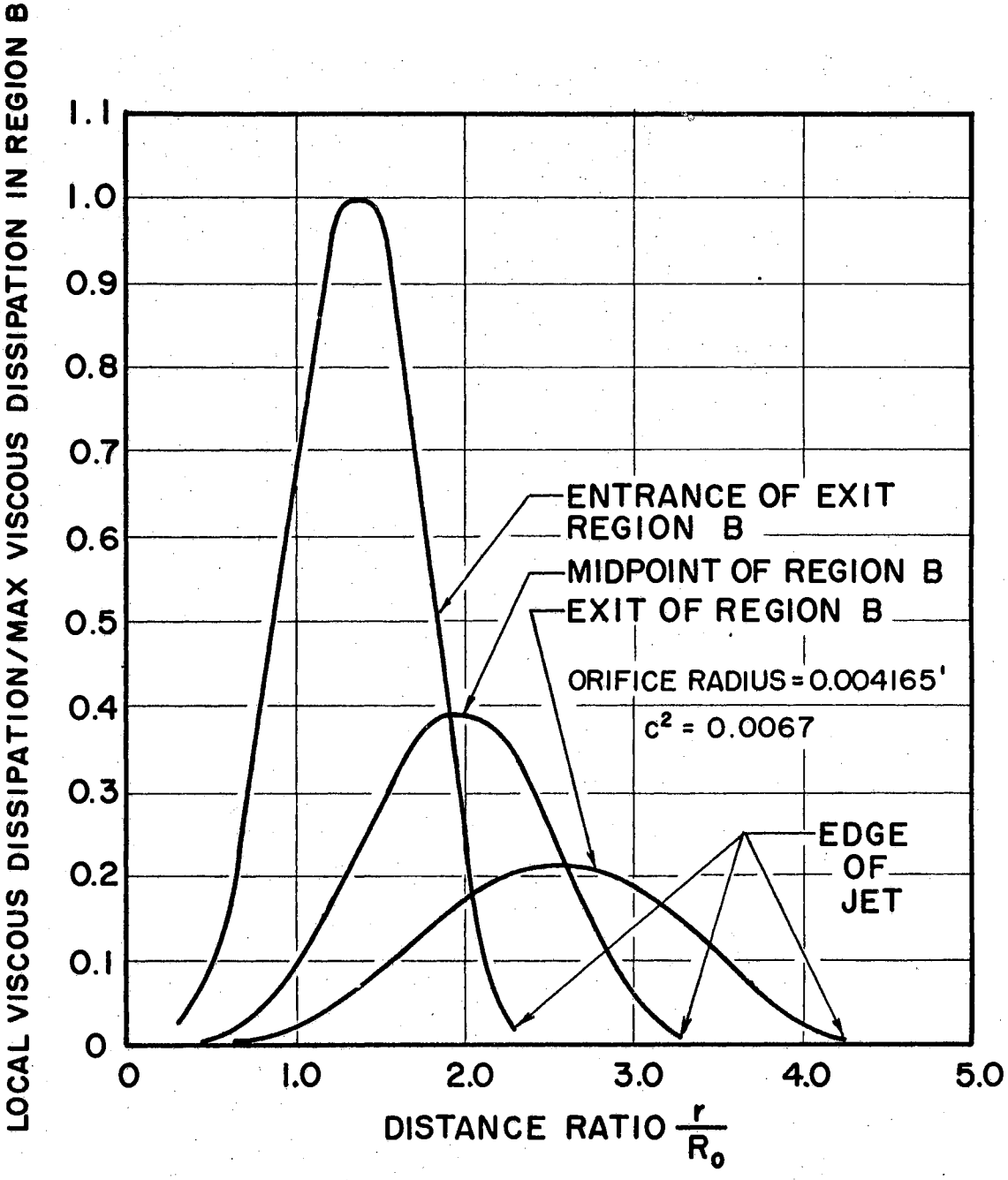

FIGURE 20

DISTRIBUTION OF THE DISSIPATED ENERGY IN THE EXIT REGION B.

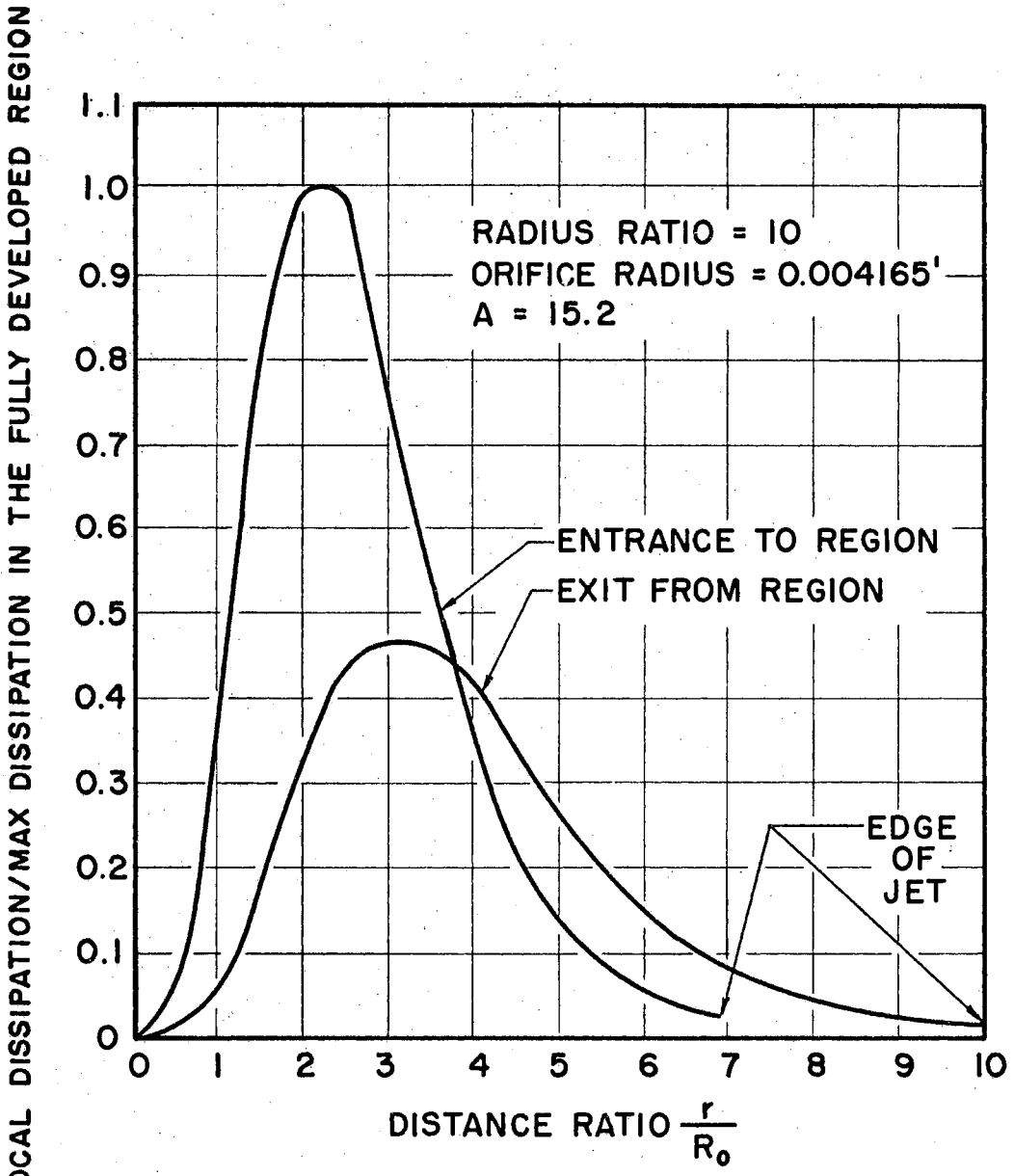

FIGURE 21

DISTRIBUTION OF DISSIPATED ENERGY IN THE FULLY DEVELOPED REGION.

stream, the conversion of energy occurs over a larger annulus to the point that at the end of Region A, the viscous dissipation of energy is occurring over the entire cross section of the jet except at the axis of the jet and the edge of the jet.

In Region B the viscous dissipation occurs over the entire jet between the center and the edge of the jet. The shape of the distribution across the radius of the jet is symmetrical and is similar to a sine-cosine function. In the Fully-Developed Region, the distribution is similar to that in Region B except that the distribution seems to spread more in a radial direction near the edge of the jet.

The relative importance of the exit regions is strikingly illustrated in Figure 22 where the axial distribution of the viscous dissipation of energy is shown as an increase in the bulk fluid temperature. Even for the case where R/R_o is quite large ($R/R_o = 10$), 89% of the increase of the bulk fluid temperature occurs in this region and only 11% occurs in the fully-developed region.

If this conversion of mechanical energy into internal energy is to result in a change in the temperature of the fluid then the distribution of the temperature is also changed. The temperature distribution of a jet based on the similarity principle is shown as the solid line in Figure 23. This represents the solution of the energy equation of the form

$$u\frac{\partial T}{\partial x} + v\frac{\partial T}{\partial r} = \frac{k}{\rho c_v}\,\frac{1}{r}\frac{\partial}{\partial r}\left[r\frac{\partial T}{\partial r}\right] \qquad \text{(IV-5)}$$

The energy equation including the viscous dissipation function is of the

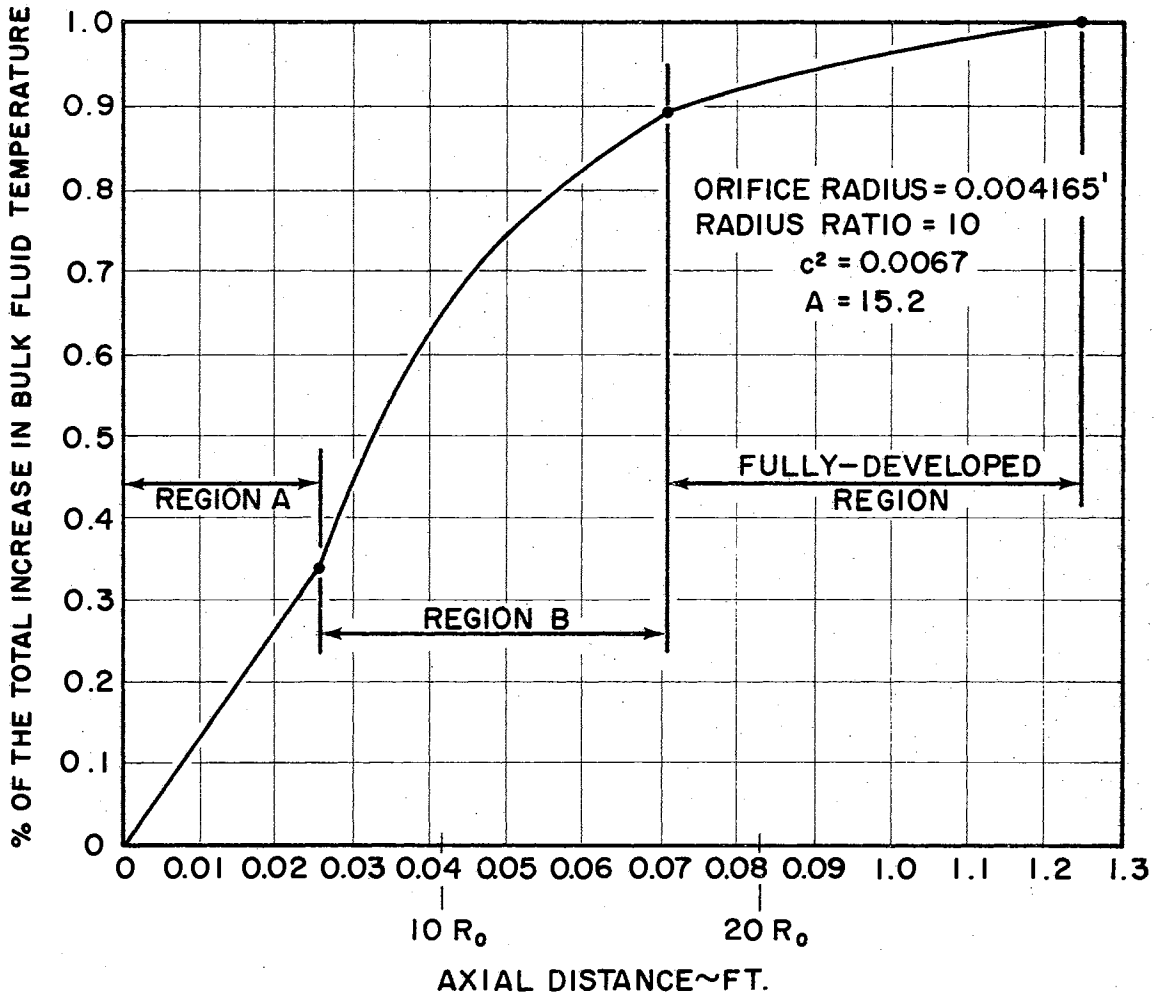

FIGURE 22

AXIAL DISTRIBUTION OF THE DISSIPATED ENERGY IN A CIRCULAR JET.

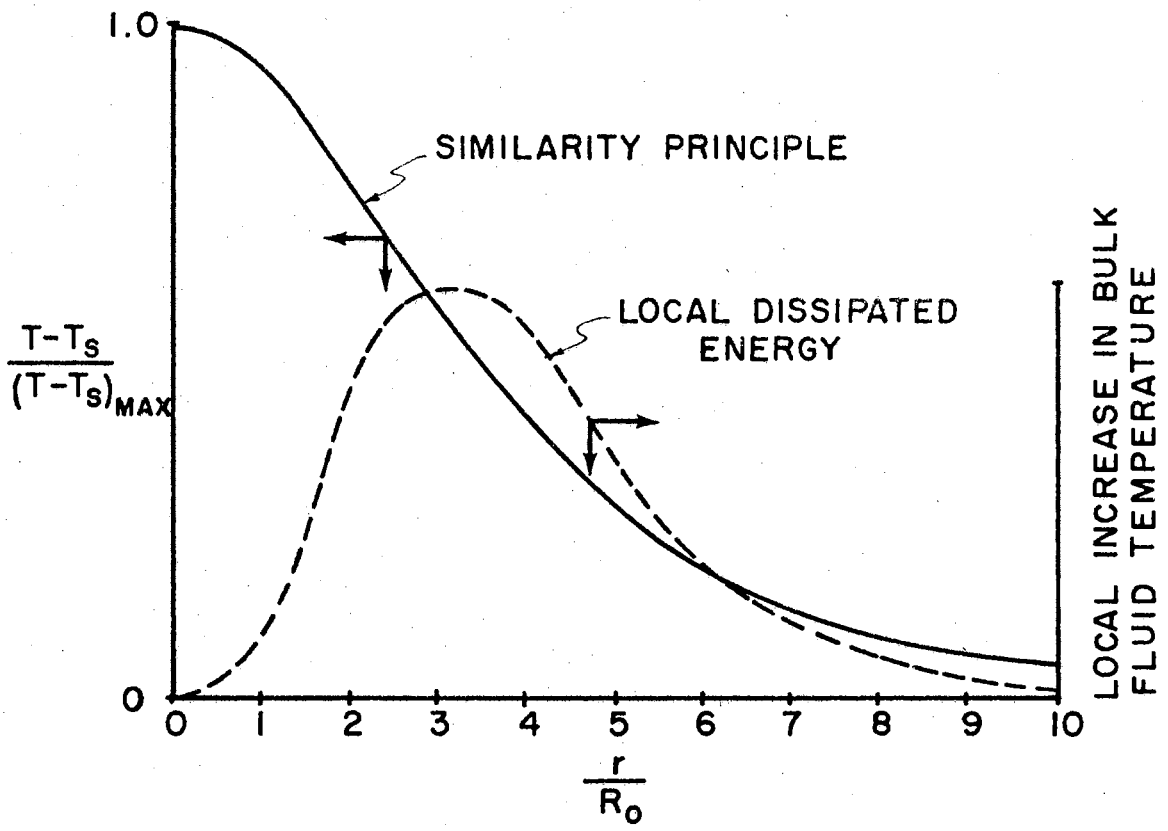

FIGURE 23

THE TEMPERATURE DISTRIBUTION IN A FULLY-DEVELOPED JET.

form

$$u \frac{\partial T}{\partial x} + v \frac{\partial T}{\partial r} = \frac{k}{\rho c_v} \frac{1}{r} \frac{\partial}{\partial r}\left[r \frac{\partial T}{\partial r}\right] + \frac{\mu}{\rho c_v} \phi \qquad \text{(IV-6)}$$

Taking the solution of equation (IV-5) and superimposing the results of evaluating the viscous dissipation function as shown in dotted line, certain qualitative conclusions may be formed. Taylor (6) found that a discrepancy existed in the temperature measurements of free-flow experiments which led him to develop a theory--the Vorticity Theory. Taylor finds that the temperature distribution spreads radially faster than described by the similarity principle based on the momentum transfer theory. His vorticity theory produces a profile which agrees with the experimental data on temperature distributions.

According to Figure 9, Taylor's vorticity theory is substantiated by experimental data; Taylor believes that the reason heat spreads radially faster than momentum is due to the added conductivity of the fluid. Squire (18) points out that this difference is not possible on the basis of the similarity principle. Squire also states that the difference is well established by experimental data, but he states that it is just by "chance."

Reviewing this information, the author suggests that the key linking these two theories - thus explaining why the vorticity theory best describes the temperature distribution and the momentum transfer theory best describes the velocity distribution - lies in the consideration of the viscous dissipation of energy. When the similarity principle is employed establishing the temperature profile from the velocity profile based on

the momentum transfer theory, the effects of viscous dissipation are not considered. When the local dissipated energy is considered by a superposition technique, the net distribution is a temperature distribution which spreads radially as described by the vorticity theory. Since each axial location has energy transported into an increase in the bulk fluid temperature, a true profile of a particular axial location must take this previously converted energy into account. In order to obtain an accurate description of the local temperature distribution in a jet, it is necessary that the energy equation be solved with the inclusion of the viscous dissipation function. If this were possible, the temperature distribution would then accurately account for the dissipated energy as well as any influence of the dissipated energy on the conduction and convection processes. Also if this equation were solved, fluids with Prandtl Numbers other than unity could be studied.

CHAPTER IX

THE INFLUENCE OF THE INPUT PARAMETERS

Additional information which aids in the understanding of the energy conversion process can be obtained by considering the effects of the input parameters. The various input parameters are:

Flow Rate - $\dot{q}$

Density - ρ

Radius Ratio - R/R_o

Empirical Constants - c^2; A

Orifice Radius - R_o

These input parameters are studied independently of each other in order to isolate the influence of each parameter on the conversion process.

The viscous dissipation of energy in Exit Region A may be written in slightly different form than equation (VI-33) as

$$\phi_f = C_1 \rho c^2 \dot{q}^3 / R_o^6 \left\{ (r_o - r_1)^{-1} \int_{-1}^{1} \left(\pi \frac{r_o - r}{r_o - r_1} \right) \left[1 + \frac{C_2 (c^2)^2 r^2}{(r_o - r_1)^2} + C_3 \frac{(c^2)^2 r R_o}{(r_o - r_1)^2} + C_4 \frac{(c^2)^2 R_o^2}{(r_o - r_1)^2} \right] r \, dr \, dx \right. \qquad \text{(IX-1)}$$

where r_o and r_1 are functions of the axial coordinate. In Exit Region B the viscous dissipation of energy is given by equation (VI-44). Substituting the definition of u_x from equation (VI-42) into equation (VI-44) and rewriting in a different form gives

$$dq_f = C_1' \rho C^2 \dot{q}^{-3} R_o^{-3.71} \left\{ \frac{C_2'}{r_o} \left[C^2 x \right]^{-2.23} \sin^3\left(\frac{\pi r}{r_o}\right) \left[1 + C_3' \frac{(C^2)^2 r^2}{r_o^2} \right] \right.$$

$$+ C_4' (C^2)^{-1.19} x^{-3.19} \frac{r}{r_o} \sin^2\left(\frac{\pi r}{r_o}\right) \left[1 + \cos\left(\frac{\pi r}{r_o}\right) \right]$$

$$\left. + C_5' (C^2)^{-2.19} x^{-4.19} \sin\left(\frac{\pi r}{r_o}\right) \left[1 + 2\cos\left(\frac{\pi r}{r_o}\right) + \cos^2\left(\frac{\pi r}{r_o}\right) \right] \right\} r\, dr\, dx \qquad \text{(IX-2)}$$

where r_o is a function of the axial coordinate. For the fully-developed region, the viscous dissipation of energy from equation (V-29) may be written as

$$dq_f = C_1'' \rho A^5 \dot{q}^{-3} R_o^{-3} \frac{r^3}{x^6} \left(1 + \frac{A^2 r^2}{4x^2} \right)^{-6} dr\, dx. \qquad \text{(IX-3)}$$

The three expressions describe the conversion of energy by the action of viscous dissipation. The input parameters appear in these expressions in different ways so that they must be considered independently.

Flow Rate and Density

The flow rate and density appear in each of the expressions for the viscous dissipation of energy in a similar manner. The flow rate appears to the third power. In determining the increase in the bulk fluid temperature due to the viscous dissipation of energy, it is necessary to divide each expression by the quantity $(q\rho)$. Upon performing this indicated division, the bulk fluid temperature increase is found to be a function of the flow rate squared. Agreement is then established with the approach of thermodynamics, which specifies that the bulk fluid temperature increase is proportional to the pressure drop which is in turn a function of the flow rate squared. Therefore, the flow rate effects of the viscous dissipation of energy appear as a constant multiplier.

Radius Ratio

The radius ratio establishes the regions which describe the expansion process. When the radius ratio is small, the entire expansion process may occur in a portion of the first and second region, i.e., Exit Regions A and B. As the radius ratio increases, more regions must be considered. Even though the radius ratio is not specified as a specific input parameter in the expressions, this ratio does establish the necessary expressions to be considered in describing the expansion process completely.

The Empirical Constants

There are two empirical constants in the expressions for the dissipation of energy in a free circular jet; one constant is c^2 appearing in the exit region expressions and the other is "A" appearing in the expression for the fully-developed region. A value for c^2 for air is given by Squire and Trouncer (19) as 0.0067. Based on the experimental determinations in a later section where MIL-H-5606A hydraulic fluid at a temperature of 80F is employed, the value of c^2 decreases in this case to 0.00538.

The fact that the constant decreases for a more dense, more viscous fluid may be explained by considering the larger potential difference in the form of pressure drop. This increased pressure difference represents a greater driving potential which results in a decrease in the rate of spread of the jet. Figure 24 shows the axial distribution of the dissipated energy in a circular jet for two different values of

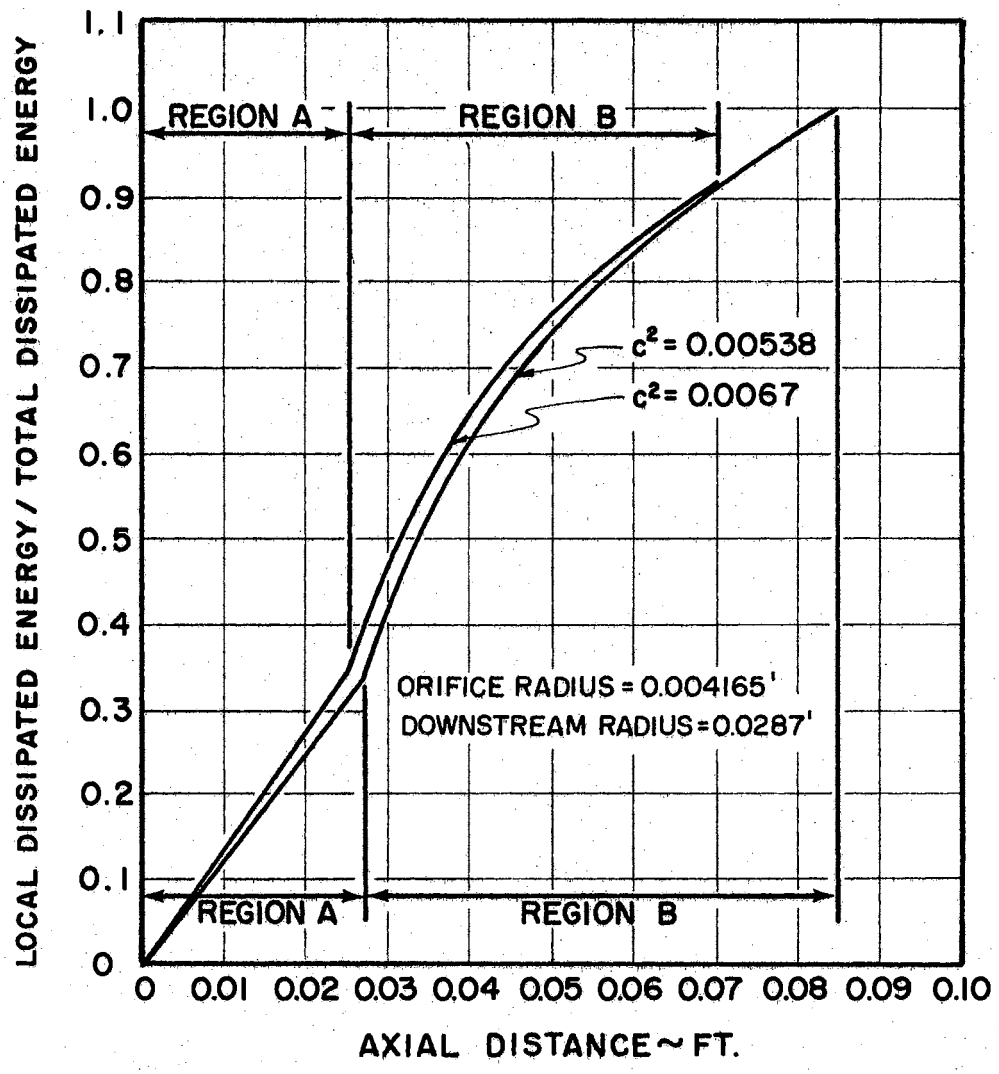

FIGURE 24

THE AXIAL DISTRIBUTION OF THE DISSIPATED ENERGY FOR DIFFERENT EMPIRICAL CONSTANTS.

c^2; each curve is for the same orifice radius, the same radius ratio, and the same flow rate. Since the radius ratio is identical in each case, the radial spread of the jet is decreased for the lower value of c^2 since a longer axial distance is required to attain the same radius. Also from Figure 24, the lower value of c^2 decreases the rate of dissipated energy; however, even though the rate is less, the axial distance of expansion is more so that the net effect is to increase the dissipated energy.

The Orifice Radius

The orifice radius has a very pronounced effect on the viscous dissipation of energy. In the expressions describing the viscous dissipation of energy in each of the three regions, the orifice radius appears in each expression in a different manner. In the expressions for Exit Region B and the Fully-Developed Region, the orifice radius is a constant multiplier. However, in equation (IX-1) for Exit Region A, the orifice radius appears in several locations in the expression. Figure 25 shows the effect of the orifice radius on the viscous dissipation of energy; each curve is for a different orifice radius but for the same flow rate, same density, and the same radius ratio, R/R_o. From this figure, it is clearly evident that small orifice diameters are characterized by large viscous dissipation. This is a result of the significant velocity gradients for the smaller orifice openings.

The various input parameters appearing in the expressions describing the viscous dissipation of energy in a circular jet have been investigated independently. These parameters are functions of the geometrical

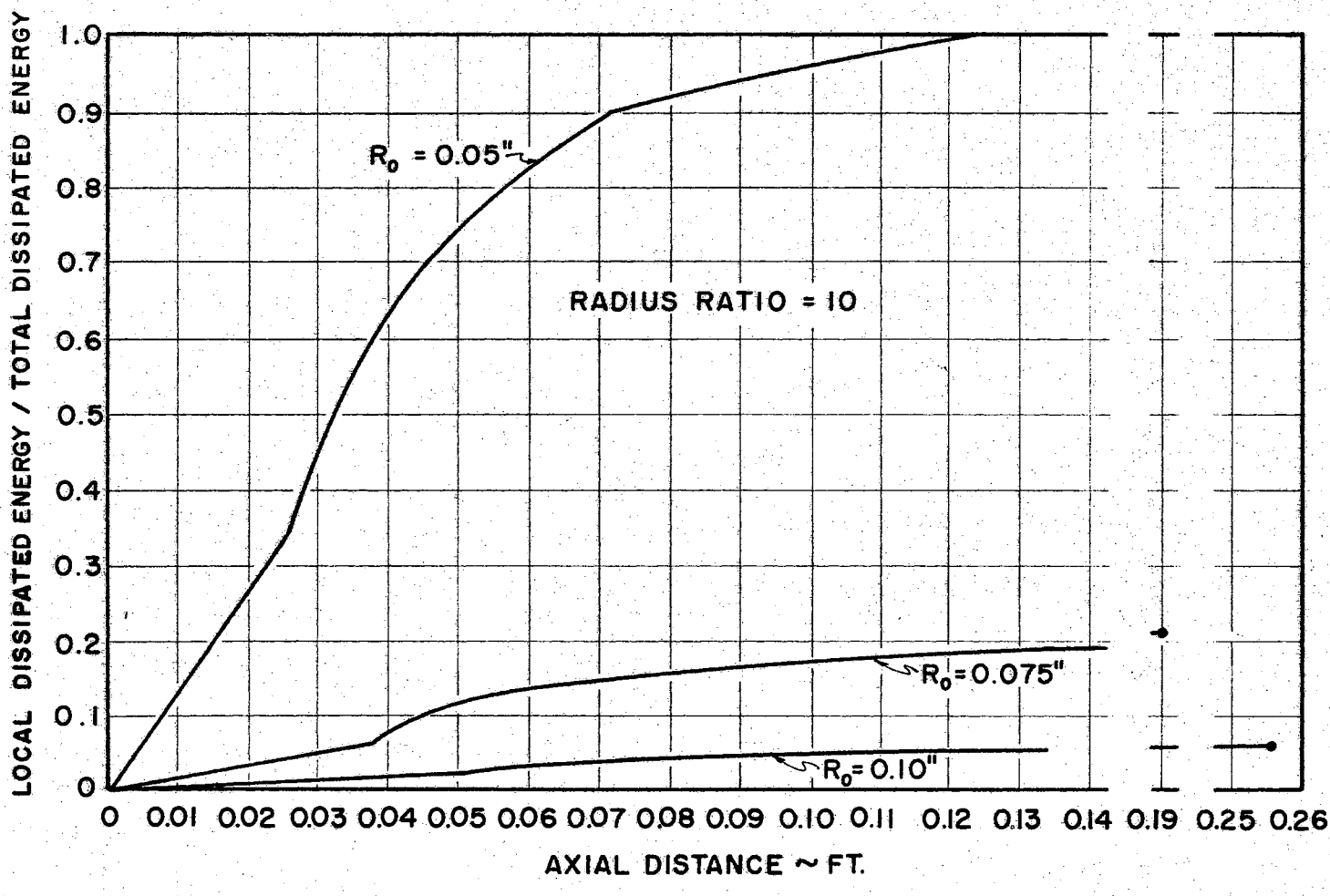

FIGURE 25

THE EFFECT OF THE ORIFICE RADIUS ON THE VISCOUS DISSIPATION OF ENERGY

flow situation as well as the characteristics of the fluid. In addition to investigating these parameters, it is necessary to establish the numerical agreement between the results obtained through the evaluation of the dissipation function and the results obtained by thermodynamics.

CHAPTER X

COMPARISON OF NUMERICAL RESULTS

In a practical situation the pressure drop is usually known and hence the corresponding increase in the bulk fluid temperature can be established from the thermodynamic relations. The consideration of the viscous dissipation function has established a means of physically describing the process for the conversion of mechanical energy into thermal energy. It is necessary to establish the quantitative agreement between the results obtained from viscous dissipation considerations with the results obtained by thermodynamic relations.

From the experimental results presented in a later section for a working fluid of MIL-H-5606A hydraulic fluid, the following situation may be considered:

$$\dot{q} = 0.0142 \text{ ft}^3/\text{sec}$$

$$R_o = 0.004165 \text{ ft}$$

$$R = 0.0287 \text{ ft}$$

$$\Delta P = 795 \text{ psi.}$$

From thermodynamic considerations shown graphically in Figure 2, the corresponding increase in the bulk fluid temperature is 6.0F.

Applying the results found by evaluation of the viscous dissipation function for the situation corresponding to:

$$\dot{q} = 0.0142 \text{ ft}^3/\text{sec}$$

$R_o = 0.004165$ ft

$R = 0.0287$ ft

$c^2 = 0.00538$

the resulting increase in the bulk fluid temperature is 4.8F. In the evaluation, it is noted that the expansion process occurs only in Exit Regions A and B. The result is based upon the empirical constant determined from the experimental data for hydraulic fluid as discussed in a later section. The comparison of results shows that the viscous dissipation approach gives results 20% below that determined from thermodynamics. This conservative value is a result of the many limiting assumptions in the development of the expressions. The two most significant limitations in the development are:

(1). The neglecting of all terms in the dissipation function containing flow normal to the axis of the jet.

(2). The neglecting of all flow patterns upstream of the restriction. The latter of these limitations is of significant importance. Since a large amount of fluid is passing through a small cross-sectional area, the velocity gradients in the entrance region of the orifice could be important and easily account for the conservative value determined by considering the flow patterns downstream of the restriction alone. No suitable analytical model is available to describe the flow patterns upstream of the orifice.

CHAPTER XI

CALCULATION OF THE AXIAL DISTRIBUTION OF THE STATIC PRESSURE

Using the results of the viscous dissipation of energy as determined by evaluation of the dissipation function, the change in the average static pressure of the jet can be expressed as a function of the axial coordinate. This evaluation is based on the assumption that the decrease in the static pressure is proportional to the increase in the bulk fluid temperature at each axial location. Figure 26 presents the axial distribution of the increase in the bulk fluid temperature for the case of a circular jet of MIL-H-5606A hydraulic fluid. Expressing the energy in terms of a local static pressure decrease produces the axial distribution of the static pressure in the jet. Comparing the analytical results to the experimental results in the previous chapter, a 20% difference is shown. If this value is considered to be accounted for in the area upstream of the restriction where the analytical model is neglected, the static pressure distribution may be extrapolated as indicated by the dotted line on Figure 26. It should be emphasized that the static pressure represented in Figure 26 is evaluated from the dissipation function and does not account for kinetic energy changes.

The energy equation from thermodynamics for a fluid element for the case of a fluid flowing steadily through a restriction may be written as

$$dh + \bar{u}\,d\bar{u} = 0 \qquad \text{(XI-1)}$$

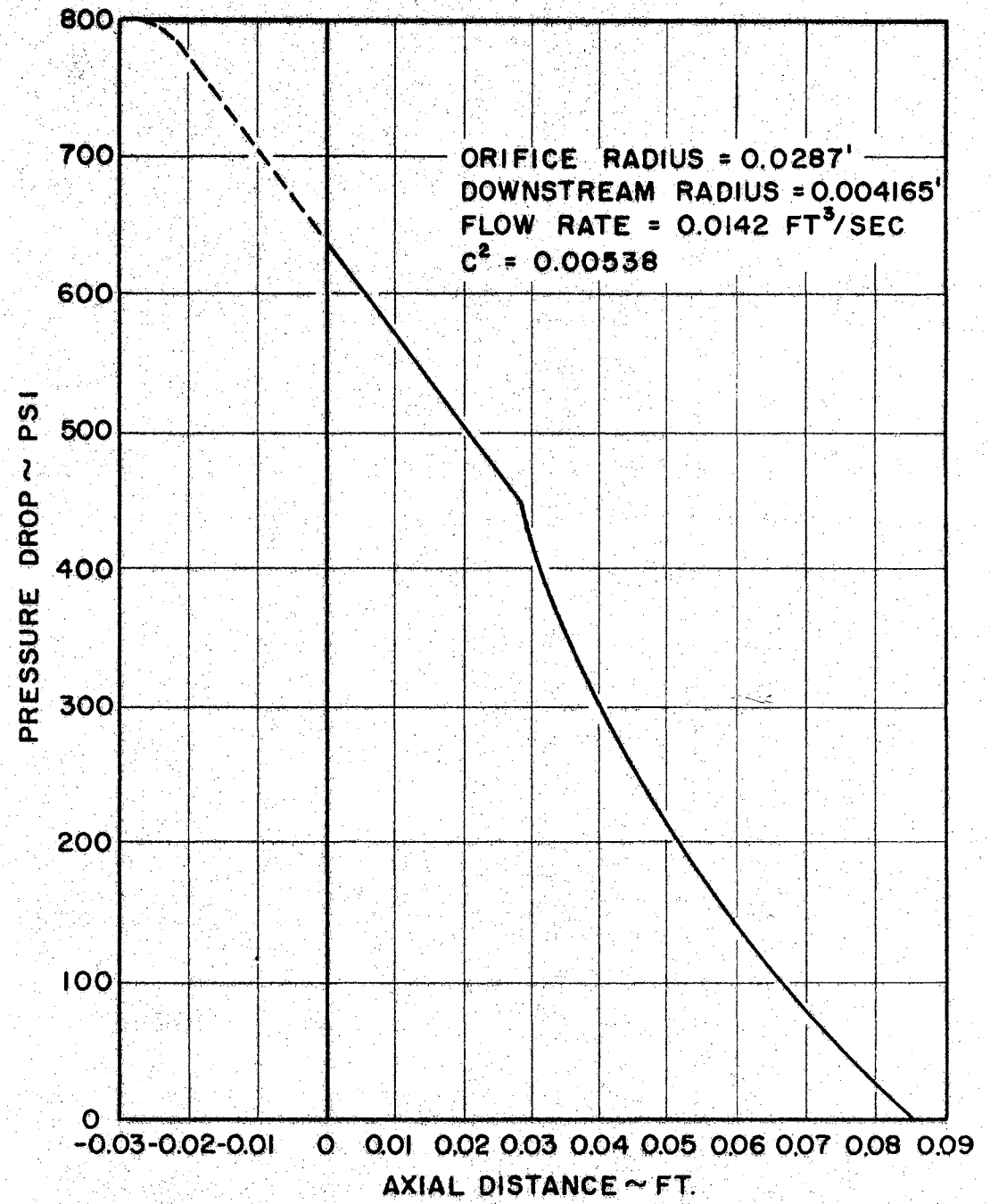

FIGURE 26

THE AXIAL DISTRIBUTION OF "STATIC" PRESSURE.

in the absence of potential energy considerations, paddle-wheel work, and heat transfer. Using the definition of enthalpy and differentiating gives

$$de + P dv + v dP + \bar{u} d\bar{u} = 0 \tag{XI-2}$$

For the case of an incompressible fluid the expression reduces to

$$de + v dP + \bar{u} d\bar{u} = 0 \tag{XI-3}$$

and since

$$de = c_v dT$$

then

$$\bar{u} d\bar{u} = -c_v dT - v dP \tag{XI-4}$$

Therefore in a throttling process, the kinetic energy considerations can affect the local bulk fluid temperature as well as the local static pressure of the fluid. In order to establish the exact nature of the distribution of the pressure it would be necessary to establish the exact behavior of the two properties - temperature and pressure. In the absence of such information, the distribution of the pressure in the jet is shown from the dissipation function information.

CHAPTER XII

EXPERIMENTAL DETERMINATIONS

The purpose of the experimental investigations is to determine the validity of the velocity distributions employed in the evaluation of the viscous dissipation function. These free-flow relations have been verified experimentally by a number of previous investigators using air as the working fluid and the empirical constants are evaluated from this data. The verification undertaken in this study involves the use of a fluid other than air. The fluid selected is MIL-H-5606A Hydraulic Fluid. This selection is based on the fact that the viscous dissipation of energy is an important factor in fluid power systems presently in operation.

Description of the Test Section

The function of the test section is to permit the experimental investigation of the turbulent flow phenomena downstream of a restriction. Cast Acrylic Resin rod is chosen for the material for containing the fluid downstream of the restriction. The material permits visual observation of the flow phenomena and the measuring devices. The material is also a good insulator thus simulating adiabatic flow conditions. It is also resistant to the action of many chemical compounds including petroleum-base oils. A list of the properties of Cado Cast

Acrylic Resin materials - as provided by the manufacturer - is presented in Table I.

The basic design of the test section is established by satisfying two needs: first, to provide a means of creating the desired turbulent action; and second, to provide a means of measuring the flow phenomena in this turbulent region.

The test section has three basic components: (1) the fluid inlet section, (2) the restriction insert, and (3) the downstream flow section. The first section provides a means of receiving the fluid with a minimum amount of entrance effects. In this first section is located an upstream static pressure tap and an O-ring seal on the upstream side of the insert. The insert simply provides the restriction to be investigated. The third section is perhaps the most important. It provides a means of viewing the flow pehnomena, a support for measuring devices, and a seal against fluid losses. Since failure of the plastic section is most likely to occur in longitudinal tension, this component is supported in longitudinal compression by means of two plates and four rods.

Details of the test section are provided in Figures 27 and 28. The provisions for the measuring devices are discussed in the next section.

Measurements and Instrumentation

In order to be able to describe the flow phenomena downstream of a restriction, it is necessary to establish the characteristics of the velocity in this region.

On the outside of the plastic cylinder, a surface is carefully prepared for the location of a smooth, flat steel plate. The plate is

TABLE I

PROPERTIES OF CADO CAST ACRYLIC RESIN

PROPERTY	VALUE	UNITS	A.S.T.M.
Thermal Conductivity	2.3	$\frac{\text{BTU in}}{\text{l+R ft}^2\,^\circ\text{F}}$	(Cenco-Fitch)
Specific Heat	0.35		
Coefficient of Linear Thermal Expansion per F	$49(10)^{-5}$		
Heat Distortion Temperature			
264 psi	160	F	D 648-45T
66 psi	170	F	
Tensile Strength			
-70F	14,300	psi	
77F	7,000	psi	D 638-46T
170F	2,900	psi	
Index of Refraction	1.49		D 542-42
Specific Gravity	1.18		D 792-48T

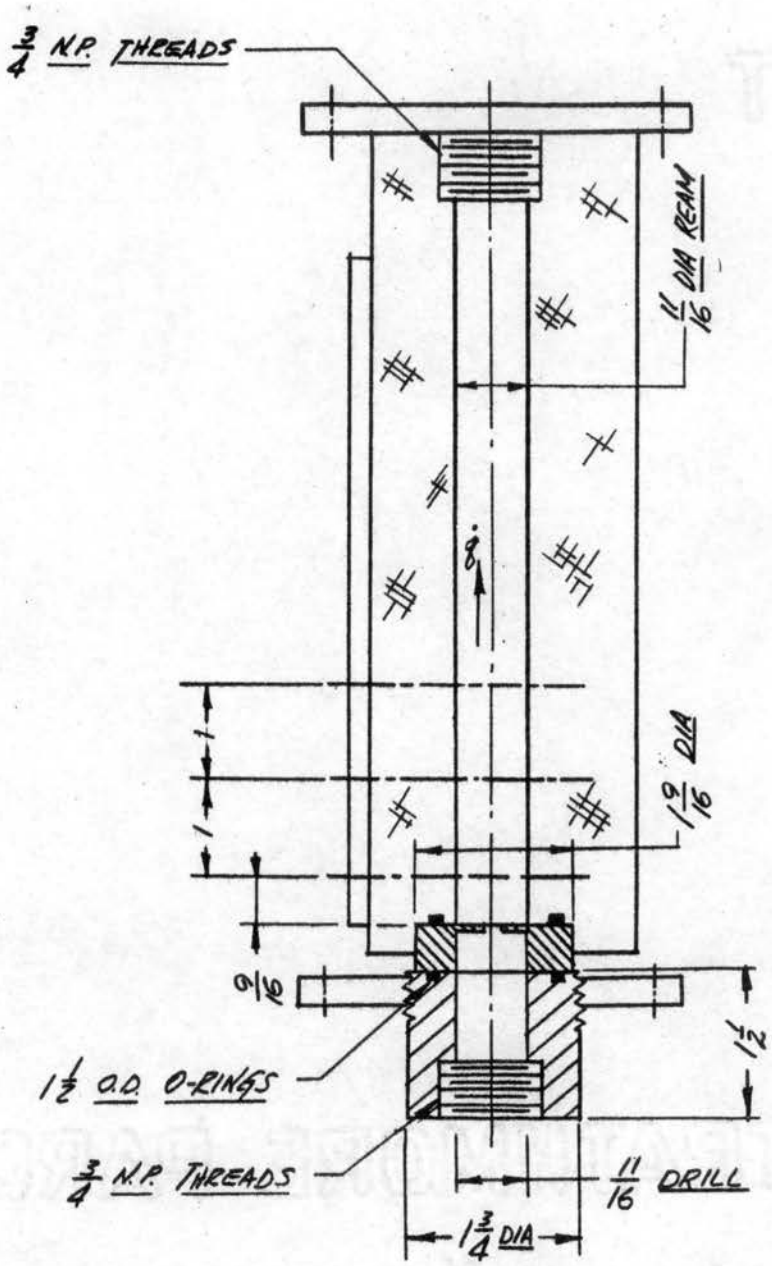

Figure 27. Details of the Test Section - I

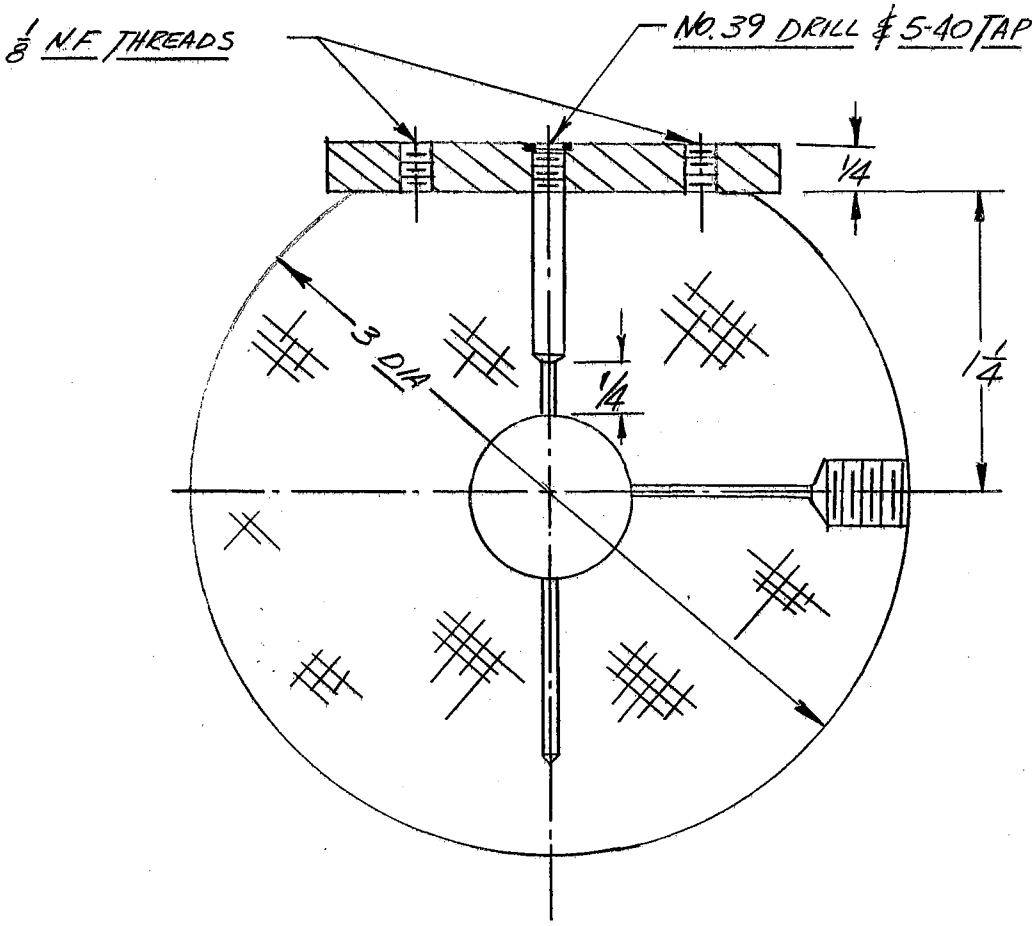

Figure 28. Details of the Test Section - II

attached to the plastic surface by an epoxy compound. This steel plate supports the measuring probe.

The probe device as shown in Figure 29 receives the information for determining the velocity profile in the region. The probe consists of a 0.058" (17 gage) diameter hypodermic tubing with a 0.018" diameter hole in one side to record the pressure. This probe traverses across the path of the fluid recording the total pressure profile. It is important to know accurately the location of the total pressure tap; to accomplish this, a modified depth gage is employed.

The depth gage is a Brown and Sharpe model 605. The small measuring rod in the original depth gage is replaced by a 0.095" (13 gage) diameter hypodermic tubing. The diameter of the steel tubing is almost identical to that of the original rod. The base of the depth gage is removed and replaced by a new base built for mounting purposes. The vernier scale mechanism is unaltered and it allows for the accurate movement of the probe across the diameter of the fluid path in a very exacting manner. The divisions on the vernier scale are in 0.05" intervals.

The steel tube is positioned with the total pressure probe always located in an upstream position. To obtain information at different axial distant locations from the restriction, the probe is removed and repositioned.

In order to establish the velocity profile, a static pressure tap is provided in the side of the plastic cylinder.

DETAILS OF SENSING PROBE

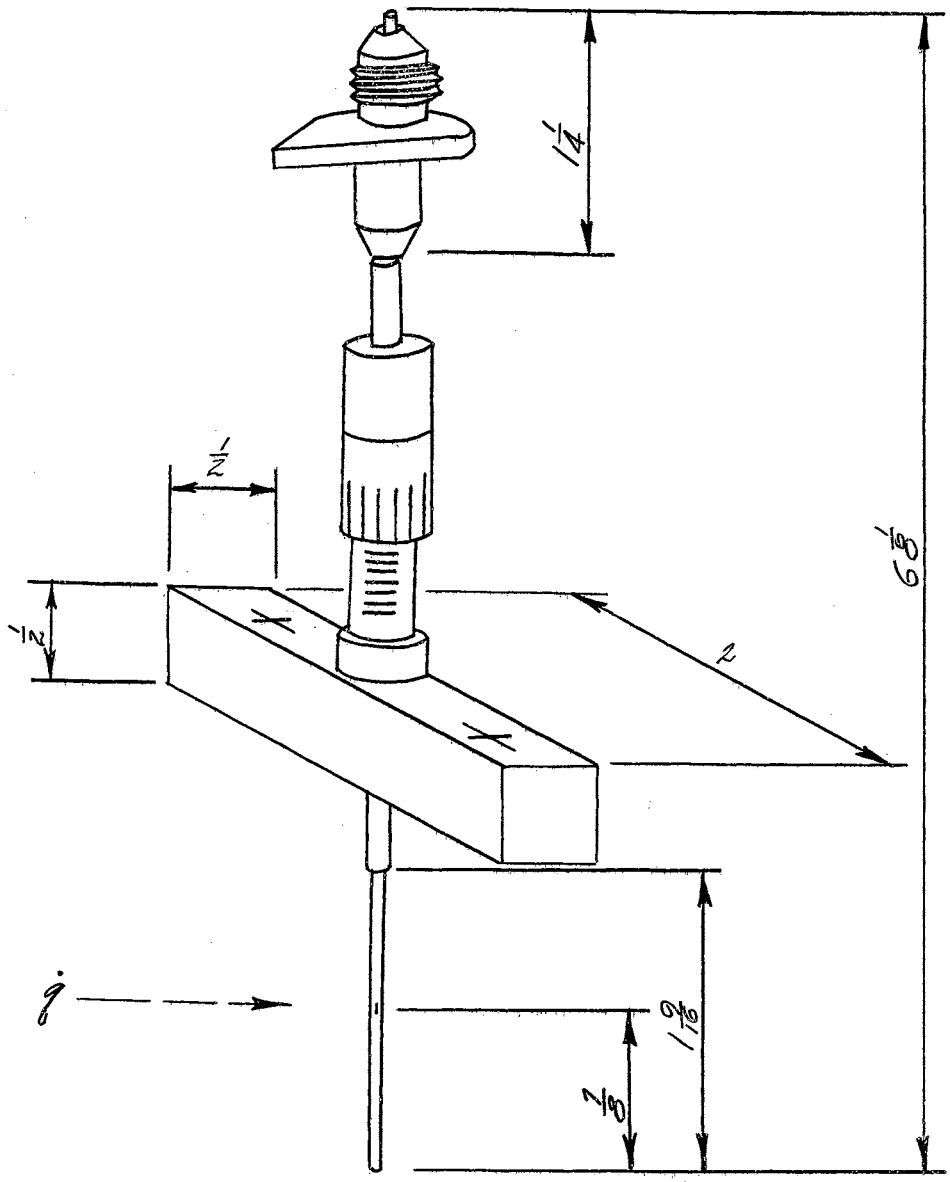

Figure 29. Details of the Sensing Probe

Presentation of Experimental Data

Downstream of the circular orifice, total traverses are performed across the radius of the section and data are recorded at .01-inch intervals. By using the static pressure measurement at the same axial location, the axial velocity can be computed for the incompressible fluid by the relation

$$u = \sqrt{\frac{2}{\rho}\left(P_{TOTAL} - P_{STATIC}\right)} \quad . \tag{XII-1}$$

For a particular section, i.e., a particular axial coordinate location, data is shown for various flow rates and pressure drop situations. The fluid media is MIL-H-5606A hydraulic fluid.

The sensing probe is located a distance of .0468 feet downstream of the orifice. The exit region model of Squire and Trouncer (19) indicates the probe to be in Exit Region B. The velocity in the axial direction in this region is given analytically as

$$u = \frac{1}{2} u_x \left(1 + \cos \frac{\pi r}{r_o}\right) \quad , \tag{XII-2}$$

The velocity ratio may be then expressed as

$$\frac{u}{u_x} = \frac{1}{2}\left(1 + \cos \frac{\pi r}{r_o}\right) \tag{XII-3}$$

where r_o is a function of the axial coordinate and contains in its definition the empirical constant c^2. Figure 30 presents the velocity ratio as determined from the experimental data. Using the technique suggested by Squire and Trounder, the empirical constant is evaluated for the case of hydraulic fluid to be .00538 as compared to a value of .0067

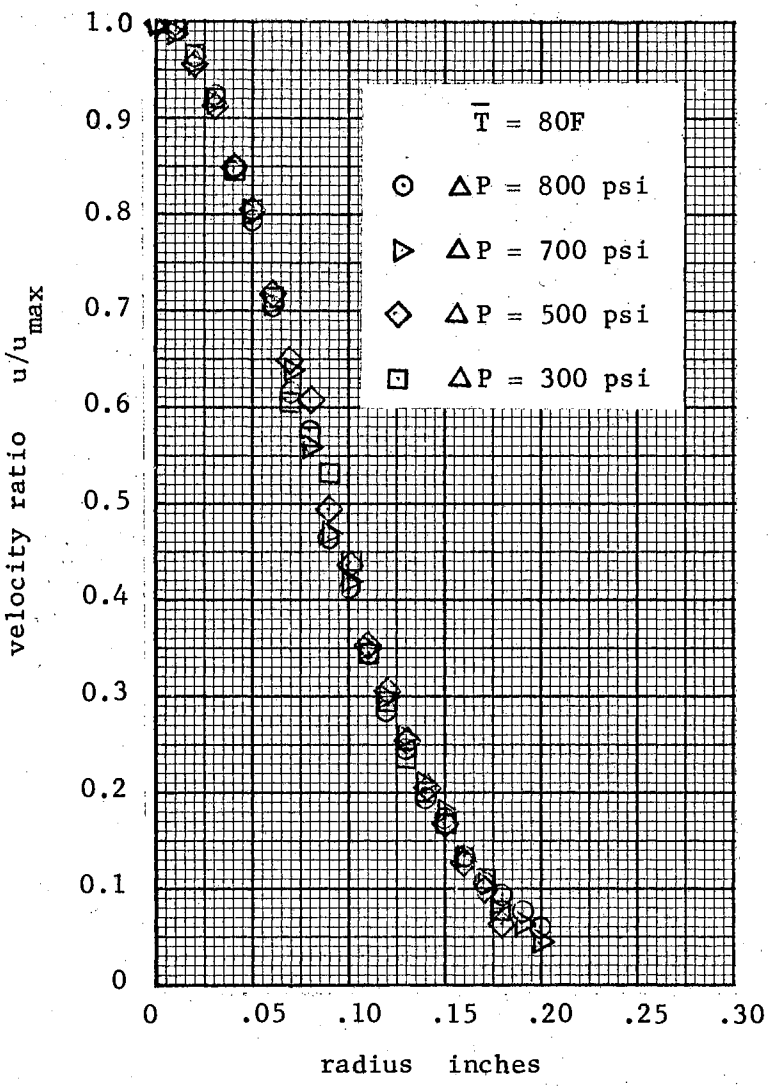

Figure 30. The Velocity Distribution for a Free Jet of Hydraulic Fluid

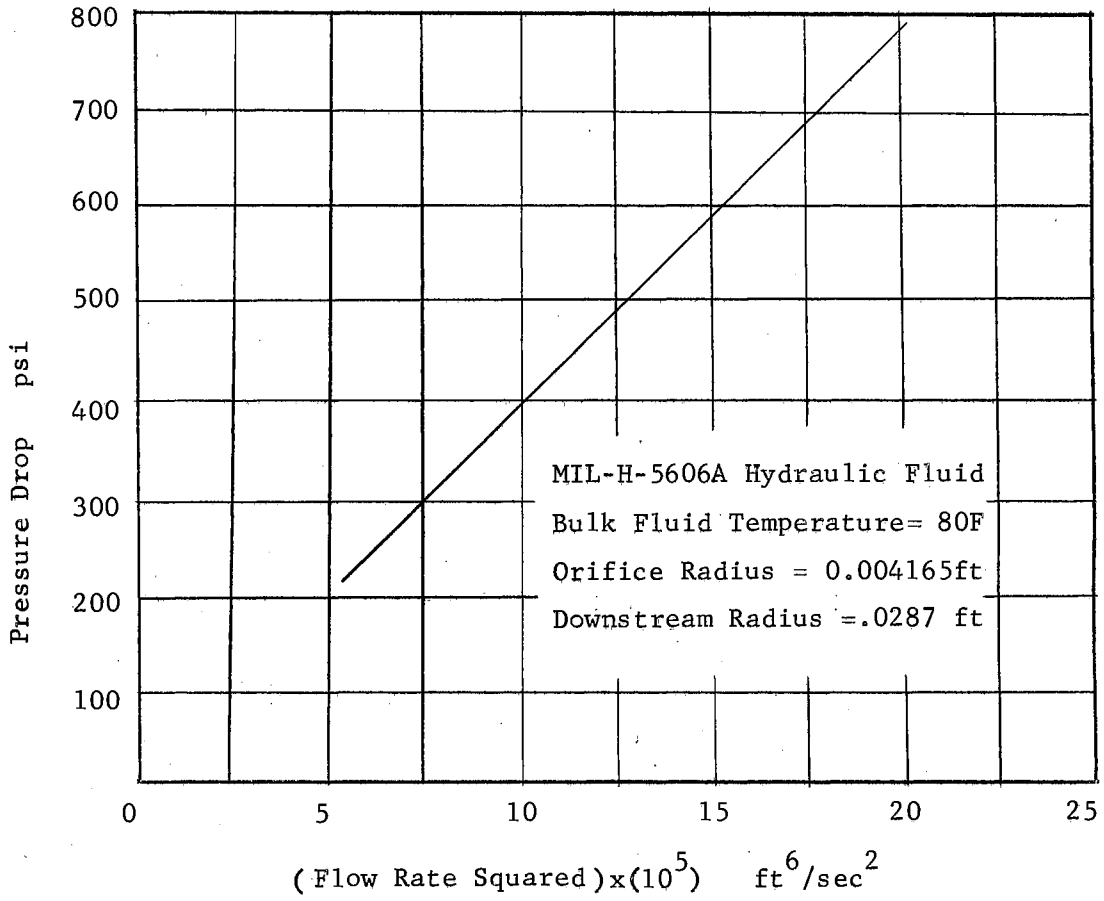

Figure 31. Flow Characteristics for the Test Orifice with Hydraulic Fluid Employed

for air. The method of determining c^2 involves the solving of the momentum flux expression and the velocity expression along with the physical measurement of the radial location corresponding to a velocity ratio of 0.5.

The characteristics of the test orifice with hydraulic oil as the working fluid are shown in Figure 31 where pressure drop is shown as a function of the flow rate.

Experimental Observations

In studying the flow phenomena downstream of an orifice using MIL-H-5606A Hydraulic Fluid as the working fluid, the presence of gas bubbles is detected. The appearance of the bubbles is a function of the degree of turbulence, the pressure drop, and the flow rate; these three factors are dependent variables. In the case of low flow rates, no bubbles are present and no visible flow patterns are evident. As the flow rates are increased, the presence of gas bubbles near the orifice is detected and the outline of the flow pattern becomes evident as illustrated in Figure 32. Downstream the bubbles seem to redissolve into the liquid. At the maximum flow rate corresponding to a pressure drop across the orifice of approximately 800 psi, not all the gas bubbles redissolved in the liquid but some remain suspended in the liquid and are carried downstream.

These bubbles are generally known as cavitation bubbles. The visible bubbles are a result of the release of gases which have been dissolved in the liquid. A smaller bubble, which may not be visible, is the vapor of the liquid. A fluid such as MIL-H-5606A hydraulic fluid is capable of dissolving a volume of air for every 110 psi increase in pressure according to LeRoy and Leslie (31). However, in a hydraulic circuit a considerably less amount of gas is usually present because systems are designed to remove the gases.

The presence of the gas bubbles in the region downstream of the restriction is important since the formation and expansion of these cavitation bubbles represents a sink. All the energy of viscous dissipation does not result in an internal energy increase but a portion of that

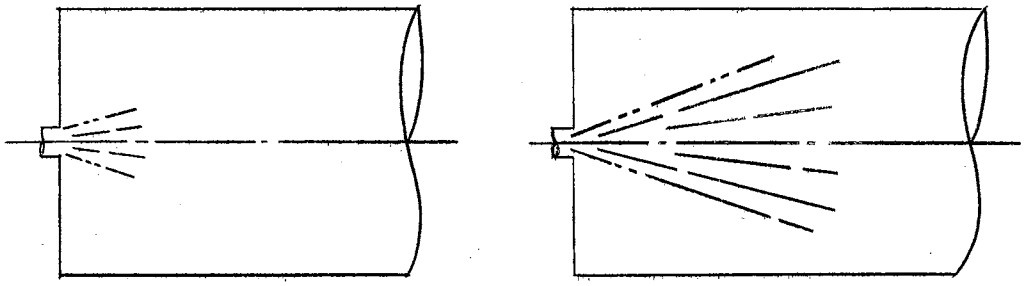

(a) P = 300 psi (b) P = 500 psi

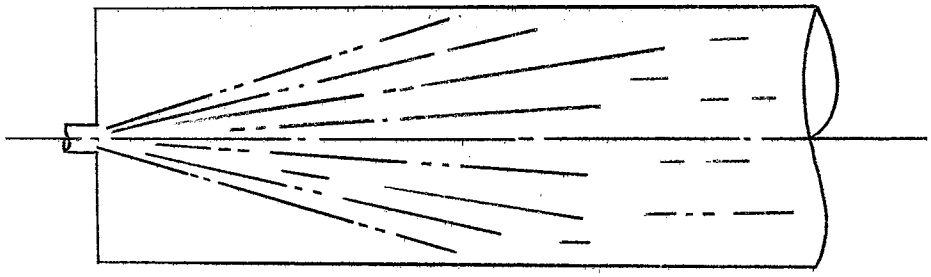

(c) P = 800 psi

Figure 32. Presence of Bubbles in Liquid Jets

energy must be transported to the bubbles.

CHAPTER XIII

CONCLUSIONS AND RECOMMENDATIONS

The analysis provides a tool for describing the physical process of converting mechanical energy into thermal energy by the action of viscous dissipation. It has been shown that as the fluid discharges from the face of the orifice, the dissipation process occurs in a narrow annulus near the edge of the jet; further downstream, the dissipation of energy occurs in a larger annulus with the maximum dissipation occurring near the midpoint between the edge of the jet and the axis of the jet.

By the evaluation of the viscous dissipation function, the maximum rate of increase of the bulk fluid temperature is found to be in the second region, Region B, approximately 3 to 4 diameters downstream of the face of the orifice. The importance of considering the first and second regions in the evaluation of the viscous dissipation of energy is illustrated by considering the situation where $R/R_o = 10$ and air is the fluid medium; all three regions must be considered in describing the expansion process. However, 89% of the dissipation of energy occurs in the first and second region, i.e., in the first eight diameters downstream of the orifice. Most of these parameters are established by the physical flow situation; however, the empirical constants, c^2 and A, are determined by the fluid medium. These empirical constants have been established for air as the working fluid by previous investigators.

Experimental tests employing MIL-H-5606A hydraulic fluid at a temperature of approximately 80F show that the value of c^2 is 0.00538 for this situation. The value for air is 0.0067. The influence of the empirical constants on the dissipation process cannot be established by simple investigation of the equations; for example, a smaller value of c^2 reduces the rate of increase of the bulk fluid temperature but does not necessarily decrease the total change in the bulk fluid temperature. For the same radius ratio the increase in the bulk fluid temperature may be larger for the smaller c^2 due to the increased axial distance in the expansion process. The viscous dissipation of energy is considered only in the expansion process and not beyond the point of contact of the wall.

Comparison of the results of the viscous dissipation of energy with the results of thermodynamics shows that the dissipation function value is 20% lower than the thermodynamic value. This comparison is made on the basis of experimental tests employing hydraulic fluid at a temperature of 80F. The empirical constant used in the evaluation process is also evaluated for this data. The conservative results are believed to be primarily due to the fact that all flow patterns upstream of the restriction are neglected. In this entrance region, the velocity gradients could increase the numerical value of the dissipated energy by nearly 20%.

By using the relations for the plane jet, the viscous dissipation process for the flow of a fluid through a slit-type restriction is shown to be similar in nature to the circular jet. In the analytical evaluation of the circular jet and the plane jet, the predominant term in the

evaluation process in the $(\partial u/\partial r)$ contribution. Even for these situations where the $(\partial u/\partial x)$ is significant, the corresponding contribution is small in comparison.

In order to obtain the exact temperature distribution in a free jet, the energy equation including the viscous dissipation function must be solved. A review of the existing mathematical solutions for partial differential equations of this type reveals no solution presently available. It is hoped that this endeavor may be extended by solving the equation by a finite difference technique. Additional experimental investigation is also suggested. These investigations should concentrate on the exit regions near the face of the restriction and the regions near where the jet boundaries contact the wall. Fluids other than air should be employed. In addition to verifying the theoretical velocity distributions, a complete investigation of the empirical constants should be undertaken. These investigations should be concerned with the physical situations of fluids passing through restrictions.

BIBLIOGRAPHY

1. Lamb, Sir H. Hydrodynamics. Dover Publications, 6th Edition, 1932, New York.

2. Bird, R. B., Stewart, W. E., and Lightfoot, E. N. Transport Phenomena. John Wiley and Sons, 1960.

3. Bennett, C. O. and Myers, J. E. Momentum, Heat and Mass Transfer. McGraw-Hill, 1962.

4. Jones, J. B. and Hawkins, G. A. Engineering Thermodynamics. John Wiley and Sons, 1960.

5. Prandtl, L. "Bericht uber Untersuchungen zur ausgebildeten Turbulenz" Zeitschrift für angewandte Mathematik und Mechanik. Vol. 5, No. 2, 1925, pp. 136-139.

6. Taylor, G. I. "The Transport of Vorticity and Heat Through Fluids in Turbulent Motion", Appendix by A. Fage and V. M. Falkner, Proc. Roy Soc London. A135, pp. 685-705, 1932.

7. Goldstein, S. "On the Velocity and Temperature Distributions in the Turbulent Wake Behind a Heated Body of Revolution," Proc Cambridge Phil Soc. pp 48-67, 1938.

8. Lord Rayleigh (Strutt, John William). Scientific Papers. Vol I, 1869-1881, Cambridge University Press, "On Capillary Phenomena of Jets," Proc Roy Soc, Vol. XXIX, pp. 71-97, 1879.

9. Chaplygin, S. "Gas Jets," NACA TM 1063, August 1944, Uvenge Zapiski Imp. Moskov Univ., Otd. Fiz.-Mat. 21, pp 1-121, 1904.

10. Tollmien, Walter. "Calculation of the Turbulent Expansion Processes," NACA TM 1085, 1945; "Berechnung turbulenter Ausbrietungsvorgänge," Zeitschrift für angewandte Mathematik und Mechanik, Vol. 6, pp. 1-12, 1926.

11. Förthmann, E. "Turbulent Jet Expansion," NACA TM 789, 1936; "Uber turbulente Strahlausbreitung," Ingenieur-Archiv, Vol. V, No. 1, pp. 42-54, 1934.

12. Kuethe, Arnold M. "Investigations of the Turbulent Mixing Regions Formed by Jets," Jour Appl Mech, Vol. 2, A-87-95, 1935.

13. Howarth, L. "Concerning the Velocity and Temperature Distributions in Plane and Axially Symmetrical Jets," Proc Cambridge Phil Soc, Vol. 34, pp 185-203, 1938.

14. Ruden, Von P. "Turbulente Ausbreitungsvorgänge im Freistrahl," Naturwissenschaften, Vol. 21, pp. 375-378, 1933.

15. Bickley, W. G. "The Plane Jet," Phil Mag. Ser. 7, Vol XXIII, No. 156, pp 727-731, April, 1937.

16. Prandtl, L. "Bemerkungen zur Theorie der freien Turbulenz," Zeitschrift fur angewandte Mathematik und Mechanik, Vol. XXII, No. 5, pp 241-243, October, 1942.

17. Görtler, H. "Berechgnung von Aufgaben der freien Turbulenz auf Grund eines neuen Naherungsansatzes," Zeitschrift für angewandte Mathematik und Mechanik, Vol. XXII, No. 5, pp 244-254, October, 1942.

18. Squire, H. B. "Reconsideration of the Theory of Free Turbulence," Phil Mag, Series 7, Vol. XXXIX, No. 288, pp B1-20, January, 1948.

19. Squire, H. B. and Trouncer, J. "Round Jets in a General Stream," British Aeronautical Research Council, Rept and Memoranda No. 1974, January, 1944, pp 1-23.

20. Emmons, Howard W. Review Number 1394, Vol. 1, No. 9, Appl Mech Reviews, September, 1948.

21. Lin, Chia-Chiao. "Velocity and Temperature Distributions in Turbulent Jets," Sci. Rep Nat Tsing Hau Univ. 4, pp 419-450, 1947.

22. Hinze, J. R., Hegge, Van der, and Zijnen, B. G. "Transfer of Heat and Matter in the Turbulent Mixing Zone of an Axially Symmetrical Jet," Appl Sci Res, Vol. A1, pp 435-461, 1949.

23. Corrsin, Stanley and Uberoi, Mahinder S. "Further Experiments on the Flow and Heat Transfer in a Heated Turbulent Air Jet," NACA Report 998, 1950.

24. Pai, Shih-i. Fluid Dynamics of Jets. D. Van Nostrand Company, 1954.

25. Schlichting, Hermann, Boundary Layer Theory, 4th Edition, 1960.

26. Wilson, Warren E. and Mitchell, Warren I. "Self-Induced Temperature Effects on Laminar Flow of Liquids," Proceedings of the First U. S. Congress on Laminar Flow of Liquids, pp. 789-795, 1951.

27. Toor, H. L. "The Energy Equation for Viscous Flow," Industrial and Engineering Chemistry, Vol. 48, No. 5, pp 922-926. 1956.

28. Brinkman, H. C. "Heat Effects in Capillary Flow I," Appl Sci Res

Vol. A2, pp 120-124, 1950.

29. Sparrow, E. M. and Siegel, R. "Laminar Tube Flow with Arbitrary Internal Heat Sources and Wall Heat Transfer," Nuclear Sci and Engineering, Vol. 4, pp 239-254, 1958.

30. Tao, L. N. "The Second Fundamental Problem in Heat Transfer of Laminar Forced Convection," Jour Appl Mech, Transactions of ASME, paper number 61-WA-108.

31. LeRoy, W. W. and Leslie, R. L. "Hydraulic Fluid Effects on System Performance," Machine Design, Nov. 22, 1962, pp 182, 184, 186, and 188.

32. Sparrow, E. M., Hallman, T. M. and Siegel, R. "Turbulent Heat Transfer in the Thermal Entrance Region of a Pipe with Uniform Heat Flux," Appl Sci Res, Sec A, Vol 7, pp 37-52, 1958.

APPENDIX A

THE GENERAL EQUATIONS OF MOTION

The equations of motion are valid for Newtonian fluids with constant density and viscosity.

Rectangular Coordinates (x,y,z)

x-component

$$\rho\left[\frac{\partial u}{\partial t}+u\frac{\partial u}{\partial x}+v\frac{\partial u}{\partial y}+w\frac{\partial u}{\partial z}\right]=-\frac{\partial p}{\partial x}+\mu\left[\frac{\partial^2 u}{\partial x^2}+\frac{\partial^2 u}{\partial y^2}+\frac{\partial^2 u}{\partial z^2}\right]+\rho g_x$$

y-component

$$\rho\left[\frac{\partial v}{\partial t}+u\frac{\partial v}{\partial x}+v\frac{\partial v}{\partial y}+w\frac{\partial v}{\partial z}\right]=-\frac{\partial p}{\partial y}+\mu\left[\frac{\partial^2 v}{\partial x^2}+\frac{\partial^2 v}{\partial y^2}+\frac{\partial^2 v}{\partial z^2}\right]+\rho g_y$$

z component

$$\rho\left[\frac{\partial w}{\partial t}+u\frac{\partial w}{\partial x}+v\frac{\partial w}{\partial y}+w\frac{\partial w}{\partial z}\right]=-\frac{\partial p}{\partial z}+\mu\left[\frac{\partial^2 w}{\partial x^2}+\frac{\partial^2 w}{\partial y^2}+\frac{\partial^2 w}{\partial z^2}\right]+\rho g_z$$

Cylindrical Coordinates (r,θ,z)

r-component

$$\rho\left[\frac{\partial v_r}{\partial t}+v_r\frac{\partial v_r}{\partial r}+\frac{v_\theta}{r}\frac{\partial v_r}{\partial \theta}-\frac{v_\theta^2}{r}+u\frac{\partial v_r}{\partial x}\right]=-\frac{\partial p}{\partial r}+\mu\left\{\frac{\partial}{\partial r}\left[\frac{1}{r}\frac{\partial}{\partial r}(rv_r)\right]\right.$$
$$\left.+\frac{1}{r^2}\frac{\partial^2 v_r}{\partial \theta^2}-\frac{2}{r^2}\frac{\partial v_\theta}{\partial \theta}+\frac{\partial^2 v_r}{\partial x^2}\right\}+g_r\rho$$

θ-component

$$\rho\left[\frac{\partial v_\theta}{\partial t}+v\frac{\partial v_\theta}{\partial r}+\frac{v_\theta}{r}\frac{\partial v_\theta}{\partial \theta}+\frac{v v_\theta}{r}+u\frac{\partial v_\theta}{\partial z}\right]=-\frac{1}{r}\frac{\partial P}{\partial \theta}+\mu\left\{\frac{\partial}{\partial r}\left[\frac{1}{r}\frac{\partial}{\partial r}(r v_\theta)\right]\right.$$
$$\left.+\frac{1}{r^2}\frac{\partial^2 v_\theta}{\partial \theta^2}+\frac{2}{r^2}\frac{\partial v_r}{\partial \theta}+\frac{\partial^2 v_\theta}{\partial z^2}\right\}+\rho g_\theta$$

z-component

$$\rho\left[\frac{\partial u}{\partial t}+v\frac{\partial u}{\partial r}+\frac{v_\theta}{r}\frac{\partial u}{\partial \theta}+u\frac{\partial u}{\partial z}\right]=-\frac{\partial P}{\partial z}+\mu\left\{\frac{1}{r}\frac{\partial}{\partial r}\left[r\frac{\partial u}{\partial r}\right]\right.$$
$$\left.+\frac{1}{r^2}\frac{\partial^2 u}{\partial \theta^2}+\frac{\partial^2 u}{\partial z^2}\right\}+\rho g_z$$

APPENDIX B

THE GENERAL ENERGY EQUATIONS

The energy equations are valid for Newtonian fluids with constant density, viscosity and thermal conductivity.

Rectangular Coordinates

$$\rho c_v\left(\frac{\partial T}{\partial t}+u\frac{\partial T}{\partial x}+v\frac{\partial T}{\partial y}+w\frac{\partial T}{\partial z}\right)=k\left[\frac{\partial^2 T}{\partial x^2}+\frac{\partial^2 T}{\partial y^2}+\frac{\partial^2 T}{\partial z^2}\right]+\mu\phi$$

where

$$\phi=2\left[\left(\frac{\partial u}{\partial x}\right)^2+\left(\frac{\partial v}{\partial y}\right)^2+\left(\frac{\partial w}{\partial z}\right)^2\right]+\left(\frac{\partial u}{\partial y}+\frac{\partial v}{\partial x}\right)^2+\left(\frac{\partial u}{\partial z}+\frac{\partial w}{\partial x}\right)^2+\left(\frac{\partial v}{\partial z}+\frac{\partial w}{\partial y}\right)^2$$

Cylindrical Coordinates

$$\rho c_v\left(\frac{\partial T}{\partial t}+v\frac{\partial T}{\partial r}+\frac{v_\theta}{r}\frac{\partial T}{\partial \theta}+u\frac{\partial T}{\partial x}\right)=k\left[\frac{1}{r}\frac{\partial}{\partial r}\left(r\frac{\partial T}{\partial r}\right)+\frac{1}{r^2}\frac{\partial^2 T}{\partial \theta^2}+\frac{\partial^2 T}{\partial x^2}\right]+\mu\phi$$

where

$$\phi=2\left[\left(\frac{\partial v}{\partial r}\right)^2+\left(\frac{1}{r}\frac{\partial v_\theta}{\partial \theta}+\frac{v}{r}\right)^2+\left(\frac{\partial u}{\partial x}\right)^2\right]+\left(\frac{\partial v_\theta}{\partial x}+\frac{1}{r}\frac{\partial u}{\partial \theta}\right)^2$$

$$+\left(\frac{\partial u}{\partial r}+\frac{\partial v}{\partial x}\right)^2+\left[\frac{1}{r}\frac{\partial v}{\partial \theta}+r\frac{\partial}{\partial r}\left(\frac{v_\theta}{r}\right)\right]^2$$

APPENDIX C

DETAILS OF EVALUATION OF THE TWO-DIMENSIONAL CIRCULAR JET

The equation to be analytically evaluated is

$$q_f = \mu_t \iiint_V \left\{ \frac{2B^2}{x^4}\left[f(\eta)^2 + 2\eta f(\eta) f'(\eta) + \eta^2 f'(\eta)^2 \right] + \frac{A^2B^2}{x^4} f'(\eta)^2 \right\} dV$$

$$= 2\pi B^2 \mu_t \int_{x=x_1}^{x=L} \int_{r=0}^{r=R_x} \left\{ \frac{2}{x^4}\underbrace{\left[f(\eta)^2 \right]}_{I_1} + \underbrace{2\eta f(\eta) f'(\eta)}_{I_2} + \underbrace{\eta^2 f'(\eta)^2}_{I_3} \right] + \frac{A^2}{x^4}\underbrace{f'(\eta)^2}_{I_4} \Bigg\} r\,dr\,dx \qquad \text{(C-1)}$$

The integration is the sum of four integrals; the first integral may be written as

$$I_1 = 2\pi \mu_t B^2 \int_{x=x_1}^{x=L} \frac{1}{x^4} \int_{r=0}^{r=R_x} f(\eta)^2 \cdot 2r\,dr\,dx$$

$$= 2\pi \mu_t B^2 \int_{x=x_1}^{x=L} \frac{1}{x^4} \int_{r=0}^{r=R_x} \left(1 + \frac{1}{4}\eta^2 \right)^{-4} 2r\,dr\,dx$$

Substituting for η gives

$$I_1 = 2\pi\mu_t B^2 \int_{z=z_1}^{z=L} \frac{1}{z^4} \int_{r=0}^{r=R_z} \left(1 + \frac{A^2 r^2}{4z^2}\right)^{-4} 2r\,dr\,dz. \tag{C-2}$$

The integration with respect to 4 involves the substitution

$$r^2 = w \; ; \; 2r\,dr = dw \tag{C-3}$$

then

$$\int (a+bw)^N dw = \frac{1}{b(N+1)} (a+bw)^{N+1}. \tag{C-4}$$

Therefore, when N = -4

$$I_1 = 2\pi\mu_t B^2 \int_{z=z_1}^{z=L} \frac{1}{z^4} \left\{ -\frac{4z^2}{3A^2} \left[1 + \frac{A^2 r^2}{4z^2}\right]^{-3} \right\}_{r=0}^{r=R_z = \frac{Rz}{L}} dz$$

$$= 2\pi\mu_t \frac{B^2}{A^2} \left(-\frac{4}{3}\right) \int_{z=z_1}^{z=L} \frac{1}{z^2} \left[\left(1 + \frac{A^2 R^2 z^2}{4L^2}\right)^{-3} - 1 \right] dz$$

$$= -\frac{8}{3}\pi\mu_t \frac{B^2}{A^2} \left[\left(1 + \frac{A^2 R^2}{4L^2}\right)^{-3} - 1 \right] \int_{z=z_1}^{z=L} \frac{dz}{z^2}$$

$$I_1 = C_1 \left(\frac{1}{z_1} - \frac{1}{L} \right) \tag{C-5}$$

where

$$C_1 = \frac{8}{3}\pi\mu_t \frac{B^2}{A^2}\left[1 - \left(1 + \frac{A^2R^2}{4L^2}\right)^{-3}\right] \tag{C-6}$$

The second integral may be written as

$$I_z = 2\pi\mu_t B^2 \int_{y=y_1}^{y=L} \frac{2}{y^4} \int_{r=0}^{r=R_x} \eta f(\eta) f'(\eta) 2r\,dr\,dy$$

$$= 4\pi\mu_t B^2 \int_{y=y_1}^{y=L} \frac{1}{y^4} \int_{r=0}^{r=R_x} \frac{\eta}{\left(1+\frac{1}{4}\eta^2\right)^2} \cdot \frac{(-\eta)}{\left(1+\frac{1}{4}\eta^2\right)^3} 2r\,dr\,dy$$

$$= -4\pi\mu_t B^2 \int_{y=y_1}^{y=L} \frac{1}{y^4} \int_{r=0}^{r=R_x} \frac{\eta^2}{\left(1+\frac{1}{4}\eta^2\right)^5} 2r\,dr\,dy.$$

Substituting the definition of η gives

$$I_z = -4\pi\mu_t B^2 \int_{y=y_1}^{y=L} \frac{A^2}{y^6} \int_{r=0}^{r=R_x} \frac{r^2\,2r\,dr}{\left(1+\frac{A^2r^2}{4y^2}\right)^5}\,dy$$

$$= -4\pi\mu_t B^2 A^2 \int_{y=y_1}^{y=L} \frac{1}{y^6} \int_{r=0}^{r=R_x} \frac{r^2\,2r\,dr}{\left(1+\frac{A^2r^2}{4y^2}\right)^5}\,dy \tag{C-7}$$

Let $w = r^2$ and $dw = 2r\,dr$, then

$$\int \frac{w\,dw}{(a+bw)^N} = \frac{1}{b^2}\left[\frac{-1}{(N-2)(a+bw)^{N-2}} + \frac{a}{(N-1)(a+bw)^{N-1}}\right] \tag{C-8}$$

so that:

$$I_z = -4\pi\mu_t B^2 A^2 \int_{x=x_1}^{x=L} \frac{1}{x^6}\left\{\frac{16x^4}{A^4}\left[\frac{-1}{3\left(1+\frac{A^2r^2}{4x^2}\right)^3}+\frac{1}{4\left(1+\frac{A^2r^2}{4x^2}\right)^4}\right]_{r=0}^{r=R_x=\frac{Rx}{L}}\right\}dx$$

$$= -4\pi\mu_t \frac{B^2}{A^2}(16)\int_{x=x_1}^{x=L}\frac{1}{x^2}\left\{-\frac{1}{3\left(1+\frac{A^2R^2}{4L^2}\right)^3}+\frac{1}{4\left(1+\frac{A^2R^2}{4L^2}\right)^4}+\frac{1}{3}-\frac{1}{4}\right\}dx$$

$$= -64\mu_t \frac{B^2}{A^2}\left[\frac{1}{12}-\frac{1}{3}\left(1+\frac{A^2R^2}{4L^2}\right)^{-3}+\frac{1}{4}\left(1+\frac{A^2R^2}{4L^2}\right)^{-4}\right]\int_{x=x_1}^{x=L}\frac{dx}{x^2}$$

$$= -64\mu_t \frac{B^2}{A^2}\left[\frac{1}{12}-\frac{1}{3}\left(1+\frac{A^2R^2}{4L^2}\right)^{-3}+\frac{1}{4}\left(1+\frac{A^2R^2}{4L^2}\right)^{-4}\right]\left(\frac{1}{x_1}-\frac{1}{L}\right)$$

Let

$$C_z = -64\mu_t \frac{B^2}{A^2}\left[\frac{1}{12}-\frac{1}{3}\left(1+\frac{A^2R^2}{4L^2}\right)^{-3}+\frac{1}{4}\left(1+\frac{A^2R^2}{4L^2}\right)^{-4}\right] \qquad \text{(C-9)}$$

Then

$$I_z = C_z\left(\frac{1}{x_1}-\frac{1}{L}\right) \qquad \text{(C-10)}$$

The third integral may be integrated next

$$I_3 = 2\pi\mu_t B^2 \int_{x=x_1}^{x=L}\frac{1}{x^4}\int_{r=0}^{r=R_x}\eta^2 f(\eta)^2\, 2r\,dr\,dx$$

$$I_3 = 2\pi\mu_t B^2 \int_{x=x_1}^{x=L} \frac{1}{x^4} \int_{r=0}^{r=R_x} \frac{\eta^4}{\left(1+\frac{1}{4}\eta^2\right)^6} 2r\,dr\,dx$$

Substituting for η gives

$$I_3 = 2\pi\mu_t B^2 \int_{x=x_1}^{x=L} \frac{A^4}{x^8} \int_{r=0}^{r=R_x} \frac{r^4\, 2r\,dr}{\left(1+\frac{A^2r^2}{4x^2}\right)^6} dx \qquad \text{(C-11)}$$

Again let $w = r^2$ and $dw = 2r\,dr$, then

$$\int \frac{w^2\,dw}{(a+bw)^N} = \frac{1}{b^3}\left[\frac{-1}{(N-3)(a+bw)^{N-3}} + \frac{2a}{(N-2)(a+bw)^{N-2}} + \frac{-a^2}{(N-1)(a+bw)^{N-1}}\right] \qquad \text{(C-12)}$$

Therefore,

$$I_3 = 2\pi\mu_t B^2 A^4 \int_{x=x_1}^{x=L} \frac{1}{x^8}\left\{\frac{4^3x^6}{A^6}\left[-\frac{1}{3}\left(1+\frac{A^2r^2}{4x^2}\right)^{-3} + \frac{1}{2}\left(1+\frac{A^2r^2}{4x^2}\right)^{-2} - \frac{1}{5}\left(1+\frac{A^2r^2}{4x^2}\right)^{-5}\right]_{r=0}^{r=R_x}\right\} dx$$

$$I_3 = 128\pi\mu_t \frac{B^2}{A^2}\left[\frac{1}{30} - \frac{1}{3}\left(1+\frac{A^2R^2}{4L^2}\right)^{-3} + \frac{1}{2}\left(1+\frac{A^2R^2}{4L^2}\right)^{-4} - \frac{1}{5}\left(1+\frac{A^2R^2}{4L^2}\right)^{-5}\right] \int_{x=x_1}^{x=L} \frac{dx}{x^2}$$

Let

$$C_3 = 128\pi\mu_t \frac{B^2}{A^2}\left[\frac{1}{30} - \frac{1}{3}\left(1+\frac{A^2R^2}{4L^2}\right)^{-3} + \frac{1}{2}\left(1+\frac{A^2R^2}{4L^2}\right)^{-4} - \frac{1}{5}\left(1+\frac{A^2R^2}{4L^2}\right)^{-5}\right] \tag{C-13}$$

Then

$$I_3 = C_3\left(\frac{1}{L} - \frac{1}{\chi_1}\right) \tag{C-14}$$

The remaining integral to be evaluated is

$$I_4 = \pi\mu_t B^2A^2\int_{\chi=\chi_1}^{\chi=L}\frac{1}{\chi^4}\int_{r=0}^{r=R_\chi} f'^2(\eta)\, 2r\,dr\,d\chi$$

$$= \pi\mu_t B^2A^2\int_{\chi=\chi_1}^{\chi=L}\frac{1}{\chi^4}\int_{r=0}^{r=R_\chi}\frac{\eta^2}{\left(1+\frac{1}{4}\eta^2\right)^3}\, 2r\,dr\,d\chi$$

and substituting for η gives

$$I_4 = \pi\mu_t B^2A^4\int_{\chi=\chi_1}^{\chi=L}\frac{1}{\chi^6}\int_{r=0}^{r=R_\chi}\frac{r^2\, 2r\,dr}{\left(1+\frac{A^2r^2}{4\chi^2}\right)^3}\, d\chi$$

Integrating by equation (C-8) yields

$$I_4 = \pi\mu_t B^2A^4\int_{\chi=\chi_1}^{\chi=L}\frac{1}{\chi^6}\left\{\frac{16\chi^4}{A^4}\left[-\frac{1}{4}\left(1+\frac{A^2r^2}{4\chi^2}\right)^{-4} + \frac{1}{5}\left(1+\frac{A^2r^2}{4\chi^2}\right)^{-5}\right]_{r=0}^{r=R_\chi=\frac{R\chi}{L}}\right\} d\chi$$

$$= \pi\mu_t B^2A^2\int_{\chi=\chi_1}^{\chi=L}\frac{1}{\chi^2}\frac{16}{A^4}\left[\frac{1}{20} - \frac{1}{4}\left(1+\frac{A^2R^2}{4L^2}\right)^{-4} + \frac{1}{5}\left(1+\frac{A^2R^2}{4L^2}\right)^{-5}\right] d\chi$$

$$I_4 = C_4\left(\frac{1}{x_1} - \frac{1}{L}\right) \tag{C-15}$$

where

$$C_4 = +16\pi\mu_t B^2\left[\frac{1}{20} - \frac{1}{4}\left(1+\frac{A^2R^2}{4L^2}\right)^{-4} + \frac{1}{5}\left(1+\frac{A^2R^2}{4L^2}\right)^{-5}\right] \tag{C-16}$$

Therefore the integration is the sum of the four integrals

$$\beta_t = (C_1 + C_2 + C_3 + C_4)\left(\frac{1}{x_1} - \frac{1}{L}\right) \tag{C-17}$$

If the edge of the jet is arbitrarily established to be the point where the axial velocity has reduced to 0.05 of its maximum value, then from the relation

$$\frac{u}{u_{max}} = \left(1+\frac{1}{4}\eta^2\right)^{-2} \tag{C-18}$$

the corresponding value of η at the edge of the jet is denoted as η_o and has a value of 3.725; the arbitrary value of 0.05 was selected as corresponding to the accepted value in entrance effects. Sparrow, Hallman, and Siegel (32) define an entrance length as the length required to obtain conditions within 5% of fully-developed conditions. The equation (C-18) is shown in Figure 33.

Applying this technique to the free jet analysis, η_o is a constant value when x = L and when r = R

$$\eta_o = \frac{AR}{L} = 3.725 \tag{C-19}$$

Since the quantity $\left(1+\frac{A^2R^2}{4L^2}\right)$ appears frequently in the results of the integration and since it can be evaluated in terms of a constant, η_o, the values are given in tabular form where

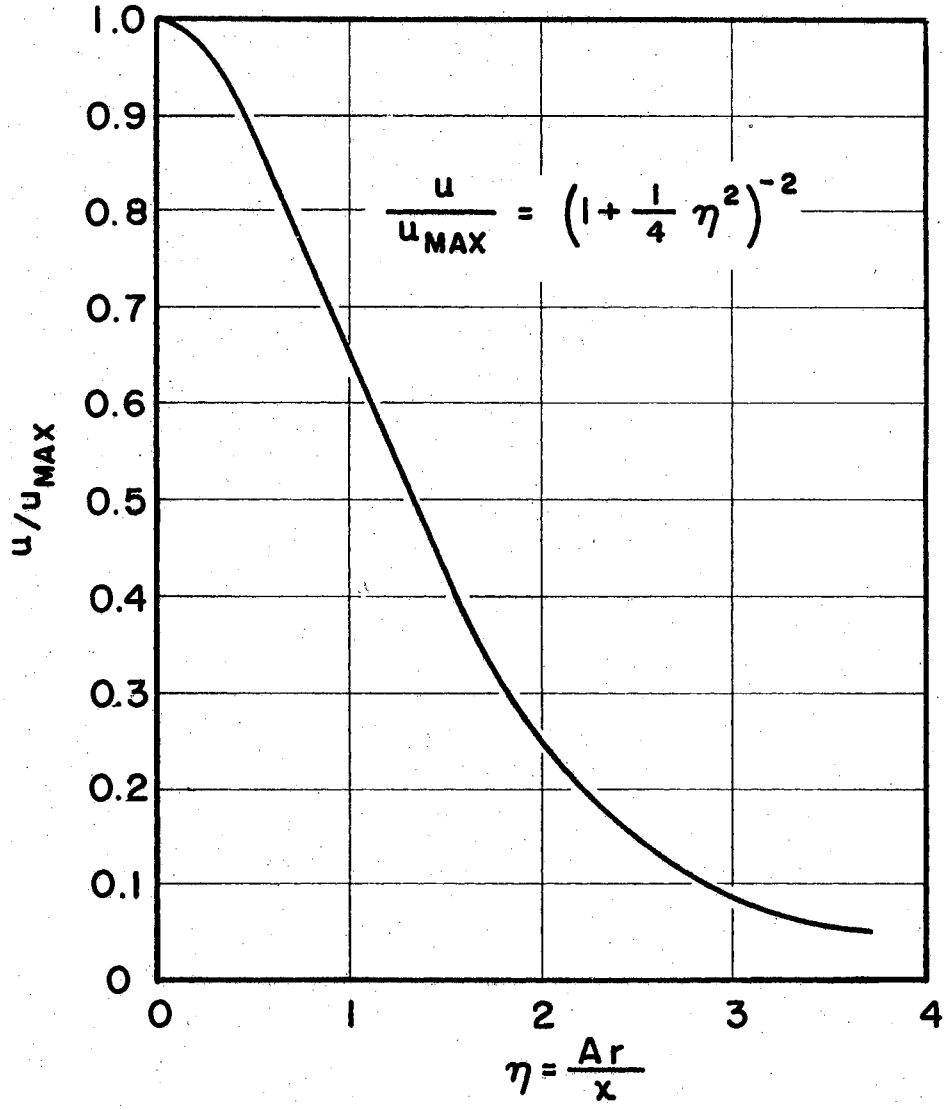

FIGURE 33

VELOCITY RATIO DISTRIBUTION FOR SCHLICHTING'S CIRCULAR JET.

$$a = \left(1 + \frac{A^2 R^2}{4L^2}\right) \tag{C-20}$$

then

$$\begin{aligned} a &= 4.47 \\ 1/a^2 &= 0.0501 \\ 1/a^3 &= 0.01121 \\ 1/a^4 &= 0.00251 \\ 1/a^5 &= 0.000562 \end{aligned} \tag{C-21}$$

Equation (C-1) is evaluated to be

$$\begin{aligned} g_f &= C\left(\frac{1}{x_1} - \frac{1}{L}\right) = \mu_t \pi \frac{B^2}{A^2}\left[1.33 + 0.792A^2\right]\left(\frac{1}{x_1} - \frac{1}{L}\right) \\ &= \mu_t \frac{3K}{4}\left[1.33 + 0.792A^2\right]\left(\frac{1}{x_1} - \frac{1}{L}\right) \\ &= \mu_t K\left[1.00 + 0.593A^2\right]\left(\frac{1}{x_1} - \frac{1}{L}\right) \end{aligned} \tag{C-22}$$

where K is the mass momentum given as

$$K = \frac{1}{\pi}\left(\dot{g}/R_o\right)^2 \tag{C-23}$$

APPENDIX D

DETAILS OF EVALUATION OF THE TWO-DIMENSIONAL PLANE JET

The relation to be evaluated analytically is given as

$$q_p = 4B_1^2\mu_t \iiint_V \left\{ \frac{2}{x^3}\left[\eta^2 \frac{\sinh^2\eta}{\cosh^6\eta} - \frac{\eta}{2}\frac{\sinh\eta}{\cosh^5\eta} + \frac{1}{16}\frac{1}{\cosh^4\eta} \right] + \frac{A_1^2}{x^3}\frac{\sinh^2\eta}{\cosh^6\eta} \right\} dV \qquad \text{(D-1)}$$

The integration is the sum of four integrals. The first integral is

$$I_1 = 8B_1^2\mu_t \iiint_V \frac{\eta^2 \sinh^2\eta}{x^3\cosh^6\eta}\, dV$$

$$= 8B_1^2\mu_t \int_{x=x_1}^{x=L} \int_{y=-Y_x}^{y=+Y_x} \frac{1}{x^3}\frac{A_1^2 y^2}{x^2}\frac{\sinh^2\left(\frac{A_1 y}{x}\right)}{\cosh^6\left(\frac{A_1 y}{x}\right)}\, dy\, dx$$

$$= \frac{8B_1^2}{A_1}\mu_t \int_{x=x_1}^{x=L} \frac{1}{x^2} \int \left(\frac{A_1 y}{x}\right)^2 \frac{\sinh^2\left(\frac{A_1 y}{x}\right)}{\cosh^6\left(\frac{A_1 y}{x}\right)} \left[\left(\frac{A_1}{x}\right) dy\right] dx \qquad \text{(D-2)}$$

$$\int w^2 \frac{\sinh^2 w}{\cosh^6 w}\,dw = -\frac{1}{5}\frac{w^2 \sinh w}{\cosh^5 w} - \frac{1}{10}\frac{w}{\cosh^4 w} + \frac{1}{10}\left(\tanh w - \frac{\tanh^3 w}{3}\right) \qquad \text{(D-3)}$$

Therefore the first integration becomes

$$I_1 = \frac{8B_1^2}{A_1}\mu_t \int_{x=x_1}^{x=L} \frac{1}{x^2}\left\{-\frac{1}{5}\left(\frac{A_1 y}{x}\right)^2 \frac{\sinh\left(\frac{A_1 y}{x}\right)}{\cosh^5\left(\frac{A_1 y}{x}\right)} - \frac{\left(\frac{A_1 y}{x}\right)}{10\cosh^4\left(\frac{A_1 y}{x}\right)} + \frac{1}{10}\left[\tanh\left(\frac{A_1 y}{x}\right) - \frac{\tanh^3\left(\frac{A_1 y}{x}\right)}{3}\right]\right\}_{y=-Y_x=-\frac{Yx}{L}}^{y=Y_x=\frac{Yx}{L}} dx \qquad \text{(D-4)}$$

Letting C_1 be defined as

$$C_1 = \frac{8B_1^2}{A_1}\mu_t\left\{-\frac{2}{5}\left(\frac{A_1 Y}{L}\right)^2 \frac{\sinh\left(\frac{A_1 Y}{L}\right)}{\cosh^5\left(\frac{A_1 Y}{L}\right)} - \frac{1}{5}\left(\frac{A_1 Y}{L}\right)\cosh^{-4}\left(\frac{A_1 Y}{L}\right) + \frac{1}{5}\tanh\left(\frac{A_1 Y}{L}\right) - \frac{2}{3}\tanh^3\left(\frac{A_1 Y}{L}\right)\right\} \qquad \text{(D-5)}$$

then

$$I_1 = C_1\left(\frac{1}{x_1} - \frac{1}{L}\right)$$

The second integral may now be considered

$$I_2 = 4B_1^2\mu_t \int_{x=x_1}^{x=L}\int_{y=-Y_x}^{y=Y_x} \frac{2}{x^3}\left(-\frac{1}{2}\right)\eta\frac{\sinh\eta}{\cosh^5\eta}\,dy\,dx \qquad \text{(D-6)}$$

$$I_z = -4B_1^2 \mu_t \int_{x=x_1}^{x=L} \frac{1}{x^3} \int_{y=-Y_x}^{y=Y_x} \left(\frac{A_1 y}{x}\right) \frac{\sinh\left(\frac{A_1 y}{x}\right)}{\cosh^5\left(\frac{A_1 y}{x}\right)} \, dy \, dx$$

$$= -\frac{4B_1^2}{A_1} \mu_t \int_{x=x_1}^{x=L} \frac{1}{x^2} \int_{y=-Y_x}^{y=+Y_x} \left(\frac{A_1 y}{x}\right) \frac{\sinh\left(\frac{A_1 y}{x}\right)}{\cosh^5\left(\frac{A_1 y}{x}\right)} \left[\frac{A_1}{x} dy\right] dx \qquad \text{(D-7)}$$

The integration with respect to y is of the form

$$\int w \frac{\sinh w}{\cosh^5 w} \, dw = -\frac{1}{4} \frac{w}{\cosh^4 w} + \frac{1}{4}\left(\tanh w - \frac{\tanh^3 w}{3}\right)$$

(D-8)

therefore

$$I_z = -\frac{4B_1^2}{A_1} \mu_t \int_{x=x_1}^{x=L} \frac{1}{x^2} \left\{ -\frac{1}{4} \frac{A_1 y/x}{\cosh^4 \frac{A_1 y}{x}} + \frac{1}{4}\left[\tanh\left(\frac{A_1 y}{x}\right) - \frac{1}{3}\tanh^3\left(\frac{A_1 y}{x}\right)\right] \right\}_{y=-Y_x=-\frac{Yx}{L}}^{y=Y_x=\frac{Yx}{L}} dx \qquad \text{(D-9)}$$

Letting

$$C_z = -\frac{4B_1^2 \mu_t}{A_1}\left[-\frac{1}{2}\left(\frac{A_1 Y}{L}\right)\frac{1}{\cosh\left(\frac{A_1 Y}{L}\right)} + \frac{1}{2}\tanh\left(\frac{A_1 Y}{L}\right) - \frac{1}{6}\tanh^3\left(\frac{A_1 Y}{L}\right)\right] \qquad \text{(D-10)}$$

Then

$$I_2 = C_2\left(\frac{1}{x_1} - \frac{1}{L}\right) \tag{D-11}$$

Considering the third integral,

$$I_3 = \frac{4B_1^2\mu_t}{16}\int_{x=x_1}^{x=L}\int_{y=-Y_x}^{y=Y_x}\frac{z}{x^3}\cosh^{-4}\eta\, dy\, dx$$

$$= \frac{B_1^2\mu_t}{2A_1}\int_{x=x_1}^{x=L}\frac{1}{x^2}\int_{y=-Y_x}^{y=Y_x}\cosh^{-4}\left(\frac{A_1 y}{x}\right)\left[\left(\frac{A_1}{x}\right)dy\right]dx$$

$$= \frac{B_1^2}{A_1}\frac{\mu_t}{2}\int_{x=x_1}^{x=L}\frac{1}{x^2}\left\{\tanh\left(\frac{A_1 y}{x}\right) - \frac{1}{3}\tanh^3\left(\frac{A_1 y}{x}\right)\right\}_{y=-Y_x=-\frac{Yx}{L}}^{y=Y_x=\frac{Yx}{L}}dx$$

Letting

$$C_3 = \frac{B_1^2\mu_t}{2A_1}\left[2\tanh\left(\frac{A_1 Y}{L}\right) - \frac{2}{3}\tanh^3\left(\frac{A_1 Y}{L}\right)\right] \tag{D-12}$$

then

$$I_3 = C_3\left(\frac{1}{x_1} - \frac{1}{L}\right) \tag{D-13}$$

The last integral may be considered

$$I_4 = 4B_1^2A_1^2\mu_t\int_{x=x_1}^{x=L}\int_{y=-Y_x}^{y=Y_x}\frac{1}{x^3}\,\frac{\sinh^2\eta}{\cosh^6\eta}\,dy\,dx$$

$$I_4 = 4B_1^2 \mu_t A_1 \int_{x=x_1}^{x=L} \frac{1}{x^2} \int_{y=-Y_x}^{y=Y_x} \sinh^2\left(\frac{A_1 y}{x}\right) \cosh^{-6}\left(\frac{A_1 y}{x}\right) \left[\left(\frac{A_1}{x}\right) dy\right] dx \tag{D-14}$$

The integration with respect to y is of the form

$$\int \frac{\sinh^2 w}{\cosh^6 w}\, dw = -\frac{1}{5}\frac{\sinh w}{\cosh^5 w} + \frac{1}{5}\tanh w - \frac{1}{15}\tanh^3 w \tag{D-15}$$

so that

$$I_4 = 4\mu_t A_1 B_1^2 \int_{x=x_1}^{x=L} \frac{1}{x^2}\left\{-\frac{1}{5}\sinh\left(\frac{A_1 y}{x}\right)\cosh^{-5}\left(\frac{A_1 y}{x}\right) + \frac{1}{5}\tanh\left(\frac{A_1 y}{x}\right) - \frac{1}{15}\tanh^3\left(\frac{A_1 y}{x}\right)\right\}_{y=-Y_x=-\frac{Yx}{L}}^{y=Y_x=\frac{Yx}{L}} dx$$

Letting

$$C_4 = 4\mu_t A_1 B_1^2\left[-\frac{2}{5}\sinh\left(\frac{A_1 Y}{L}\right)\cosh^{-5}\left(\frac{A_1 Y}{L}\right) + \frac{2}{5}\tanh\left(\frac{A_1 Y}{L}\right) - \frac{2}{15}\tanh^3\left(\frac{A_1 Y}{L}\right)\right] \tag{D-16}$$

Then

$$I_4 = C_4\left(\frac{1}{x_1} - \frac{1}{L}\right) \tag{D-17}$$

So that the entire integration is

$$q_f = (C_1 + C_2 + C_3 + C_4)\left(\frac{1}{x_1} - \frac{1}{L}\right) \tag{D-18}$$

Introducing the arbitrary edge of the jet as the point corresponding to $U/U_{max} = 0.05$ as in the case of the circular jet, the plane jet value for the corresponding η_o may be found for the expression

$$u/u_{max} = 1 - \tanh^2 \eta \qquad \text{(D-19)}$$

where η_o is found to have a value of 2.19. The above velocity ratio is shown in Figure 34. The hyperbolic constants may be evaluated for $\eta = \eta_o = AR/L$ as

η_o	$\sinh \eta_o$	$\cosh \eta_o$	$\cosh^4 \eta_o$	$\cosh^5 \eta_o$	$\tanh \eta_o$	$\tanh^3 \eta_o$
2.19	4.412	4.524	419	1900	0.975	0.926

Using this information, the coefficients appearing in the integration terms become

$$\left.\begin{aligned} C_1 &= 1.0024\, \mu_t \frac{B_1^2}{A_1} \\ C_2 &= 1.3219\, \mu_t \frac{B_1^2}{A_1} \\ C_3 &= 0.6664\, \mu_t \frac{B_1^2}{A_1} \\ C_4 &= 1.0712\, \mu_t A_1 B_1^2 \end{aligned}\right\} \qquad \text{(D-20)}$$

Combining these results, the viscous dissipation of energy is given as

$$g_f = \mu_t \frac{B_1^2}{A_1}\left[0.3669 + 1.0712\, A_1^2\right]\left(\frac{1}{x_1} - \frac{1}{L}\right) \qquad \text{(D-21)}$$

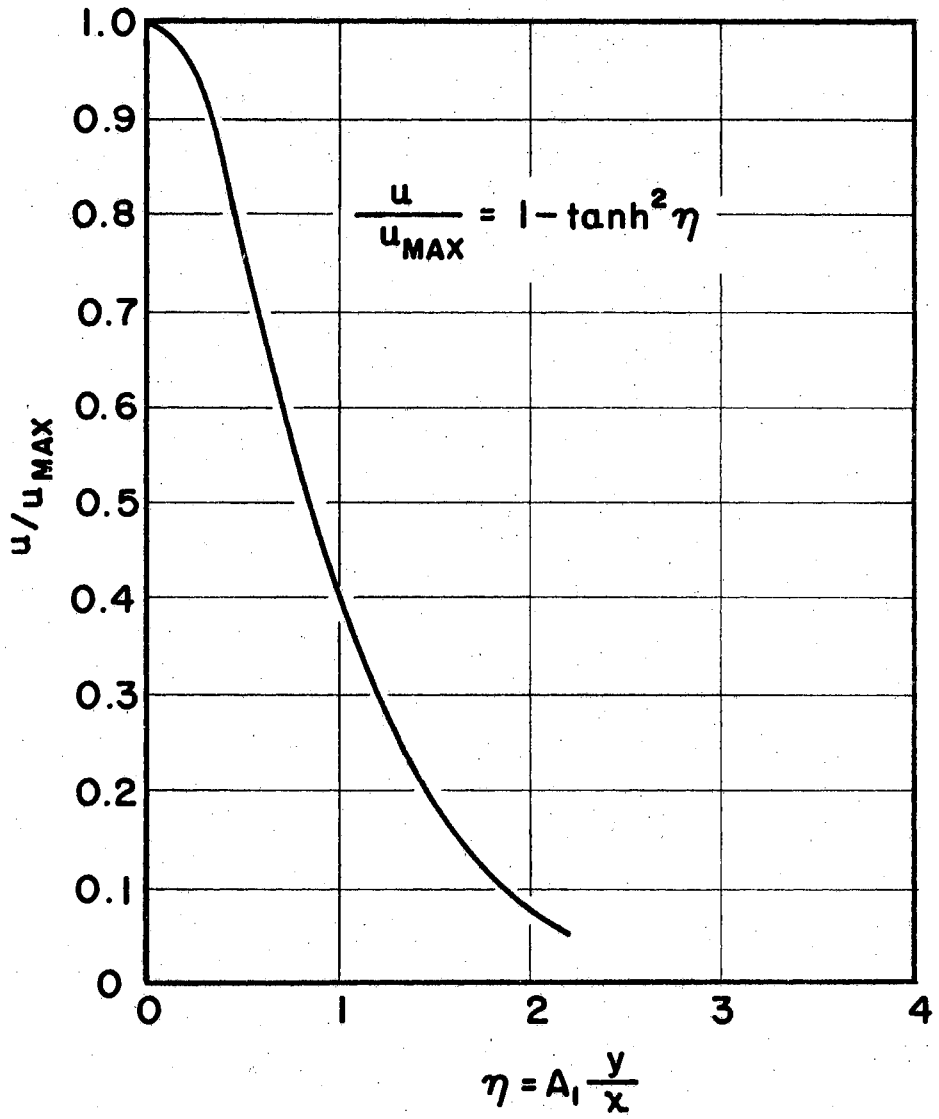

FIGURE 34

VELOCITY RATIO DISTRIBUTION FOR SCHLICHTING'S PLANE JET.

APPENDIX E

COMPUTER PROGRAMS FOR THE DETERMINING OF THE VISCOUS DISSIPATION OF ENERGY

The flow diagrams appearing on the following pages represent the calculation procedure for the evaluation of equations (VI-33), (VI-44) and (V-29). These expressions when evaluated over the entire jet provide the quantitative value of the dissipated energy in a circular jet.

Each computation represents the amount of energy dissipated in a fluid element with a volume of

$$\Delta V = 2\pi R \Delta R \Delta X$$

At each particular axial location, the dissipated energy is calculated in intervals of ΔR across the radius of the jet at that particular axial location. When the evaluation is complete at one axial location the next axial location is considered.

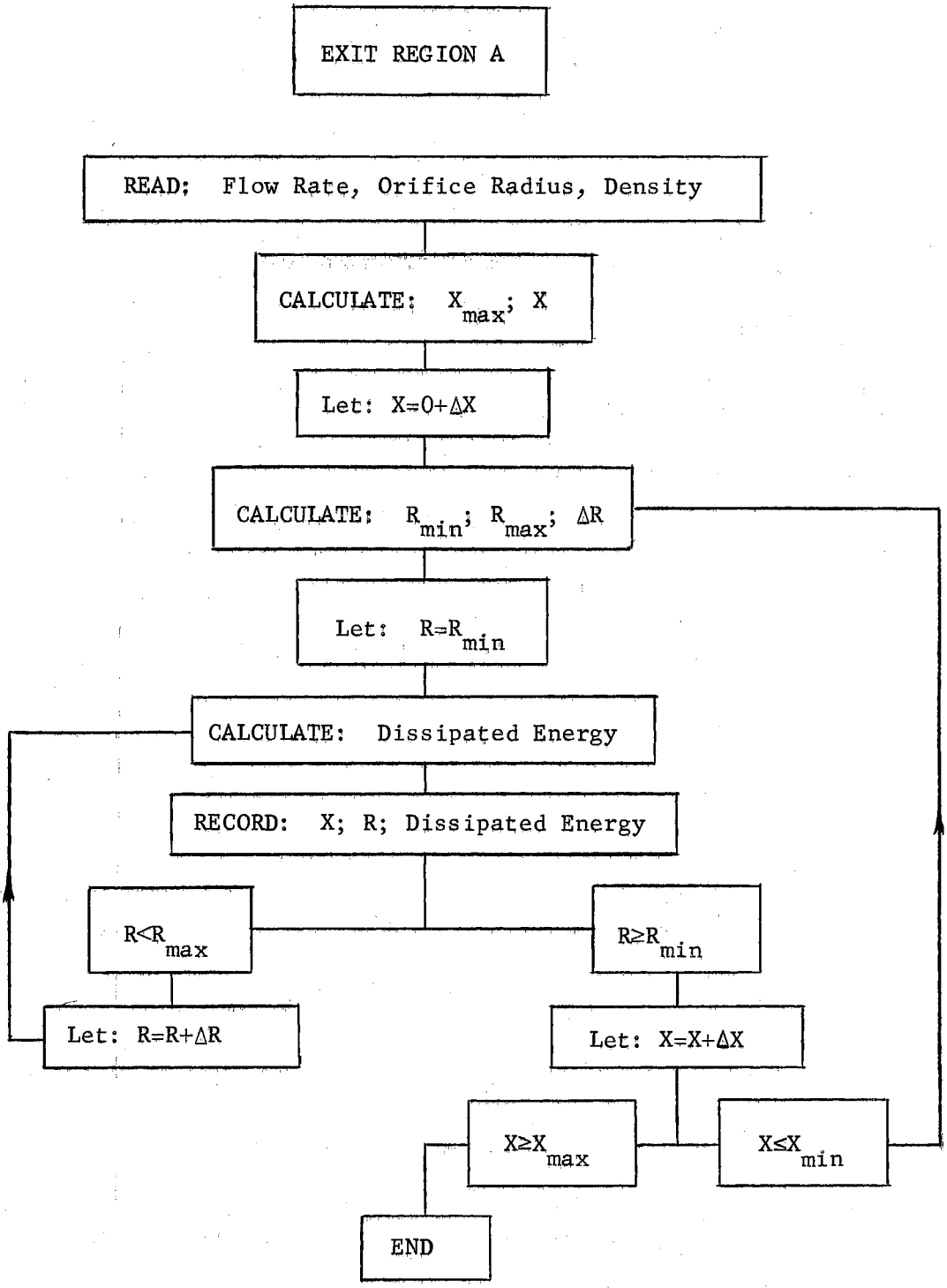
EXIT REGION A
READ: Flow Rate, Orifice Radius, Density
CALCULATE: X_{max}; X
Let: X=0+ΔX
CALCULATE: R_{min}; R_{max}; ΔR
Let: R=R_{min}
CALCULATE: Dissipated Energy
RECORD: X; R; Dissipated Energy
R<R_{max}
R≥R_{min}
Let: R=R+ΔR
Let: X=X+ΔX
X≥X_{max}
X≤X_{min}
END

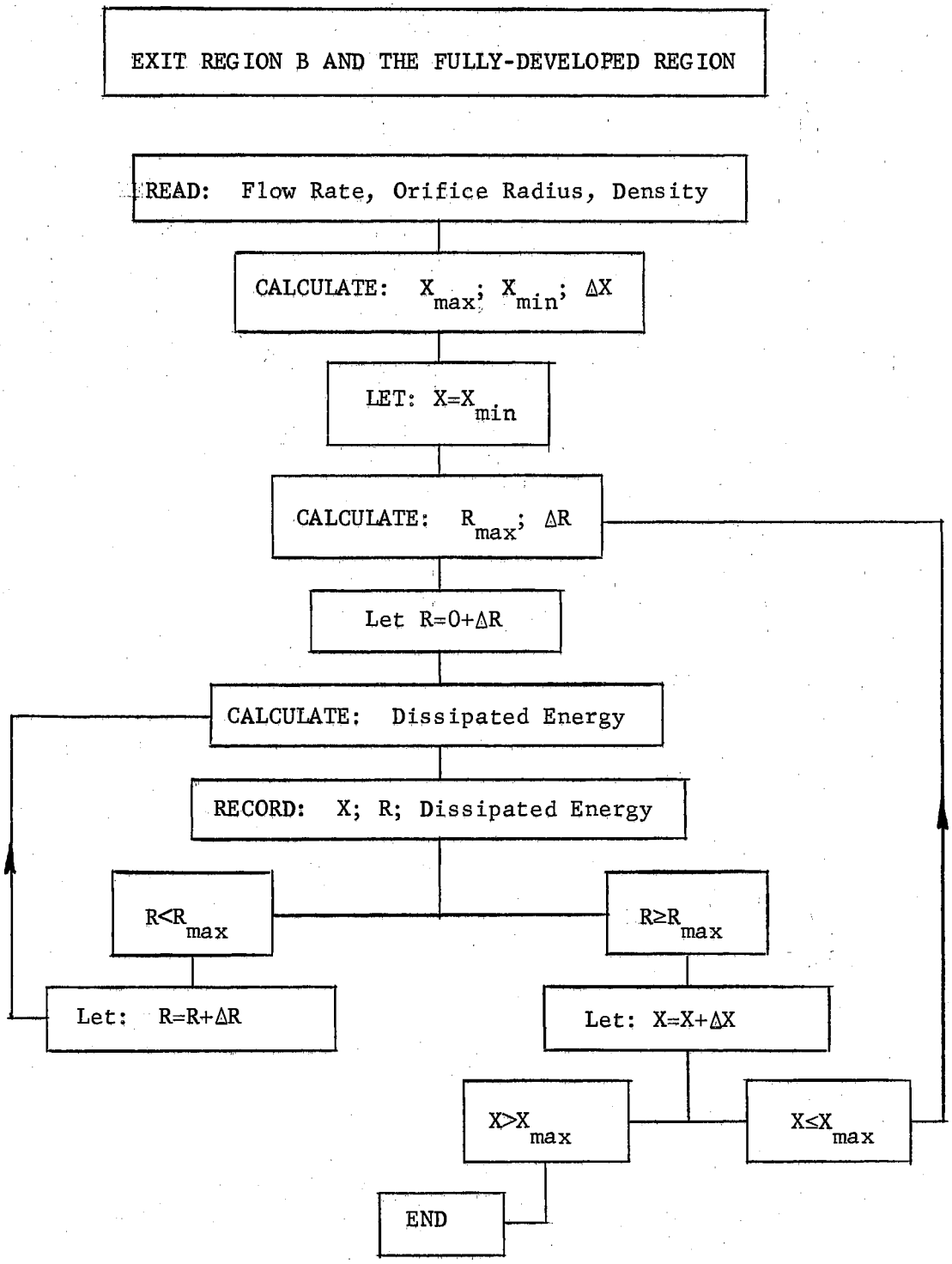
EXIT REGION B AND THE FULLY-DEVELOPED REGION
READ: Flow Rate, Orifice Radius, Density
CALCULATE: X_{max}; X_{min}; ΔX
LET: $X=X_{min}$
CALCULATE: R_{max}; ΔR
Let $R=0+\Delta R$
CALCULATE: Dissipated Energy
RECORD: X; R; Dissipated Energy
$R<R_{max}$
$R\geq R_{max}$
Let: $R=R+\Delta R$
Let: $X=X+\Delta X$
$X>X_{max}$
$X\leq X_{max}$
END

VITA

Jimmy Elster Cox

Candidate for the Degree of

Doctor of Philosophy

Thesis: INVESTIGATION OF THE VISCOUS DISSIPATION OF ENERGY IN TURBULENT FLOWS

Major Field: Mechanical Engineering

Biographical:

Personal Data: The writer was born in Waco, Texas, August 29, 1935, the son of Elster and Ernestine Cox.

Education: He graduated from North Dallas High School, Dallas, Texas, in 1953 and the following September entered Southern Methodist University where he graduated with a Bachelor of Science Degree in Mechanical Engineering in 1958 and a Master of Science Degree in Mechanical Engineering in 1960. In 1960, the writer entered Oklahoma State University where he completed the requirements for the Doctor of Philosophy Degree in August, 1963.

Experience: The writer's primary industrial experience was obtained at Chance Vought Corporation in Dallas, Texas, where he worked in the various sections of the engineering department for a total time of approximately three years. He also taught for one year in the Mechanical Engineering Department at Southern Methodist University and for three years at Oklahoma State University where his duties varied from half-time to full-time responsibilities.

Professional Organizations: The writer is a member of the following professional organizations: The American Society of Mechanical Engineers, The American Society for Engineering Education, Pi Tau Sigma Fraternity, and Sigma Tau Fraternity.